A Study of Dynamics of

Coupled Nonlinear Circuits

A Thesis
Presented to
The Academic Faculty

by

José Luis Sánchez Hernández

In Partial Fulfillment
of the Requirements for the Degree
Doctor of Philosophy

School of Mathematics
Georgia Institute of Technology
December 2004

A Study of Dynamics of

Coupled Nonlinear Circuits

Approved by:

Dr. Shui–Nee Chow, Advisor
School of Mathematics
Georgia Institute of Technology

Dr. Luca Dieci
School of Mathematics
Georgia Institute of Technology

Dr. Wang Yang
School of Mathematics
Georgia Institute of Technology

Dr. Vainstein Feodor
School of Electrical and Computer Engineering
Georgia Institute of Technology

Dr. Yi Yingfei
School of Mathematics
Georgia Institute of Technology

Date Approved: December 14, 2004

Dedication

To God ....

To Laura and my Parents

ACKNOWLEDGEMENTS

There have been many individuals without whom the completion of this work would not have been possible.

I would like to thank my advisor, Professor Shui–Nee Chow, for his support and orientation through all my studies at Georgia Tech. In addition to supporting and guiding my research efforts, I also thank him for introducing me to the fascinating world of Applied Mathematics.

I would like to thank Professors Luca Dieci, Wang Yang, Yi Yingfei, and Feodor Vainstein for serving as members of my defense. I am also thankful to professor Jack Hale for his support while I was working on my thesis.

Several people have made my stay here at Georgia Tech a wonderful one and I would like to thank them. Ms. Cathy Jacobson, English Language Consultant in School of Mathematics, has been especially helpful from the first day I came to Georgia Tech till now. I thank her for helping me improve my oral expression and my writing techniques in English. Ms. Rena Brakebill, Assistant Undergraduate Coordinator, for lots of useful advice on handling classes and videotaping. I wish also to thanks my officemates, Becky Upchurch, for all her help while I was here at Georgia Tech and Marcio Gaimero for all his help while I was working in my research.

A lot of people contributed to my education and professional formation back in Venezuela. I would like to acknowledge Professor Nelson Merentes, for introducing me to the world of Set-valued functions and Nemystky Operators. From here we got a paper that will appear in the "Bulletin of the Polish Academy of Sciences Mathematics", 2005. Professors Hugo Leiva and Marcos Lizana because they encouraged me to come to Georgia Tech. They helped me in many different ways during my years at my second alma mater: UCV.

I have been enriched by friends and colleagues in the School of Mathematics and outside as

we share so many good moments together. In particular, I am thankful to Luis Hernandez-Urena, Victor Morales Duarte, Lucrecia Vizcaino, Luis Gonzalez, Alicia Fermin, José Miguel Renom, Claudia Antonini, Jian Chen, Mei Xiang, Cinzia Elia, Andrés Sercovich, and José Enrique Figueroa-Lopez for their friendship. I will miss you all.

I would like to thank my family for their steady support and love. Thanks to my parents: Elor and Juana. Thanks to my siblings : Beatriz, Elor, and Joel. Last, but not least, I would like to thank my wife, Laura Cardoza. My life has positively change for the better since we got married. Thanks you for being so patient and understanding with me, as I sometimes put my research before you. This work would not exist without her support and love.

TABLE OF CONTENTS

LIST OF TABLES

LIST OF FIGURES

SUMMARY

We consider a type of forced "Van Der Pol" oscillator where the forced function is periodic and oscillatory around the t-axis. This problem derived from an electrical circuit model. The important issues here is that this circuit presents the spiking phenomena over a one time period and it has an important applications in signal processing and digital communication. The three most important problems that we addressed here in this thesis are to compute the number of spikes a solution completes in one time period (It can be used to transform the analog signal into digital information), how the dynamics of the number of spikes change with respect to the parameters amplitude (k) and frequency (ω), and when the coupled circuits synchronize (i.e., the driver and the respond are synchronous). Sophisticated mathematical and numerical analysis has been developed that enable us to give a complete study of the problems above described.

CHAPTER I

INTRODUCTION

The model that we consider can be used in various applications such as communications and electronic circuits (gated oscillator, sigma-delta modulator, delta modulator, clock multipliers, etc). When applied to communications, the model can be used as a fundamental modulation and demodulation technique. The Circuit receivers can be used as devices that generate pulses from the received analog signal and perform demodulation based on pulse counting and related algorithms. One of the possible circuit realizations exhibits the "S-curve" transfer characteristic (figure 1). The transfer characteristic consists of three different regions. The two lines at the top and bottom have positive slope, $\frac{1}{R_F}$ and they represent the regions in which the Op-Amp is operating in the saturated (nonlinear) mode (figure 1), the middle segment has a negative slope, $\frac{-R_1}{R_2 R_F}$ (negative resistance) and represents the region in which the Op-Amp is operating linearly. It is this negative resistance region that allows the Op-Amp to oscillate and produce pulses bounded by the positive and negative saturation voltages. By using the Principle of Duality, the "N-curve" family of circuits can be derived. In this case, the realization of the circuits can be based on the Op-Amp or devices such as the tunnel diode, etc. The transfer function of a tunnel diode exhibits the "N-curve" transfer characteristic inherently, which is a dual of the "S-curve" family. By connecting an inductor and a tunnel diode in series, we can produce pulses that are separated by periods of silence. This family of circuits responds to the voltage level of the input signal. In this case, the duration when the input signal is above a certain threshold voltage determines the duration that the circuit operates in the unstable region and consequently the number of pulses generated.

The circuit produces different sets of pulses with respect to the different frequencies of the signal or different amplitudies of the signal. The information symbols are encoded and transmitted through the channel. At the receiver, the circuit produces different sets of

pulses with respect to the different frequencies or different amplitudies of the signal. It is one of the most important features of this circuit because it enables one information symbol to be carried in one RF carrier cycle. Systems such as PAM, QAM, FSK, etc, that people are using today required thousands of cycles to capture one symbol. The information symbol can be recovered by simply counting the spikes, i.e., f_1 (A_1) produces 2 spikes, f_2 (A_2) produces 3 spikes, f_3 (A_3) produces 4 spikes, etc, where f is the frequency and A is the amplitud of the input function f.

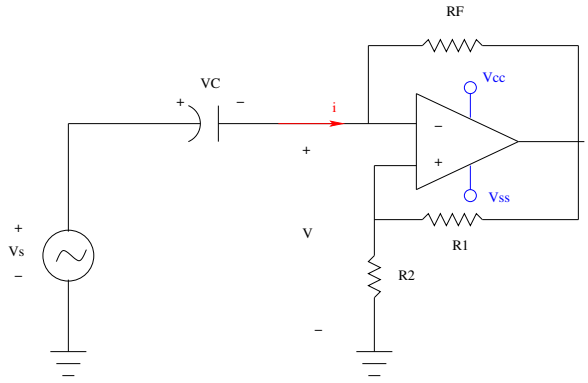

Figure 1: Circuit Diagram of the model

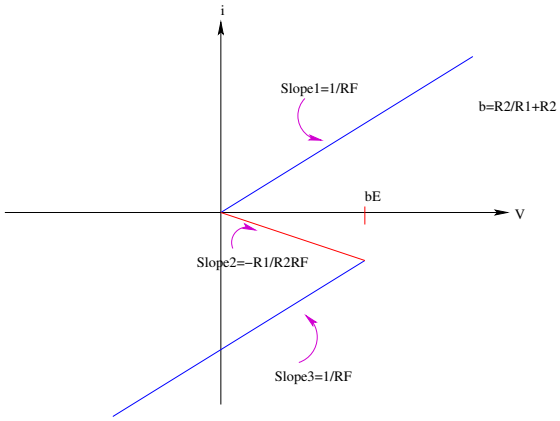

Figure 2: Characteristics curve

Coupled nonlinear oscillators model a wide variety of major technological and physical systems. An important and useful property of a nonlinear oscillator is that it can synchronize to another oscillator given the proper coupling. An array of coupled nonlinear oscillators can synchronize to a common frequency even though the frequencies of the free running

oscillators are not the same. If a pair of similar or even identical systems is coupled one may observe identical synchronization. This kind of identical synchronization, however, cannot be expected for coupled systems that are of completely different nature (e.g., an electrical circuit coupled to a mechanical system). Also, in reality, it is not possible to have identical nonlinear oscillators. This is the most important reason why different definitions of generalized synchronization (GS) have been proposed during the last years all of them depending on the application [1], [4], [25], [32], [16].

Synchronization phenomena of oscillators and coupled oscillators have been studied by physicists, engineers and mathematicians [4], [2], [40], [3], [20], [22], [21] . While this brings many interesting questions to mathematicians, it has also been applied to many areas such as communications, signal processing, etc. Its history goes back to the 17th century when the famous Dutch scientist Christiaan Huygens (1673) reported on his observation of synchronization of the two pendulum clocks. The systematic study of this phenomenon, experimental as well as theoretical, was started by Edwards Appleton (1922) [6] and Balthasar van der Pol (1927) [43]. They showed that the frequency of a triode generator can be entrained, or synchronized, by a weak external signal with slightly different frequency. These studies were of high practical importance because such generators became basic elements of radio communication systems.

The next impact to development of the theory of synchronization was given by Andronov and Vitt (1930) [5] further developed methods of van der Pol and generalized his results. Mutual synchronization of two weakly nonlinear oscillators was analytically treated by Mayer (1935) [28]. The development of rigorous mathematical tools of the synchronization theory started with works on circle map [13] and forced relaxation oscillators [9] and [10]. Recent development has been highly influenced by Arnold [7] and Kuramoto [27]. During the last decade synchronization of chaotic systems has been explored very intensively by many reserchers in various fields ranging from physics, mathematics to engineering, where for the latter the main motivation has been potential practical aplications in communication systems (Pecora and Carroll, 1990 [33]; Kocarev and Parlitz, 1995 [24]).

Synchronization of nonlinear oscillators both in their regular and chaotic states is presently

one of the main research topics in the field of nonlinear science since the pioneering work of Pecora and Carrol [34]. Among many examples we mention synchronization of pacemaker cells of the hard [35], central patter generation [26], [37] chemical waves [27], rhythmic activity in the brain [18], and pattern recognition [42]. However, despite the amount of theoretical and experimental results already obtained, a great deal of effort is still required to find optimal parameters to shorten the synchronization time, define the synchronization threshold parameters [36], and avoid loss of synchronization [11] and instability during the synchronization process. This problem is important in all the mentioned fields where synchronization finds or will find practical applications. For instance, in communication systems, the range of time during which the chaotic oscillators are not synchronized corresponds to the range of time during which the encoded message can not be recovered or sent. More than a grave and irreversible loss of information, this is a catastrophe in digital communications since the first bits of standardized bit strings contain the signalization data or identity card of the message.

In conventional communication sytems, thousands of RF carrier cycles are required to reliably extract the information contained in a carrier signal. This is because the receiver requires time to synchronise with the carrier signal. With this circuit the information can be decoded in every transmitted cycle since the synchronization depends on the coupling and not the time, i.e., we can send one information symbol to be carried per one RF carrier cycle. Thus, it promises very high-speed data transmisssion. For example in order to send information we can use different number of spikes per cycle to represent sets of information symbols and we can do it by changing the amplitud or the frequency as we proved in Chapter II.

Another important piece of information that we need to know in any electronic circuit model that can be applied to communication is the Lyapunov exponents. Lyapunov exponents are the average exponential rates of divergence or convergence of nearby orbits in phase space. Since nearby orbits correspond to nearly identical states, exponential orbital divergence means that systems whose initial differences we may not be able to resolve will soon behave quite differently (predictive ability is rapidly lost). Any system containing at least one

positive Lyapunov exponent is defined to be chaotic, with the magnitude of the exponent reflecting the time scale on which system dynamics become unpredictable.

Any continuous time-dependent dynamical system without a fixed point will have at least one zero exponent [19], corresponding to the slowly changing magnitude of a principal axis tangent to the flow. Axes that are on the average contracting (expanding) correspond to negative (positive) exponents. The sum of the Lyapunov exponents is the time-averaged divergence of the phase space velocity; hence any dissipative dynamical system will have at least one negative exponent, the sum of all of the exponents is negative, and the post-transient motion of trajectories will occur on a zero volume limit set, an attractor.

The exponential expansion indicated by a positive Lyapunov exponent is incompatible with motion on a bounded attractor unless some sort of folding process merges widely separated trajectories. Each positive exponent reflects a "direction" in which the system experiences the repeated stretching and folding that decorrelates nearby states on the attractor. Therefore, the long-term behavior of an initial condition that is specified with any uncertainty cannot be predicted; this is chaos. An attractor for a dissipative system with one or more positive Lyapunov exponents is said to be "strange" or "chaotic".

The signs of the Lyapunov exponents provide a qualitative picture of a system's dynamics. One dimensional maps are characterized by a single Lyapunov exponent which is positive for chaos, zero for a marginally stable orbit, and negative for a periodic orbit. In a three-dimensional continuous dissipative dynamical system the only possible spectra, and the attractors they describe, are as follows: $(+, 0, -)$, a strange attractor; $(0, 0, -)$, a two-torus; $(0, -, -)$, a limit cycle; and $(-, -, -)$, a fixed point. In a continous four-dimensional dissipative system there are three possible types of strange attractors: their Lyapunov spectra are $(+, +, 0, -)$, $(+, 0, 0, -)$, and $(+, 0, -, -)$.

Since we are studiying the synchronization problem from the information point of view it is very important to know the Lyapunov exponents associated to our system, because the magnitudes of the Lyapunov exponents quantify an attractor's dynamics in information theoretic terms. The exponents measure the rate at which system processes create or destroy information [39]; thus the exponents are expressed in bits of information/s or bits/orbit for

a continuous system and bits/iteration for a discrete system. For example if a system has a positive exponent of magnitude 2.16bits/s and an initial point were specified with an accuracy of one part per million (20bits), the future behavior could not be predicted after about $9s$ $[20bits/(2.16bits/s)]$, corresponding to about 20 orbits. After this time the small initial uncertainty will essentially cover the entire attractor, reflecting 20 bits of new information that can be gained from an additional measurement of the system. This new information arises from scales smaller than our initial uncertainty and results in an inability to specify the state of the system except to say that it is somewhere on the attractor. This process is sometimes called an information gain (reflecting new information from the heat bath), and sometimes is called an information loss (bits shifted out of a phase space variable "register" when bits from the heat bath are shifted in). On the other hand, the average rate at which information contained in transients is lost can be determined from the negative exponents.

1.1 Outline of the Thesis

The thesis is organized as follows.

In the first part of Chapter II we introduce the circuit model and the dynamical systems that describe it. This chapter is devoted to the first two main results of the thesis, namely the formula that gives the number of spikes for a given piecewise periodic continuous function oscillatoring around the t-axis with amplitude k and frequency ω. To obtain it we compute the asymptotic expansion of the one-cycle solution of system 4. The construction of the asymptotic solution is based on the matched expansion combined with some specific techniques used in [31], [41]. Motivated from a simpler example in [41] (where the solution is symmetric about the horizontal axis and the exact solution can be explicitly obtained), our second result tells us how the dynamics of the number of spikes change with respect to the parameters $k > 0$ and $\omega > 0$. By the first result we know that the number of spikes depends of the following parameters $\delta_1 > 0$, $\delta_2 < 0$, $y_0 < 0$, $k > 0$, and $\omega > 0$. But since the first three parameter correspond to the circuits we decided to study only the parameters $k > 0$ and $\omega > 0$. These are the most important parameters for the application.

In Chapter III we describe the kind of coupling that we are going to use with our model.

The most important kind of coupling from the applications point of view that we did here is the unidirectional coupling.

In Chapter IV, using a generalized synchronization definition [16], we show our last result. We prove that the coupled circuits have a generalized synchronization with respect to the coupling. Here we prove it for both cases of (unidirectional and bidirectional) couplings. For the unidirectional coupling we show that it is perfect synchronous in information sense as this synchronization does not depent on time, it depends only on the initial condition and the coupling.

Many investigators have studied two mutually coupled oscillators (mutual synchronization), because two oscillators' case is a prototype modeling to understand the phenomena in a large number of coupled oscillators. On the other hand, forced synchronization is also studied in the filed of physiology [8], chemistry (forced Brusselator [30]) and electric engineering (forced Van der Pol [23]). However we cannot find the study of connecting mutual synchronization and forced synchronization.

In Chapter V we do the numerical simulation using Matlab. We also Calculate the Lyapunov exponent associated at our coupled systems. From this information we also show that the original system has synchronization on the generalized case.

CHAPTER II

SPIKES SOLUTIONS AND THEIR DEPENDENCE ON THE PARAMETERS FOR A NONLINEAR CIRCUIT

2.1 Introduction

We consider a singularly perturbed system of differential equations with periodic forcing which is derived from an electrical circuit model as shown in figure 3 (used in modulation and demodulation schemes). The circuit diagram that described our model is shown in figure 1. It consist of a linear capacitor, a linear inductor and a nonlinear negative resistor. The system presents the spiking phenomena over a one time period that has important application in signal processing and in the technology in communication. Our main goal in this chapter will be to show how the number of spikes change with respect to the parameters $(\delta_1, \delta_2, y^*, k, \omega)$ and to get a formula for the number of spikes given a piecewise continuous periodic forcing function $f(t)$.

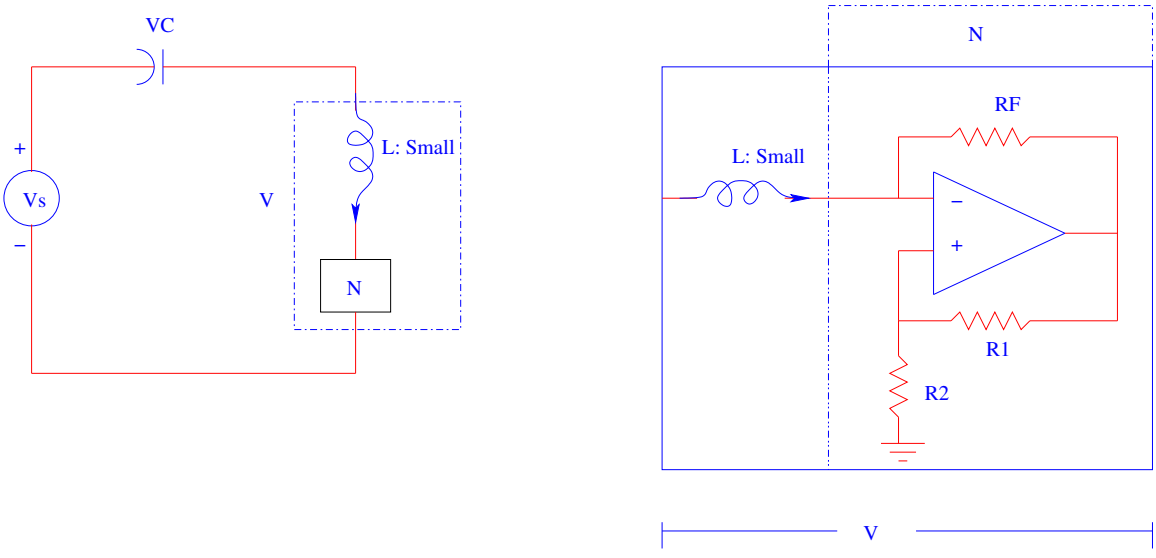

Figure 3: Circuit diagram of the model

2.2 Mathematical Model

An electronic circuit is an interconnection of components which can be modeled by a system of singularly perturbed differential equations using Kirchoff voltage and current laws. The type of circuits we considere (figure 3) can be modeled as:

$$\begin{cases} \frac{dv}{d\tau} = \frac{dv_s}{d\tau} - \frac{i}{C}, \\ \mu \frac{di}{d\tau} = v - \varphi(i), \end{cases} \tag{1}$$

and v_s is the input voltage. The characteristic function $\varphi(i)$ is defined as: where C is the capacitance, μ ($\mu = L$) is the inductance, and v_s is the input voltage. The characteristic function $\varphi(i)$ is defined as:

$$\varphi(i) = \begin{cases} \delta_1 i, & if \quad i \geq 0, \\ \delta_2 i, & if \quad i_0 \leq i < 0, \\ \delta_1 (i - i_0) + \delta_2 i_0, & if \quad i_0 \leq i, \end{cases} \tag{2}$$

where $\delta_1 > 0$ and $\delta_2 < 0$, and the v coordinate at one of the corner point is $v_0 = \delta_2 i_0$. It is shown in figure 4.

In the circuits we concern C and μ will be very small, but $0 < \frac{\mu}{C} << 1$. The problem

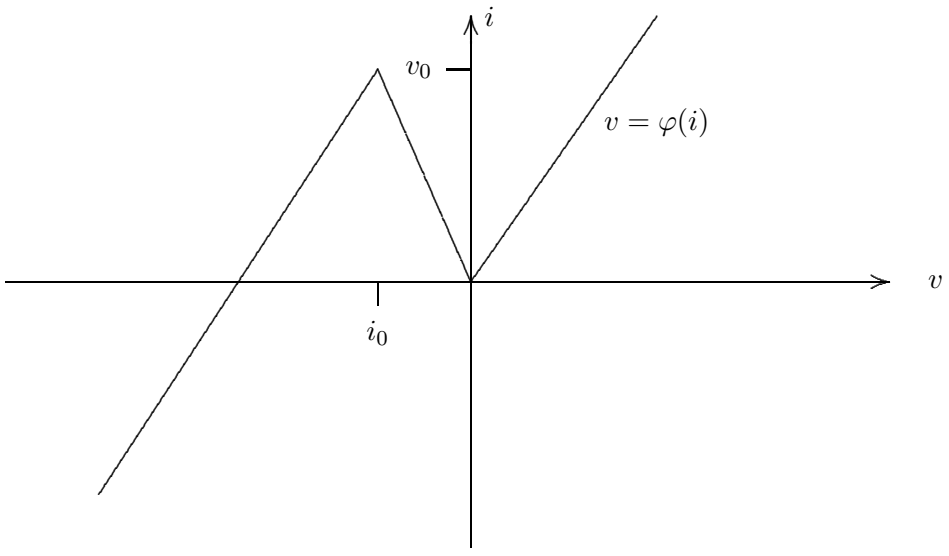

Figure 4: Function $v = \varphi(i)$

is thus a singularly perturbed problem with two small parameters. To ease the numerical computation and also the theoretical analysis we make a time variable transformation

$$\tau = Ct, \quad v = x, \quad i = y, \quad \frac{dv_s}{dt} = f(t). \tag{3}$$

The differential equations then become

$$\begin{cases} \frac{dx}{dt} = f(t) - y, \\ \epsilon \frac{dy}{dt} = x - \varphi(y), \end{cases} \tag{4}$$

where $\epsilon = \frac{\mu}{C} > 0$ is a small parameter, $f(t)$ is a forced periodic function, and

$$\varphi(y) = \begin{cases} \delta_1 y, & if \quad y > 0, \\ \delta_2 y, & if \quad y_0 < y \leq 0, \\ \delta_1 y + y_0(\delta_2 - \delta_1), & if \quad y \leq y_0, \end{cases} \tag{5}$$

$\delta_1 > 0$ and $\delta_2 < 0$. The graph of the function $x = \varphi(y)$ is of (single) N-shape, see figure 5. In this work we assume that $f(t)$ is a piecewise continuos function oscillatory around t axis (i.e. around $y = 0$ alternating from positive side to negative side). A practical example for $f(t)$ are $f(t) = kcos(\omega t)$ or $v_s = \frac{k}{\omega} sin(\omega t)$, and $f(t)$ =triangular waveform or $f(t)$ =the slope of the triangular waveform.

Remark 2.2.1.

$$\varphi(y) = \frac{\delta_1}{2} \{2y - y_0 + |y| - |y - y_0|\} + \frac{\delta_2}{2} \{y_0 + |y - y_0| - |y|\}, \tag{6}$$

hence $\varphi(y) = \delta_2 y_0 - \varphi(y_0 - y)$.

Eliminating x in (4) yields a second order differential equation for y:

$$\epsilon \frac{d^2y}{dt^2} + \varphi'(y) \frac{dy}{dt} + y = f(t), \tag{7}$$

where

$$\varphi'(y) = \begin{cases} \delta_1, & if \quad y \geq 0; \\ \delta_2, & if \quad y_0 \leq y < 0; \\ \delta_1, & if \quad y < y_0. \end{cases} \tag{8}$$

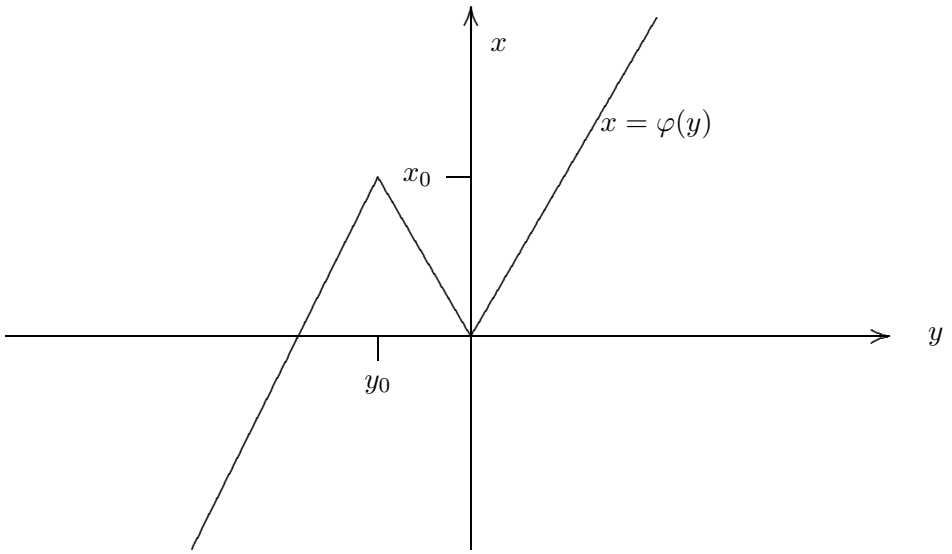

Figure 5: Function $x = \varphi(y)$

Note that $\varphi'(y)$ is of piecewise constant. For the special function $f(t) = kcos(\omega t)$ exact solution can be obtained and then properties of the solution can be analyzed based on the exact solution. For the purpose of generality our discussion will not be based on exact solution but on aymptotic analysis which is applicable to general $f(t)$.

2.3 Formation of a spike solution

The system (4) or the equation (7) is not autonomous because of the input signal term $f(t)$. We first study phase plane solution for each fixed $f(t)$. We then let time flow to obtain the properties of the dynamic solution.

The systems is of "Van Der Pol type" modeling an electronic circuit with a piecewise current-voltage characteristic $x = \varphi(y)$. Since ϵ is small it corresponds to relaxation oscillations which exhibit two distinct and characteristic phases: one during which energy is stored up slowly and another in which the energy is discharged nearly instantaneously when a certain critical state is attained.

Let $\Gamma : x = \varphi(y)$ be the characteristic curve of the system. Consider a solution that starts at a point $P = (x(0), y(0))$. This is a singularly perturbed systems. We can expect slow

motion to be primarily determined by the reduced system

$$\begin{cases} \frac{dx}{dt} = f(t) - y, \\ 0 = x - \varphi(y), \end{cases} \tag{9}$$

whereas fast motions will follow the stretched system

$$\frac{dy}{ds} = x - \varphi(y), \tag{10}$$

with x as a parameter and $s = \frac{t-t_0}{\epsilon}$ for some appropriate t_0 [31]. We have that slow motions will lie on the characteristic curve (manifold) Γ, whereas fast motion will occur off Γ. The fixed point is the intersection point of the curve Γ and the horizontal line $i = f(t)$. If $f(t)$ is between zero and y_0 the fixed point is unstable. The solution will never reach it if it is not the starting point. If $f(t)$ is larger than zero or smaller than y_0 then the fixed point is stable and the solution will approach it. Hence, in the time segment when $f(t) > 0$ or $f(t) < y_0$, there is no cycling solution. A detailed description of phase plane solution is given below.

Suppose that the starting point P is away from Γ, $\frac{dy}{dt}$ is approximately $+\infty$ or $-\infty$ and we expect y to move almost instantaneously toward Γ (approximately satisfying the fast system), whereas x will hardly vary (see figure 6).

First consider the case where $y_0 < f(t) < 0$. Let P_1 be the point where the solution reaches Γ. Then $\frac{dy}{dt} = 0$ at P_1. Since $\frac{dy}{dt}$ is approximately $\pm\infty$ away from Γ, the solution curve tends to follow Γ, starting above it, until it reaches the vicinity of P_2. At this point the solution curve turns almost vertically until it intersects Γ at P_3. By the same reason the solution curve tends to follow Γ from P_3 counter–clockwise, starting below Γ, until it reaches the vicinity of P_4, where it turns almost vertically again to intersect Γ at P_5. Then it tends to follow the path from P_5 to P_2. Therefore the limit of the cycling solution as $\epsilon \to 0$ consists of the two segments P_5P_2 and P_3P_4 of Γ, and the two vertical lines P_4P_5 and P_2P_3. Thus the limit solution satisfies $x = \varphi(y)$ except at certain points (i.e. P_2 and P_4) where y has jump discontinuities. These discontinuities cause difficulty in constructing the asymptotic solution which, however, is necessary in asymptotically calculating the one-cycle time of the $P_2P_3P_4P_5$ cycle later.

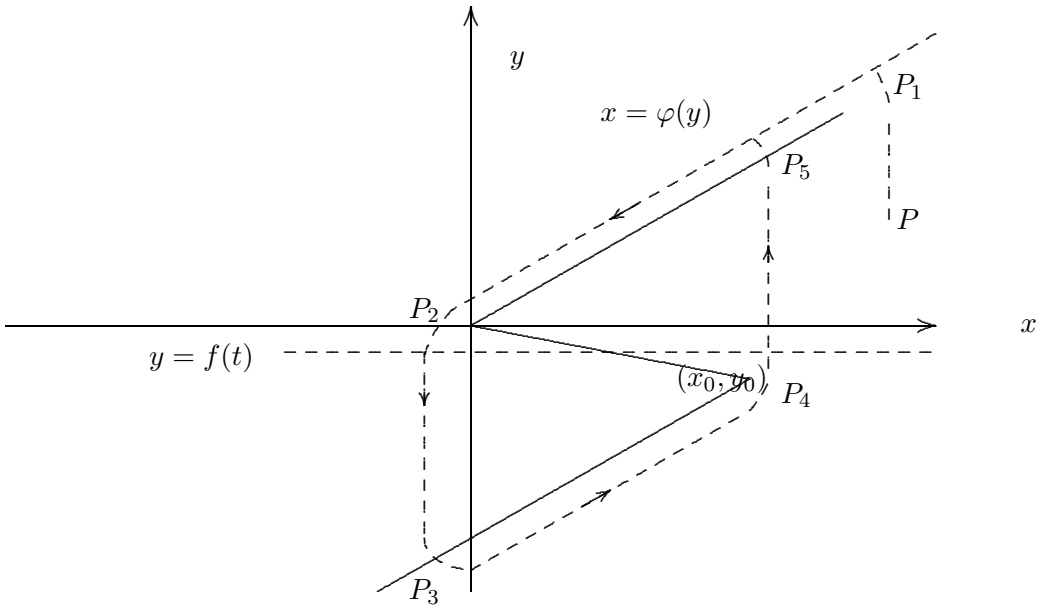

Figure 6: Phase portrait when $y_0 < f(t) < 0$

Similarly we can described the cases $f(t) \geq 0$ and $f(t) \leq y_0$. These cases are illustrated in figures (7) and (8), respectively. In these two cases we would not have a cycling solution since the solution approaches a stable fixed point.

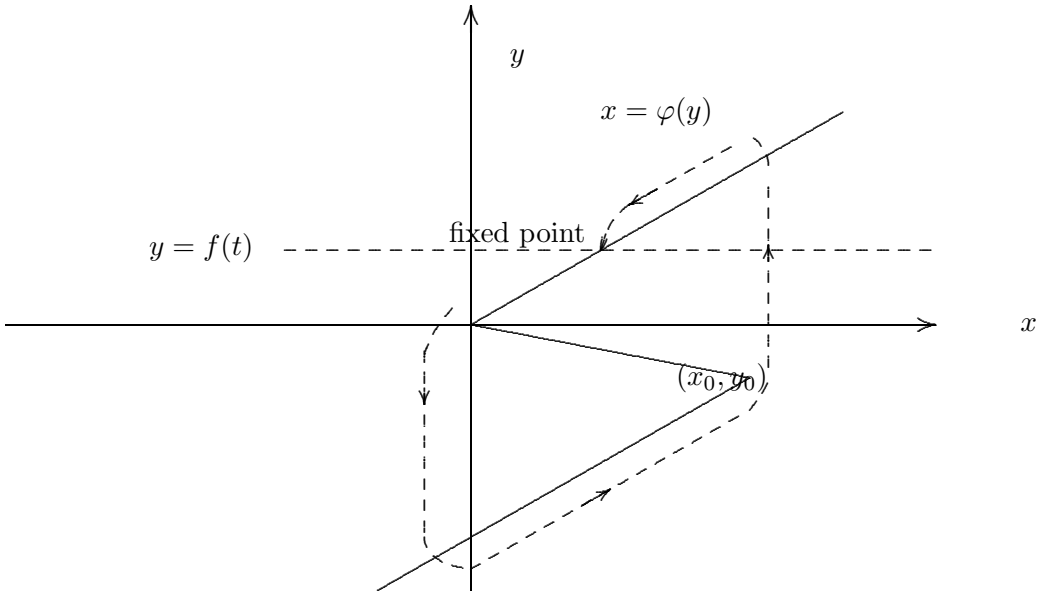

Figure 7: Phase portrait when $f(t) \geq 0$

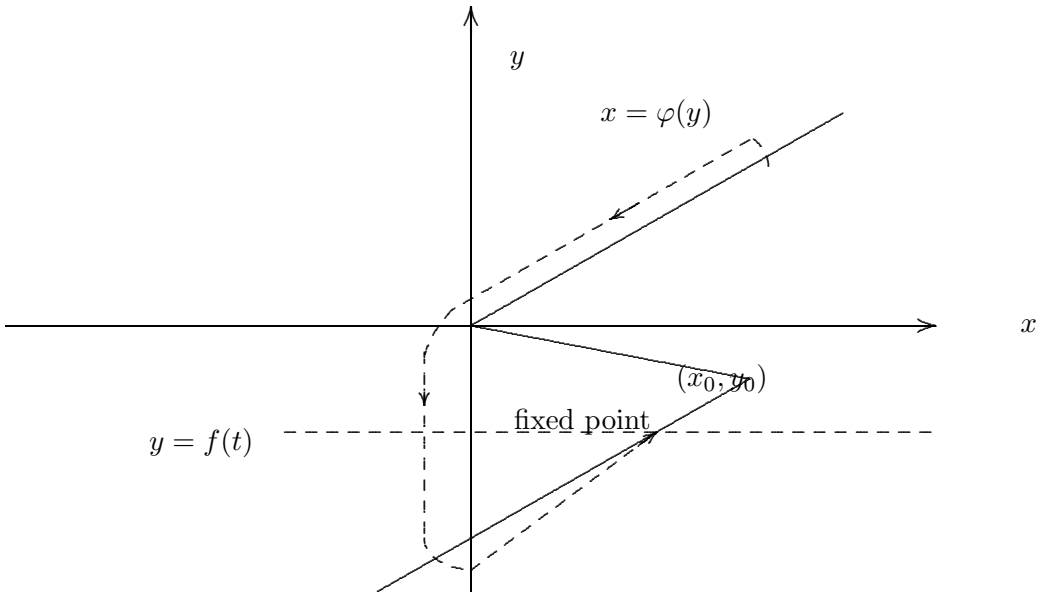

Figure 8: Phase portrait when $f(t) \leq y_0$

Now let $f(t)$ flow with time t. Suppose $f(t)$ starts from some point, say its maximum [1], and moves down. After some time, say t_+, $f(t)$ moves down to zero. During this time segment $f(t)$ is above $y = 0$. The solution of the system will be near the fixed point–the (moving) crossing point of the curves Γ and the horizontal line $y = f(t)$. After $t = t_+$, $f(t)$ moves down to the region $y_0 < y < 0$. If $f(t)$ stays long enought in the region then the solution will turn around the $P_2P_3P_4P_5$ cycle a few times. For each cycle the output voltage solution x moves from near zero to near y_0 and then turns back to near zero– producing a spike signal in $x - y$ plane. The number of cycles the solution travels (or of spikes the output voltage produces) will depend on how long $f(t)$ stays in the region and how long the solution needs to travel one cycle. We will consider this in details in the next sections.

If the minimum of $f(t)$ is larger than y_0 then after some time, say t_-, $f(t)$ will move up to positive side and the cycling behavior will stop until it turns back to below zero again. A typical such signal pattern is shown in figure 9

The computation is done by a variable order stiff solver which works pretty well for the system (4). Note that in this figure $f(t) = \frac{dv_s}{dt}$ and v_s is a sinusoidal input. From the figure

[1]The maximum should be positive since $f(t)$ is oscillatory around $y = 0$.

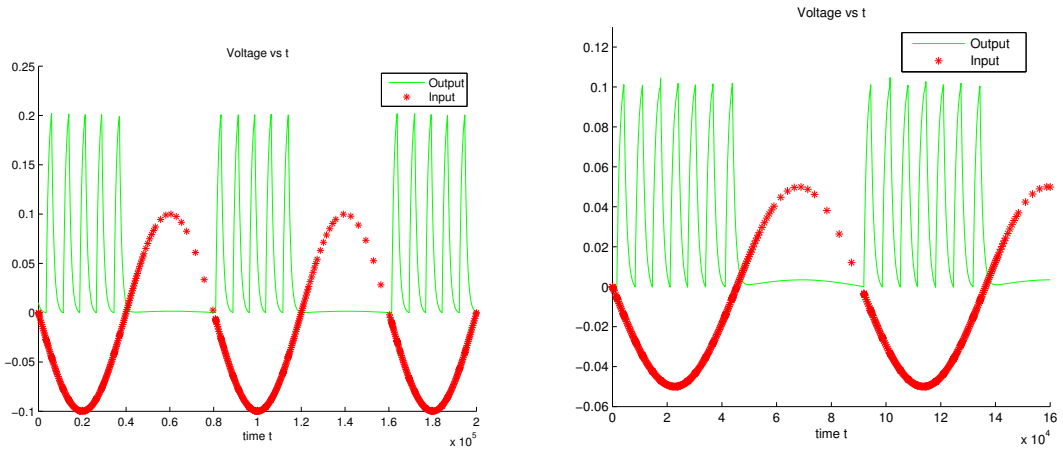

Figure 9: Input and output voltage when the minimum of $f(t)$ does not drop below y_0

9 we clearly see that the negative part of $f(t)$ corresponds to the oscillations (spikes) in the output x. If the minimum of $f(t)$ is smaller than y_0 then after $f(t)$ drops below y_0 the cycling behavior will also stop until it reaches the minimum and turns back to y_0. A typical signal pattern in this case is shown in figure 10.

From figure 10 we again see the negative part of $f(t) = \frac{dv_s}{dt}$ corresponds to the spike solution in the output x. But when $f(t)$ drops below y_0 the spikes stops so we see a flat part of x in the middle of spikes.

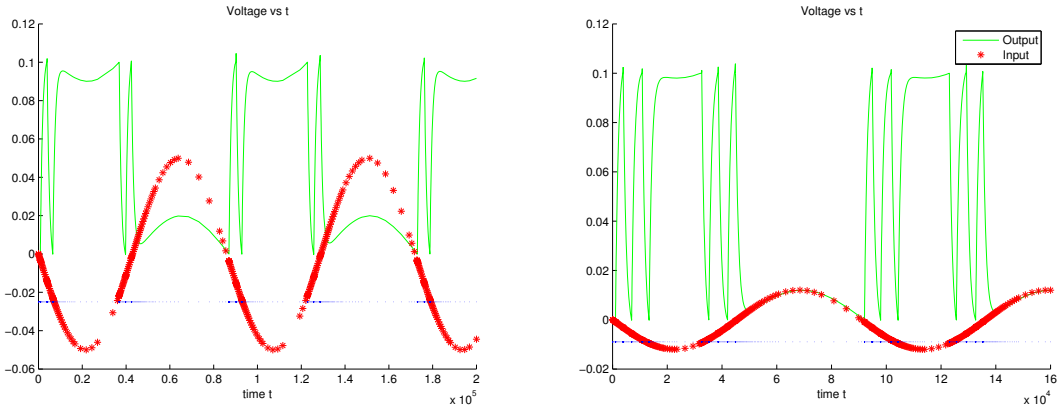

Figure 10: Input and output voltage when the minimum of $f(t)$ drops below y_0

2.4 Asymptotic expansion of the one-cycle time of the solution

The spike solution we see in figure 9-10 corresponds to output signals in electronic communications. Different number of spikes corresponds to different signals. What factors does the number of spikes depend on in the electronic circuits we propose? How do we calculate the number of spikes? These are theoretical questions we need to answer in design and analysis of electronic devices and communication systems. In this section we construct the asymptotic expansion of the periodic (cycling) solution (i.e. the $P_2P_3P_4P_5$ cycle in figure 6) of systems (4) and then provide a formula to compute the one-cycle time [2], denoted as t_0, of the solution. We then in next section use this formula to calculate the number of spikes. The computation of the one-cycle t_0 involves a construction of asymptotic expansion of the cycling solution. Zeroth order approximation of t_0 with respect to the small parameter ϵ is not very difficult to construct. It is just the time traveling from P_5 to P_2 along the characteristic curve Γ plus the time traveling from P_3 to P_4 along Γ (see figure 6) and can be calculated from the solution of the reduced system (9). In practice ϵ is not always very small. Higher order approximation of t_0 is generally needed.

Next we construct it for general oscillatory function $f(t)$. In this section we are only interested in the time segment where

$$f(t) \in (y_0, 0) \tag{11}$$

since we now consider the case that the system has cycling solution. More precise condition on the existence of the solution cycle will be summarized after the construction.

We divide the period solution cycle into four parts according to the piecewise expression of the function $\varphi(y)$ as illustrated in figure 11.

We will construct asymptotic solution of the differential equations and then the time it travels in each part.

[2] i.e. the time needed for the phase plane solution to run one $P_2P_3P_4P_5$ cycle.

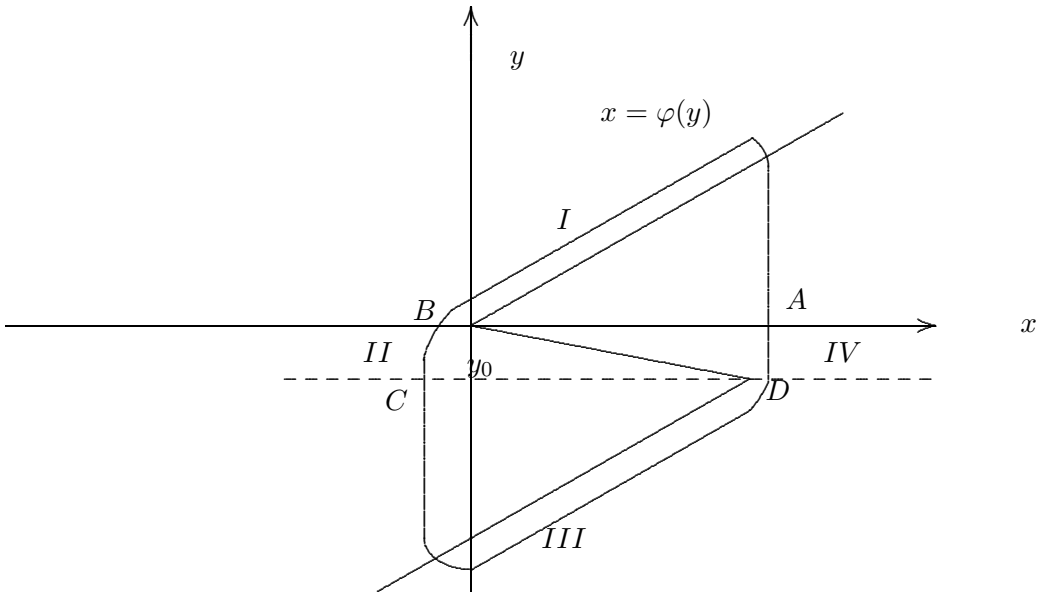

Figure 11: Phase portrait when $y_0 < f(t) < 0$

2.4.1 Matching Conditions

The construction of the asymptotic solution is based on the matched expansion combined with some specific techniques used in [31],[41]. Motivated from a simpler example in [41] (where the solution is symmetric about the horizontal axis and the exact solution can be explicitly obtained) we should include $\epsilon ln(\epsilon)$ in the expansions. Without loss of generality we will start at time $t = 0$. This can always be achieved by a time translation. Actually, in each part of the construction we will start at time $t = 0$. Hence, the one-cycle time will be the sum of the time when the solution travels to the end of each part.

The matching conditions are a set of auxiliary conditions that ensures the unique solvability of the inner expansions and the asymptotic matching of the outer and inner expansion.

Here we are considering the following two systems:

- Slow System

$$\begin{cases} \frac{dx}{dt} = f(t) - y, \\ \epsilon \frac{dy}{dt} = x - \varphi(y), \end{cases} \tag{12a}$$

- Fast System

$$\begin{cases} \frac{dx}{ds} = \epsilon(f(\epsilon s) - y), \\ \frac{dy}{ds} = x - \varphi(y). \end{cases} \tag{12b}$$

The time scale given by s is said to be fast, whereas that for t is slow. The two systems are equivalent as long as $\epsilon \neq 0$. Here we have that y is the fast variable and x is the slow variable.

For the Slow System we will center our attention on those points on the plane $x - y$ for which $x = \varphi(y)$. We study for both systems, asymptotic expansions in ϵ and $\epsilon \ln \epsilon$. For the fast system we consider the so called Inner Expansions and for the slow system we consider the so called Outer Expansions. Using the asymptotic expansions and equating like powers of ϵ and $\epsilon \ln \epsilon$ we get, corresponding to the fast system, a family of systems of differential equations and corresponding to the slow system, a family of algebraic-differential equations. We will used Van Dyke's matching principle (see [29], Section 4.1).

Van Dyke's matching rule is

$$(m \text{ term inner})(n \text{ term outer}) = (n \text{ term inner})(m \text{ term outer}) \tag{13}$$

where m and n may be taken to be any two integers which may be equal or unequal. i.e., in the outer variables expand to n terms. Then switch to inner variables and reexpand to m terms. The result is the same as first expanding in the inner to m terms, then switching to outer variables and reexpanding to n terms.

Warning: When using this matching rule you must treat log as $O(1)$.

2.4.2 The periodic solution cycle

In this subsection we will construct asymptotic solution of the differential equations and then the time it travels in each part. For it we are going to consider the four region according to the piecewise expression of the function $x = \varphi(y)$ as illustrated in figure 11.

Region I Where $\varphi(y) = \delta_1 y$.

Let the solution start at a point A near $(x_0, 0)$ (see figure 11), that is, initial conditions are

$$x(0) = x_A, \qquad y(0) = y_A = 0. \tag{14}$$

Let x_A take the following expansion:

$$x(0) = x_0 + \beta_0 \epsilon \ln \epsilon + \gamma_0 \epsilon + \cdots , \tag{15}$$

where β_0 and γ_0 are parameters to be determined later. Note that in this region both slow and fast modes are involved. We first construct the outer asymptotic expansion (slow mode solution) $x^0(t)$ and $y^0(t)$.

Suppose

$$\begin{cases} x^0(t) = x_0(t) + x_1(t)\epsilon \ln \epsilon + x_2(t)\epsilon + \cdots , \\ y^0(t) = y_0(t) + y_1(t)\epsilon \ln \epsilon + y_2(t)\epsilon + \cdots . \end{cases} \tag{16}$$

Substituting (16) into (4) and equating like powers of $\epsilon \ln \epsilon$ and ϵ we have

- For ϵ^0

$$\begin{cases} \frac{dx_0}{dt} = f(t) - y_0, \\ 0 = x_0 - \delta_1 y_0. \end{cases} \tag{17a}$$

- For $\epsilon \ln \epsilon$

$$\begin{cases} \frac{dx_1}{dt} = -y_1, \\ 0 = x_1 - \delta_1 y_1. \end{cases} \tag{17b}$$

- For ϵ

$$\begin{cases} \frac{dx_2}{dt} = -y_2, \\ \frac{dy_0}{dt} = x_2 - \delta_1 y_2. \end{cases} \tag{17c}$$

From (14) and (15), x_i, $i = 0, 1, 2$, should satisfy the following initial conditions

$$x_0(0) = x_0, \quad x_1(0) = \beta_0, \quad x_2(0) = \gamma_0. \tag{18}$$

Solving equations (17a)-(17c) with initial conditions (18), respectively, we obtain

$$\begin{cases} x_0(t) = x_0 e^{-\frac{t}{\delta_1}} + e^{-\frac{t}{\delta_1}} \int_0^t e^{\frac{\xi}{\delta_1}} f(\xi) d\xi, \\ y_0(t) = \frac{x_0}{\delta_1} e^{-\frac{t}{\delta_1}} + \frac{1}{\delta_1} e^{-\frac{t}{\delta_1}} \int_0^t e^{\frac{\xi}{\delta_1}} f(\xi) d\xi, \\ x_1(t) = \beta_0 e^{-\frac{t}{\delta_1}}, \\ y_1(t) = \frac{\beta_0}{\delta_1} e^{-\frac{t}{\delta_1}}, \\ x_2(t) = \gamma_0 e^{-\frac{t}{\delta_1}} + \frac{1}{\delta_1^3}(\delta_1 f(0) - x_0) t e^{-\frac{t}{\delta_1}} + \frac{1}{\delta_1^2} e^{-\frac{t}{\delta_1}} \int_0^t \int_0^\xi e^{\frac{\eta}{\delta_1}} f'(\eta) d\eta d\xi, \\ y_2(t) = (\frac{\gamma_0}{\delta_1} + \frac{x_0}{\delta_1^3}) e^{-\frac{t}{\delta_1}} + \frac{1}{\delta_1^4}(\delta_1 f(0) - x_0) t e^{-\frac{t}{\delta_1}} - \frac{1}{\delta_1^2} f(t) \\ \qquad + \frac{1}{\delta_1^3} e^{-\frac{t}{\delta_1}} \int_0^t \int_0^\xi e^{\frac{\eta}{\delta_1}} f'(\eta) d\eta d\xi + \frac{1}{\delta_1^3} e^{-\frac{t}{\delta_1}} \int_0^t e^{\frac{\xi}{\delta_1}} f(\xi) d\xi. \end{cases} \tag{19}$$

Hence,

$$\begin{cases} x^0(t) = x_0 e^{-\frac{t}{\delta_1}} + e^{-\frac{t}{\delta_1}} \int_0^t e^{\frac{\xi}{\delta_1}} f(\xi) d\xi + \beta_0 e^{-\frac{t}{\delta_1}} \epsilon \ln \epsilon \\ \qquad + \left[\gamma_0 e^{-\frac{t}{\delta_1}} + \frac{1}{\delta_1^3}(\delta_1 f(0) - x_0) t e^{-\frac{t}{\delta_1}} + \frac{1}{\delta_1^2} e^{-\frac{t}{\delta_1}} \int_0^t \int_0^\xi e^{\frac{\eta}{\delta_1}} f'(\eta) d\eta d\xi \right] \epsilon \\ \qquad + \dots, \\ y^0(t) = \frac{x_0}{\delta_1} e^{-\frac{t}{\delta_1}} + \frac{1}{\delta_1} e^{-\frac{t}{\delta_1}} \int_0^t e^{\frac{\xi}{\delta_1}} f(\xi) d\xi + \frac{\beta_0}{\delta_1} e^{-\frac{t}{\delta_1}} \epsilon \ln \epsilon \\ \qquad + \left[(\frac{\gamma_0}{\delta_1} + \frac{x_0}{\delta_1^3}) e^{-\frac{t}{\delta_1}} + \frac{1}{\delta_1^4}(\delta_1 f(0) - x_0) t e^{-\frac{t}{\delta_1}} - \frac{1}{\delta_1^2} f(t) \right. \\ \qquad \left. + \frac{1}{\delta_1^3} e^{-\frac{t}{\delta_1}} \int_0^t \int_0^\xi e^{\frac{\eta}{\delta_1}} f'(\eta) d\eta d\xi + \frac{1}{\delta_1^3} e^{-\frac{t}{\delta_1}} \int_0^t e^{\frac{\xi}{\delta_1}} f(\xi) d\xi \right] \epsilon + \dots. \end{cases} \tag{20}$$

We then construct the inner asymptotic expansion (fast mode solution). Making the stretched time transformation $s = \frac{t}{\epsilon}$ in the system (4), we have

$$\begin{cases} \frac{dx}{ds} = \epsilon(f(\epsilon s) - y), \\ \frac{dy}{ds} = x - \delta_1 y, \end{cases} \tag{21}$$

satisfying initial conditions (14) where $x(0)$ has expansion (15). Let $x^i(s)$ and $y^i(s)$ stand for inner expansion and assume

$$\begin{cases} x^i(s) = \bar{x}_0(s) + \bar{x}_1(s)\epsilon \ln \epsilon + \bar{x}_2(s)\epsilon + \dots, \\ y^i(s) = \bar{y}_0(s) + \bar{y}_1(s)\epsilon \ln \epsilon + \bar{y}_2(s)\epsilon + \dots. \end{cases} \tag{22}$$

Substituting (22) into (21) and equating like powers of ϵ and $\epsilon \ln \epsilon$, we have

- For ϵ^0

$$\begin{cases} \frac{d\bar{x}_0}{ds} = 0, \\ \frac{d\bar{y}_0}{ds} = \bar{x}_0 - \delta_1 \bar{y}_0. \end{cases} \tag{23a}$$

- For $\epsilon \ln \epsilon$

$$\begin{cases} \frac{d\bar{x}_1}{ds} = 0, \\ \frac{d\bar{y}_1}{ds} = \bar{x}_1 - \delta_1 \bar{y}_1. \end{cases} \tag{23b}$$

- For ϵ

$$\begin{cases} \frac{d\bar{x}_2}{ds} = f(0) - \bar{y}_0, \\ \frac{d\bar{y}_2}{ds} = \bar{x}_2 - \delta_1 \bar{y}_2. \end{cases} \tag{23c}$$

From (14) $\bar{y}_i$, $i = 0, 1, 2$, should satisfy the following initial conditions

$$\bar{y}_0(0) = \bar{y}_1(0) = \bar{y}_2(0) = 0. \tag{24}$$

Solving equations (23a)-(23c) with initial conditions (24), respectively, we obtain

$$\begin{cases} \bar{x}_0(s) = c_0, \\ \bar{y}_0(s) = -\frac{c_0}{\delta_1} e^{-\delta_1 s} + \frac{c_0}{\delta_1}, \\ \bar{x}_1(s) = c_1, \\ \bar{y}_1(s) = -\frac{c_1}{\delta_1} e^{-\delta_1 s} + \frac{c_1}{\delta_1}, \\ \bar{x}_2(s) = -\frac{c_0}{\delta_1^2} e^{-\delta_1 s} + (f(0) - \frac{c_0}{\delta_1}) s + c_2, \\ \bar{y}_2(s) = [\frac{1}{\delta_1^2}(f(0) - \frac{c_0}{\delta_1}) - \frac{c_2}{\delta_1}] e^{-\delta_1 s} - \frac{c_0}{\delta_1^2} s e^{-\delta_1 s} + \frac{1}{\delta_1^2}(f(0) - \frac{c_0}{\delta_1})(\delta_1 s - 1) + \frac{c_2}{\delta_1}. \end{cases} \tag{25}$$

Hence,

$$\begin{cases} x^i(t) = c_0 + c_1 \epsilon \ln \epsilon + [-\frac{c_0}{\delta_1^2} e^{-\delta_1 s} + (f(0) - \frac{c_0}{\delta_1}) s + c_2] \epsilon + \cdots, \\ y^i(t) = -\frac{c_0}{\delta_1} e^{-\delta_1 s} + \frac{c_0}{\delta_1} + [-\frac{c_1}{\delta_1} e^{-\delta_1 s} + \frac{c_1}{\delta_1}] \epsilon \ln \epsilon + [\frac{1}{\delta_1^2}(f(0) - \frac{c_0}{\delta_1}) - \frac{c_2}{\delta_1}] e^{-\delta_1 s} \\ \qquad\qquad -\frac{c_0}{\delta_1^2} s e^{-\delta_1 s} + \frac{1}{\delta_1^2}(f(0) - \frac{c_0}{\delta_1})(\delta_1 s - 1) + \frac{c_2}{\delta_1}] \epsilon + \cdots. \end{cases} \tag{26}$$

Here c_0, c_1, c_2 are constants which will be determined by matching with the outer solution. Using Van Dyke's matching principle (see [29] , Section 4.1) we have

$$c_0 = x_0, \quad c_1 = \beta_0, \quad \textit{and} \quad c_2 = \gamma_0 \tag{27}$$

and the composite asymtotic solution

$$\begin{cases} x^I(t) = x_0 e^{-\frac{t}{\delta_1}} + e^{-\frac{t}{\delta_1}} \int_0^t e^{\frac{\xi}{\delta_1}} f(\xi) d\xi + \beta_0 e^{-\frac{t}{\delta_1}} \epsilon \ln \epsilon + \Big[\gamma_0 e^{-\frac{t}{\delta_1}} \\ \qquad + \frac{1}{\delta_1^3}(\delta_1 f(0) - x_0) t e^{-\frac{t}{\delta_1}} - \frac{x_0}{\delta_1^2} e^{-\delta_1 \frac{t}{\epsilon}} + \frac{1}{\delta_1^2} e^{-\frac{t}{\delta_1}} \int_0^t \int_0^\xi e^{\frac{\eta}{\delta_1}} f'(\eta) d\eta d\xi \Big] \epsilon + \cdots, \\ y^I(t) = \frac{x_0}{\delta_1} e^{-\frac{t}{\delta_1}} - \frac{x_0}{\delta_1} e^{-\delta_1 \frac{t}{\epsilon}} + \frac{1}{\delta_1} e^{-\frac{t}{\delta_1}} \int_0^t e^{\frac{\xi}{\delta_1}} f(\xi) d\xi - \frac{x_0}{\delta_1^2} t e^{-\delta_1 \frac{t}{\epsilon}} \\ \qquad + [\frac{\beta_0}{\delta_1} e^{-\frac{t}{\delta_1}} - \frac{\beta_0}{\delta_1} e^{-\delta_1 \frac{t}{\epsilon}}] \epsilon \ln \epsilon + \{ (\frac{\beta_0}{\delta_1} + \frac{x_0}{\delta_1^3}) e^{-\frac{t}{\delta_1}} + \frac{1}{\delta_1^4}(\delta_1 f(0) - x_0) t e^{-\frac{t}{\delta_1}} \\ \qquad - \frac{1}{\delta_1^2} f(t) + \frac{1}{\delta_1^3} e^{-\frac{t}{\delta_1}} \int_0^t \int_0^\xi e^{\frac{\eta}{\delta_1}} f'(\eta) d\eta d\xi + \frac{1}{\delta_1^3} e^{-\frac{t}{\delta_1}} \int_0^t e^{\frac{\xi}{\delta_1}} f(\xi) d\xi \\ \qquad + [\frac{1}{\delta_1^2}(f(0) - \frac{x_0}{\delta_1}) - \frac{\gamma_0}{\delta_1}] e^{-\delta_1 \frac{t}{\epsilon}} \} \epsilon + \cdots. \end{cases} \tag{28}$$

Thus the time t_1 needed for the solution of (4) to travel from A to B is determined by

$$y^I(t) = 0. \tag{29}$$

Assume

$$t_1 = p_1 + q_1 \epsilon \ln \epsilon + r_1 \epsilon + \cdots. \tag{30}$$

Then by (28) and (29), p_1, q_1, and r_1 satisfy the following equations, respectively

$$\int_0^{p_1} e^{\frac{\xi}{\delta_1}} f(\xi) d\xi = -x_0, \tag{31}$$

$$q_1 = -\frac{\beta_0}{f(p_1)} e^{-\frac{p_1}{\delta_1}}, \tag{32}$$

$$r_1 = \frac{1}{\delta_1} - \frac{\delta_1}{f(p_1)} L_1(p_1) e^{-\frac{p_1}{\delta_1}}, \tag{33}$$

where

$$L_1(p_1) = \frac{\gamma_0}{\delta_1} + \frac{1}{\delta_1^4}(\delta_1 f(0) - x_0) p_1 + \frac{1}{\delta_1^3} \int_0^{p_1} \int_0^\xi e^{\frac{\eta}{\delta_1}} f'(\eta) d\eta d\xi. \tag{34}$$

We then have

$$x^I(t_1) = \alpha_1 + \beta_1 \epsilon \ln \epsilon + \gamma_1 \epsilon + \cdots, \tag{35}$$

where

$$\alpha_1 = \beta_1 = 0, \qquad \gamma_1 = \frac{f(p_1)}{\delta_1}. \tag{36}$$

Region II where $\varphi(y) = \delta_2 y$.

Only fast mode is involved in this region. As indicated earlier we will start at $t = 0$ again

in this region. Introducing the stretched time $s = \frac{t}{\epsilon}$ we have

$$\begin{cases} \frac{dx}{ds} = \epsilon(f(\epsilon s) - y), \\ \frac{dy}{ds} = x - \delta_2 y, \end{cases} \tag{37}$$

with initial conditions

$$\begin{cases} x(0) = \alpha_1 + \beta_1 \epsilon \ln \epsilon + \gamma_1 \epsilon + \cdots, \\ y(0) = 0. \end{cases} \tag{38}$$

Suppose

$$\begin{cases} x^{II}(s) = \bar{x}_0(s) + \bar{x}_1(s)\epsilon \ln \epsilon + \bar{x}_2(s)\epsilon + \cdots, \\ y^{II}(s) = \bar{y}_0(s) + \bar{y}_1(s)\epsilon \ln \epsilon + \bar{y}_2(s)\epsilon + \cdots. \end{cases} \tag{39}$$

Substituting (39) into (37) and equating like powers of ϵ and $\epsilon \ln \epsilon$, we have

- For ϵ^0

$$\begin{cases} \frac{d\bar{x}_0}{ds} = 0, \\ \frac{d\bar{y}_0}{ds} = \bar{x}_0 - \delta_2 \bar{y}_0. \end{cases} \tag{40a}$$

- For $\epsilon \ln(\epsilon)$

$$\begin{cases} \frac{d\bar{x}_1}{ds} = 0, \\ \frac{d\bar{y}_1}{ds} = \bar{x}_1 - \delta_2 \bar{y}_1. \end{cases} \tag{40b}$$

- For ϵ

$$\begin{cases} \frac{d\bar{x}_2}{ds} = f(0) - \bar{y}_0, \\ \frac{d\bar{y}_2}{ds} = \bar{x}_2 - \delta_2 \bar{y}_2. \end{cases} \tag{40c}$$

From (38), $\bar{x}_i$ and $\bar{y}_i$, $i = 0, 1, 2$, should satisfy the following initial conditions

$$\bar{x}_0(0) = \alpha_1, \quad \bar{x}_1(0) = \beta_1, \quad \bar{x}_2(0) = \gamma_1, \quad \bar{y}_0(0) = \bar{y}_1(0) = \bar{y}_2(0) = 0. \tag{41}$$

Noting $\alpha_1 = \beta_1 = 0$ and solving equations (40a)-(40c) with initial conditions (41), respectively, we obtain

$$\begin{cases} \bar{x}_0(s) \equiv 0, \\ \bar{y}_0(s) \equiv 0, \\ \bar{x}_1(s) \equiv 0, \\ \bar{y}_1(s) \equiv 0, \\ \bar{x}_2(s) = f(0)s + \gamma_1, \\ \bar{y}_2(s) = \frac{1}{\delta_2^2}(f(0) - \delta_2^2\gamma_1)e^{-\delta_2 s} + \frac{f(0)}{\delta_2^2}s + \frac{1}{\delta_2^2}(\delta_2^2\gamma_1 - f(0)). \end{cases} \tag{42}$$

Hence, changing the time variable back to t, yields

$$\begin{cases} x^{II}(t) = f(0)t + \gamma_1\epsilon + \dots, \\ y^{II}(t) = \frac{f(0)}{\delta_2}t + [\frac{1}{\delta_2^2}(f(0) - \delta_2\gamma_1)e^{-\delta_2\frac{t}{\epsilon}} + \frac{1}{\delta_2^2}(\delta_2\gamma_1 - f(0))]\epsilon + \cdots. \end{cases} \tag{43}$$

Solving

$$y^{II}(t) = i_0, \tag{44}$$

we obtain

$$t_2 = \frac{1}{\delta_2^2}\epsilon\ln\epsilon + \frac{1}{\delta_2^2}\epsilon\ln\left\{\frac{f(0) - \delta_2\gamma_1}{\delta_2 x_0}\right\} + \cdots, \tag{45}$$

which is the time needed for the solution to travel from B to C in figure 11. We can also compute

$$x^{II}(t_2) = \alpha_2 + \beta_2\epsilon\ln\epsilon + \gamma_2\epsilon + \cdots, \tag{46}$$

where

$$\alpha_2 = 0, \quad \beta_2 = \frac{f(0)}{\delta_2}, \quad \gamma_2 = \frac{f(0)}{\delta_2}\ln\left\{\frac{f(0) - \delta_2\gamma_1}{\delta_2 x_0}\right\} + \gamma_1. \tag{47}$$

Region III where $\varphi(y) = \delta_1 y + (\delta_2 - \delta_1)y_0$.

The construction is similar to that for Region I. Denoting $a = (\delta_1 - \delta_2)y_0$ we can obtain

the following composite expansion

$$\begin{cases} x^{III}(t) = ae^{-\frac{t}{\delta_1}} - a + e^{-\frac{t}{\delta_1}} \int_0^t e^{\frac{\xi}{\delta_1}} f(\xi)d\xi + \beta_2 e^{-\frac{t}{\delta_1}} \epsilon \ln \epsilon + [\frac{1}{\delta_1}(\frac{x_0}{\delta_2} - \frac{a}{\delta_1})e^{-\delta_1 \frac{t}{\epsilon}} \\ \qquad + \left[\gamma_2 e^{-\frac{t}{\delta_1}} + \frac{1}{\delta_1^3}(\delta_1 f(0) - a)te^{-\frac{t}{\delta_1}} + \frac{1}{\delta_1^2} e^{-\frac{t}{\delta_1}} \int_0^t \int_0^\xi e^{\frac{\eta}{\delta_1}} f'(\eta)d\eta d\xi\right] \epsilon + \cdots, \\ y^{III}(t) = \frac{a}{\delta_1} e^{-\frac{t}{\delta_1}} + \frac{1}{\delta_1} e^{-\frac{t}{\delta_1}} \int_0^t e^{\frac{\xi}{\delta_1}} f(\xi)d\xi + \left(\frac{x_0}{\delta_2} - \frac{a}{\delta_1}\right) e^{-\delta_1 \frac{t}{\epsilon}} + \frac{1}{\delta_1}\left(\frac{x_0}{\delta_2} - \frac{a}{\delta_1}\right) te^{-\delta_1 \frac{t}{\epsilon}} \\ \qquad + \left(\frac{\beta_2}{\delta_1} e^{-\frac{t}{\delta_1}} - \frac{\beta_2}{\delta_1} e^{-\delta_1 \frac{t}{\epsilon}}\right) \epsilon \ln \epsilon + \left\{\left(\frac{\gamma_2}{\delta_1} + \frac{a}{\delta_1^3}\right) e^{-\frac{t}{\delta_1}} + \frac{1}{\delta_1^4}(\delta_1 f(0) - a)\, te^{-\frac{t}{\delta_1}} \right. \\ \qquad -\frac{1}{\delta_1^2} f(t) + \frac{1}{\delta_1^3} e^{-\frac{t}{\delta_1}} \int_0^t \int_0^\xi e^{\frac{\eta}{\delta_1}} f'(\eta)d\eta d\xi + \frac{1}{\delta_1^3} e^{-\frac{t}{\delta_1}} \int_0^t e^{\frac{\xi}{\delta_1}} f(\xi)d\xi \\ \qquad \left. + \left[\frac{1}{\delta_1^2}(f(0) - \frac{a}{\delta_1}) - \frac{\gamma_2}{\delta_1}\right] e^{-\delta_1 \frac{t}{\epsilon}}\right\} \epsilon + \cdots. \end{cases} \tag{48}$$

The time for the solution to travel from C to D is obtained from

$$y^{III}(t_3) = y_0, \tag{49}$$

that is,

$$t_3 = p_3 + q_3 \epsilon \ln \epsilon + r_3 \epsilon + \cdots, \tag{50}$$

where p_3, q_3, r_3 are determine by the following equations

$$\int_0^{p_3} e^{\frac{\xi}{\delta_1}} f(\xi)d\xi = \frac{\delta_1}{\delta_2} x_0 e^{\frac{p_3}{\delta_1}} - a, \tag{51}$$

$$q_3 = -\frac{\delta_2 \beta_2}{x_0 - \delta_2 f(p_3)} e^{-\frac{p_3}{\delta_1}}, \tag{52}$$

$$r_3 = \frac{\delta_1}{\delta_2(\delta_2 f(p_3) - x_0)} f(p_3) - \frac{\delta_1 \delta_2}{\delta_2 f(p_3) - x_0} L_3(p_3) e^{-\frac{p_3}{\delta_1}}, \tag{53}$$

and in (53)

$$L_3(p_3) = \frac{\gamma_2}{\delta_1} + \frac{x_0}{\delta_1^2} e^{\frac{p_3}{\delta_1}} + \frac{1}{\delta_1^4}(\delta_1 f(0) - a)p_3 + \frac{1}{\delta_1^3} \int_0^{p_3} \int_0^\xi e^{\frac{\eta}{\delta_1}} f'(\eta)d\eta d\xi. \tag{54}$$

We can then obtain

$$x^{III}(t_3) = \alpha_3 + \beta_3 \epsilon \ln \epsilon + \gamma_3 \epsilon + \cdots, \tag{55}$$

where

$$\alpha_3 = x_0, \quad \beta_3 = 0, \quad \gamma_3 = \frac{\delta_1}{\delta_2^2} f(p_3) - \frac{x_0}{\delta_1 \delta_2}. \tag{56}$$

Region IV where $\varphi(y) = \delta_2 y$ again.

The construction is similar to that in Region II. The composite asymptotic expansion in this region is

$$\begin{cases} x^{IV}(t) = x_0 + (f(0) - \frac{x_0}{\delta_2})t + \gamma_3\epsilon + \dots, \\ y^{IV}(t) = \frac{x_0}{\delta_2} + \frac{1}{\delta_2}(f(0) - \frac{x_0}{\delta_2})t + \{\frac{1}{\delta_2^2}(f(0) - \frac{x_0}{\delta_2}) - \frac{\gamma_3}{\delta_2}\}e^{-\delta_2\frac{t}{\epsilon}} + \\ \qquad + \frac{\gamma_3}{\delta_2} - \frac{1}{\delta_2^2}(f(0) - \frac{x_0}{\delta_2})\}\epsilon + \cdots. \end{cases} \tag{57}$$

The time needed for the solution to travel from D to E is determined from

$$y^{IV}(t_4) = 0. \tag{58}$$

Assume

$$t_4 = \frac{1}{\delta_2}\epsilon\ln\epsilon + \frac{1}{\delta_2}\epsilon\ln\left\{\frac{\gamma_3}{x_0} - \frac{f(0)}{\delta_2 x_0} + \frac{1}{\delta_2^2}\right\} + \cdots. \tag{59}$$

We can calculate

$$x^{IV}(t_4) = x_0 + \frac{1}{\delta_2}(f(0) - \frac{x_0}{\delta_2})\epsilon\ln\epsilon + [\frac{1}{\delta_2}(f(0) - \frac{x_0}{\delta_2})\ln(\frac{\gamma_3}{x_0} - \frac{f(0)}{\delta_2 x_0} + \frac{1}{\delta_2^2}) + \gamma_3] + \cdots. \tag{60}$$

To obtain a cycling solution E must coincide with A. We thus have the following formula for calculating β_0 and γ_0:

$$\beta_0 = \frac{1}{\delta_2}(f(0) - \frac{x_0}{\delta_2}), \tag{61}$$

$$\gamma_0 = \frac{1}{\delta_2}(f(0) - \frac{x_0}{\delta_2})\ln(\frac{\gamma_3}{x_0} - \frac{f(0)}{\delta_2 x_0} + \frac{1}{\delta_2^2}) + \gamma_3. \tag{62}$$

Hence, the one–cycle time of the phase plane solution of the system (4), is

$$\begin{aligned} t_0 &= t_1 + t_2 + t_3 + t_4 \\ &= p_1 + p_3 + (q_1 + q_3 + \frac{2}{\delta_2})\epsilon\ln\epsilon + [r_1 + r_3 + \frac{1}{\delta_2}\ln\left\{\frac{\delta_1 f(0) - \delta_2 f(p_1)}{\delta_1\delta_2 x_0}\right\} \\ &+ \frac{1}{\delta_2}\ln\left\{\frac{\delta_1 f(p_3) - \delta_2 f(0)}{\delta_2^2 x_0} + \frac{\delta_1 - \delta_2}{\delta_1\delta_2^2}\right\}]\epsilon + \cdots, \end{aligned} \tag{63}$$

where p_1 and p_3 can be obtained by solving the nonlinear equations (31) and (51), respectively, and other parameters can be obtained directly from formulas (32), (33), (52), and (53). Also, for sufficiently small ϵ, in order to have a cycling solution and in order that the nonlinear equations (31) and (51) have a solution we need to assume that

$$p_1 + p_3 < t_-, \tag{64}$$

where t_- is the time segment for $f(t) \in (y_0, 0)$ in each "full oscillation" of $f(t)$. Here the full oscillation means that $f(t)$ completes a maximum-minimum-maximum cycle or any of its shift.

2.5 Formula for computing the number of spikes and numerical demonstrations

As we analyzed above when $f(t)$ locates and stays long enough in the region $(y_0, 0)$ (e.g. (64) is valid) the phase plane solution will produce cycles in certain time segments (where $f(t) \in (y_0, 0)$) or the output voltage will produce spikes. Generally, from the phase plane analysis the number of spikes produced in the output voltage can be determined by the following formula

$$\text{The number of spikes in one full oscillation of } f(t) = \left[\frac{t_-}{t_0}\right] + 1 \tag{65}$$

if $\quad \frac{t_-}{t_0} \in (\left[\frac{t_-}{t_0}\right], \left[\frac{t_-}{t_0}\right] + 1)$,

where [.] stands for chopping to integer, t_- is the time $f(t)$ spends in the region $(y_0, 0)$ in one full oscillation of $f(t)$ and t_0 is the time needed for the phase plane solution running one $P_2P_3P_4P_5$ cycle. Since $f(t)$ is given it is not difficult to obtain t_-. The formula for computing t_0 (i.e. (63)) has been found in the previous section after a construction of uniform asymptotic expansion of the cycling solution. From the formula we can see that the number of spikes depends mainly on the slopes of the characteristic curve Γ, y_0 (or x_0), and the function $f(t)$.

Next we are going to consider a coupled of special cases where the formula may be simpler. Then we run some numerical experiments to demonstrate the correctness of these formulas. In numerical simulation, taking numerical errors into account, it is better to choose parameters so that $\frac{t_-}{t_0}$ locates near the middle of the interval $(\left[\frac{t_-}{t_0}\right], \left[\frac{t_-}{t_0}\right] + 1)$ to ensure that the expected number of spikes is produced.

Case I. Periodic piecewise linear input

$$v_s(t) = \begin{cases} -kt + A, & t \in [0, t_-], \\ kt - 3A, & t \in [t_-, 2t_-], \end{cases} \tag{66}$$

that is,

$$f(t) = \begin{cases} -k, & t \in [0, t_-], \\ k, & t \in [t_-, 2t_-], \end{cases} \tag{67}$$

where $0 < k < -y_0$, $t_- = \frac{2A}{k}$, $A > 0$. Then the parameters in the formula (63) can be obtained explicitly:

$$\begin{aligned} p_1 &= \delta_1 \ln\{1 + \frac{x_0}{\delta_1 k}\}, \\ q_1 &= -\frac{\beta_0}{f(p_1)} e^{-\frac{p_1}{\delta_1}} = -\frac{\delta_1(x_0 + \delta_2 k)}{\delta_2^2(x_0 + \delta_1 k)}, \\ r_1 &= \frac{1}{\delta_1} - \frac{\delta_1}{f(p_1)} L_1(p_1) e^{-\frac{p_1}{\delta_1}} = \frac{1}{\delta_1} + \frac{\delta_1^2}{\delta_1 k + x_0} L_1(p_1), \end{aligned} \tag{68}$$

where

$$\begin{aligned} L_1(p_1) = &-\frac{x_0 + \delta_2 k}{\delta_1 \delta_2^2} \ln\left\{-\frac{\delta_1^2 k + \delta_2 x_0}{\delta_1 \delta_2^2 x_0} + \frac{x_0 + \delta_2 k}{x_0 \delta_2^2}\right\} - \frac{\delta_1^2 k + \delta_2 x_0}{\delta_1^2 \delta_2^2} \\ &- \frac{x_0 + \delta_1 k}{\delta_1^3} \ln\left\{1 + \frac{x_0}{\delta_1 k}\right\}. \end{aligned} \tag{69}$$

And

$$\begin{aligned} p_3 &= \delta_1 \ln\{1 - \frac{\delta_2 x_0}{\delta_1(\delta_2 k + x_0)}\}, \\ q_3 &= -\frac{\delta_2 \beta_2}{x_0 - \delta_2 f(p_3)} e^{-\frac{p_3}{\delta_1}} = -\frac{\delta_1 k}{\delta_1 \delta_2 k + (\delta_1 - \delta_2) x_0}, \\ r_3 &= \frac{\delta_1 k}{\delta_2(x_0 + \delta_2 k)} + \frac{\delta_1^2 \delta_2}{\delta_1 \delta_2 k + (\delta_1 - \delta_2) x_0} L_3(p_3), \end{aligned} \tag{70}$$

where

$$\begin{aligned} L_3(p_3) = &-\frac{k}{\delta_1^2} - \frac{k}{\delta_1 \delta_2} \ln\left\{-\frac{(\delta_1 + \delta_2)k}{\delta_1 \delta_2 x_0}\right\} + \frac{x_0(\delta_1 \delta_2 k + \delta_1 x_0 - \delta_2 x_0)}{\delta_1^2 \delta_2(\delta_1 \delta_2 k + \delta_1 x_0)} \\ &- \frac{\delta_1 k + a}{\delta_1^3} \ln\left\{1 - \frac{\delta_2 x_0}{\delta_1 \delta_2 k + \delta_1 x_0}\right\}. \end{aligned} \tag{71}$$

To demonstrate the above formulas we take the following data from a real electronic circuit which is modeled by (4)

$$\delta_1 = 1000, \quad \delta_2 = -10000, \quad \text{and} \quad y_0 = -0.00001. \tag{72}$$

In order to have cycling solution we take a pretty large $t_- = 50000$ so the condition (11) is satisfied. Let n be the number of spikes in each period of the input. Then from above formula we can roughly obtain a relationship between the amplitude k of $f(t)$ and the

number of spikes n.

The first formula work for values of $n \in \{1, 2, ..n^*\}$, and the second formula work for values of $n \in \{n^*, ..., 1\}$, where n^* is the maximum number of spikes that we can get on one time period. From the first formula we get the values of $k \in [0, k_1^*]$ and from the second formula we get the values of $k \in [k_2^*, \infty)$, where $k_1^* \leq k_2^*$ are the value of k for which we get maximum number of spikes.

$$k = \frac{1}{2}\left[1 - \sqrt{1 - \frac{440}{e^{\frac{50}{n}} - 1}}\right] \times 10^{-5}. \tag{73}$$

$$k = \frac{1}{2}\left[1 + \sqrt{1 - \frac{440}{e^{\frac{50}{n}} - 1}}\right] \times 10^{-5}. \tag{74}$$

The following table shows some data obtained by the above relationship.

Table 1: Periodic piecewise linear input

k	$6.3556e-11$	$4.101e-9$	$5.0194e-8$	$2.7186e-7$	$9.6296e-7$	$3.0703e-6$
n	3	4	5	6	7	8
k	$.99999e-5$	$.99959e-5$	$.99498e-5$	$.97281e-5$	$.9037e-5$	$.69297e-5$

Now we use a variable order stiff ODE solver in MATLAB to solve the system (4) with k given in the table 1. Figure 12 shows numerical solutions where the number of spikes exactly matches those given in the table.

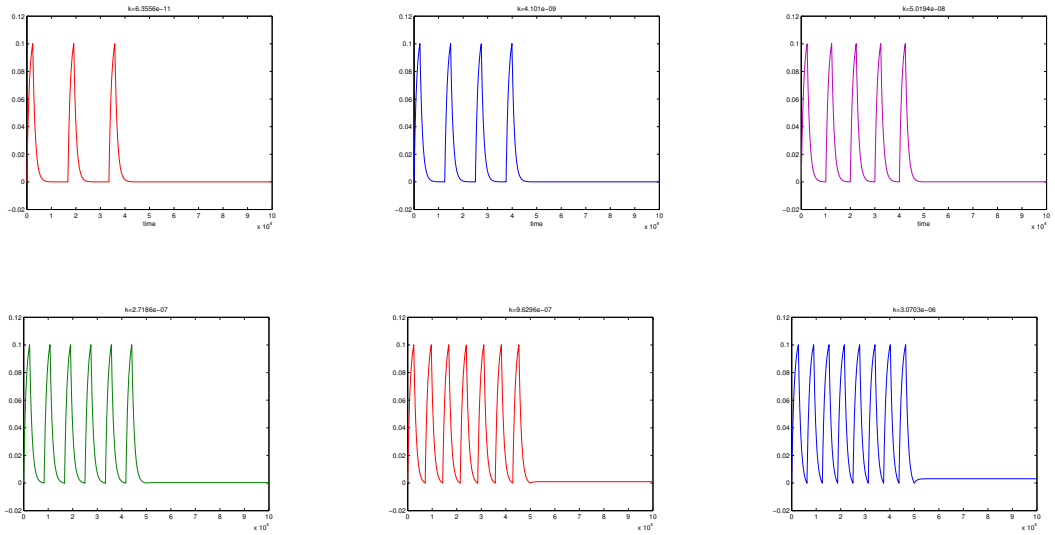

Figure 12: v vs t for various choices of k

Case II. Sinusoidal input

$$v_s = \frac{k}{\omega}\cos(\omega t) \quad \text{or} \quad f(t) = -k\sin(\omega t) \tag{75}$$

where $0 < k < -y_0$. Unlike case I, there is no explicit expression for the parameters in the cycle–time–computing formula (63). However, if we ignore the complicated $O(\epsilon)$ terms we can have a relatively simple expression for the one–cycle time:

$$t_0 = p_1 + p_3 + (q_1 + \frac{2}{\delta_2})\epsilon \ln \epsilon + O(\epsilon), \tag{76}$$

where p_1, p_3, and q_1 can be obtained from the following

$$\begin{cases} e^{\frac{p_1}{\delta_1}}(\sin(\omega p_1) - \delta_1\omega\cos(\omega p_1)) - \frac{1+\delta_1^2\omega^2}{k\delta_1}x_0 + \delta_1\omega = 0, \\ e^{\frac{p_3}{\delta_1}}(\sin(\omega p_3) - \delta_1\omega\cos(\omega p_3) + \frac{1+\delta_1^2\omega^2}{k\delta_2}x_0) - \frac{1+\delta_1^2\omega^2}{k\delta_2}(\delta_1 - \delta - 2)y_0 + \delta_1\omega = 0, \\ q - 1 = -\frac{y_0}{\delta_2 k\sin(\omega p_1)}e^{-\frac{p_1}{\delta_1}}. \end{cases} \tag{77}$$

We take the same data δ_1, δ_2, and y_0 as in case I from a real electronic circuit. In this case we are going to fix the amplitude of v_s, for example, $\frac{k}{\omega} = 0.05$ and making the frequency ω change. We can then obtain a set of data showing relationship between the frequency ω and the number of spikes n in the following table, where $f_{re} = \frac{\omega}{2\pi}$. We use the variable order stiff ODE solver again to solve the system (4) with ω given in table 2. Figure 13 shows numerical solutions where the number of spikes matches those given in the following table.

Table 2: Input function $f(t) = -k\sin(\omega t)$ or $v_s = \frac{k}{\omega}\cos(\omega t)$

$f_{re} = \frac{\omega}{2\pi}$	$3.2e-5$	$2.4e-5$	$1.7e-5$	$1.35e-5$	$1.1e-5$	$0.92e-5$
n	3	4	5	6	7	8

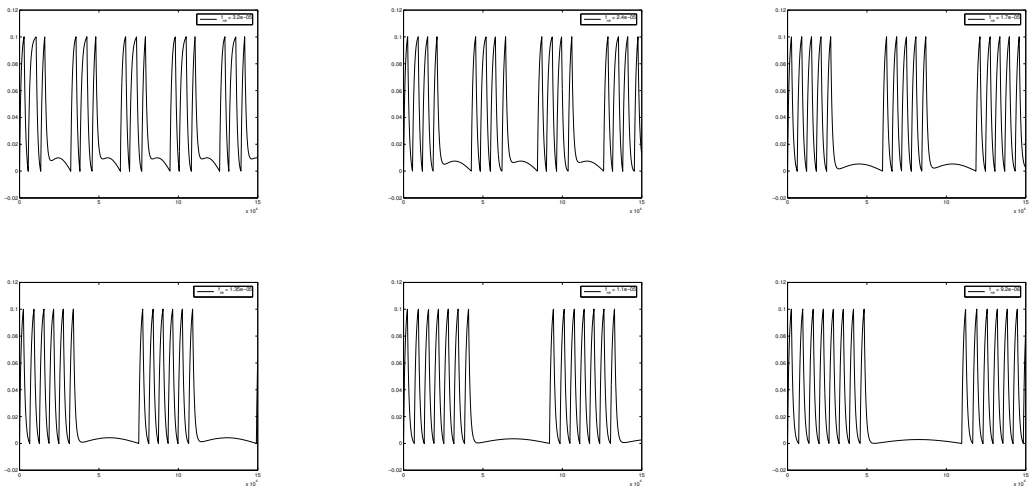

Figure 13: v vs t for various choices of ω.

2.6 Relaxation Oscillators and Networks

Relaxation oscillations comprime a large class of nonlinear dynamical systems, and arise naturally from many physical systems such as mechanics, biology, chemistry, and engineering. Such periodic phenomena are characterized by intervals of time during which little happens, interleaved with intervals of time during which considerable changes take place. In other words, relaxation oscillations exhibit more than one time scale. The dynamics of a relaxation oscillator is illustrated by the mechanical system of a seesaw in figure 14. At one side of the seesaw is there a water container which is empty at the beginning; in this situation the other side of the seesaw touches the ground. As the weight of water dripping from a tap into the container exceeds that of the other side, the seesaw flips and the container side touches the ground. At this moment, the container empties itself, and the seesaw returns quictly to its original position and the process repeats. Relaxation oscillations with a singular parameter lend themselves to analysis by singular perturbation theory [14]. Singular perturbation theory in turn yields a geometric approach to analyzing relaxation oscillation systems.

Relaxation oscillations were first observed by Van Der Pol [43] in 1926 when studying properties of a triode circuit. Such a circuit exhibits self–sustained oscillations. Van Der Pol

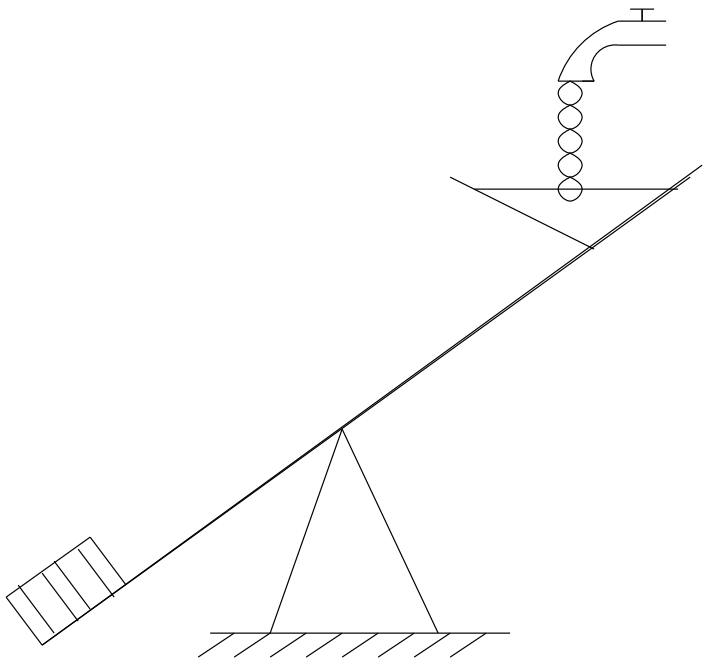

Figure 14: An example of a relaxation oscillator: a seesaw with a water container at one end (see [17])

discovered that for a certain range of the system parameters the oscillation is almost sinusoidal, but for a different range the oscillation exhibits abrupt changes.

2.6.1 Reduced systems in slow motions

From the previus section we know that the number of spikes depends on δ_1, δ_2, y^*, k, and ω. Since the parameters δ_1, δ_2, and y^* are internal parameters of the circuits we have decided to study what happen to the number of spikes when the parameters k and ω changed and δ_1, δ_2 and y^* are fixed.

Throughout this work we choose the external force $f(t)$ to be a piecewise continuous periodic function oscillatory around the t-axis with amplitude k and the natural frequency ω.

From Eq.(4) we have

$$\begin{cases} \frac{dx}{dt} = f(t) - y, \\ \epsilon \frac{dy}{dt} = x - \varphi(y), \end{cases} \tag{78}$$

where

$$\varphi(y) = \begin{cases} \delta_1 y, & if \quad y \geq 0, \\ \delta_2 y & if \qquad y^* < y < 0, \\ \delta_1 y + b, & if \quad y \leq y^*, \end{cases} \tag{79}$$

and

$$b = \frac{-y^*(\delta_1 - \delta_2)}{\delta_1}, \qquad x^* = \delta_2 y^*. \tag{80}$$

A vector field analysis indicates that the stable slow motions of Eqs.(78) consist of two sets

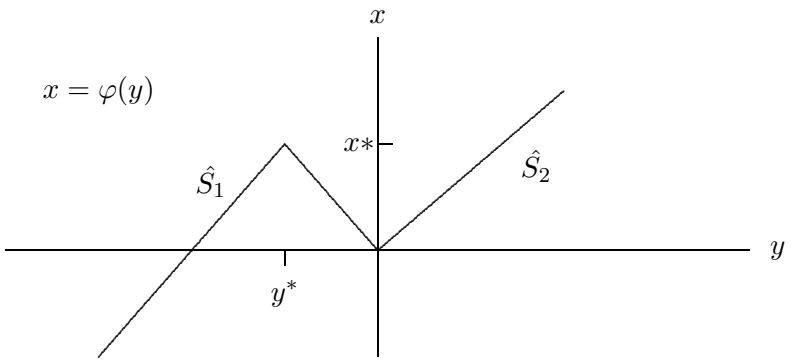

Figure 15: Manifold $x = \varphi(y)$

$\hat{S}_1$ and $\hat{S}_2$ (see figure 15) in $x - y$ plane with

$$\begin{aligned} \hat{S}_1 &= \{(x,y): \quad y = \beta x, \quad x \geq 0\}, \\ \hat{S}_2 &= \{(x,y): \quad y = \beta(x-b), \quad x \leq x^*\}, \end{aligned} \tag{81}$$

where $\beta = \frac{1}{\delta_1}$.

We can show that the attracting part of the slow motions are those points (x, y) with $0 \leq x \leq x^*$, namely,

$$\begin{aligned} S_1 &= \{(x,y): \quad y = \beta x, \quad 0 \leq x \leq x^*\}, \\ S_2 &= \{(x,y): \quad y = \beta(x-b), \quad 0 \leq x \leq x^*\}. \end{aligned} \tag{82}$$

The fundamental property of Eqs.(78) is the relaxation oscillation of its solutions. For sufficiently small $\epsilon > 0$, a solution starting at any point will converge quickly to a small neighborhood of one piece of stable slow motion and stays there for a relatively long time period. Because of an external force $f(t)$ the solution will eventually be pushed out of

this neighborhood and then quickly jumps to a small neighborhood of another piece of stable motion. When time varies the solutions repeat this pattern which can create many interesting dynamical phenomena, such as stable periodic solution, period doubling, chaos, etc.

However, the main purpose in this work is not to further explore those properties mentioned above but in a total different direction that has important application to practical problems, such as signal process, neuron networks, and wireless communication, etc.

Since the dynamics of the singularly perturbed system (78) has a close connection with the dynamics of this reduced system as $\epsilon \to 0$, it is natural way to study the reduced system on the slow motion.

From Eq.(78) we see that the reduced system on S_1 and S_2 are given respectively by the following differential equations:

$$\frac{dx}{dt} = f(t) - \beta x, \qquad 0 \le x \le x^*, \tag{83a}$$

$$\frac{dx}{dt} = f(t) + \beta(b - x), \qquad 0 \le x \le x^*. \tag{83b}$$

Let us describe the dynamics of the original singularly perturbed system (78). A solution of the reduced system (83a)-(83b) is describe as follows:

If a solution starts at S_1 with $x(0) = x_0$[3] $\in [0, x^*]$, then $x(t)$ is subject to Eq.(83a) before $x(t)$ reaches 0. If there is a first time $t_1 > 0$ such that $x(t_1) = 0$, then the solution is considered jumping to S_2 immediately and so that $x(t)$ is given by Eq.(83b) with the initial condition $x(t_1) = 0$. If there is again a first time $t_2 > t_1$ such that $x(t_2) = x^*$, then the solution returns to S_1 and hence $x(t)$ is governed by Eq.(83a) again with the initial condition $x(t_2) = x^*$. In such a way the solution is defined by Eqs.(83a)-(83b) alternatively. That is,

$$\begin{aligned} &\tfrac{dx}{dt} = f(t) - \beta x, \\ &t \in [0, t_1] \ \text{ with } \ x(0) = x_0 \in [0, x^*], \quad x(t_1) = 0, \\ &t \in [t_{2j}, t_{2j+1}] \ \text{ with } \quad x(t_{2j}) = x^*, \ \ x(t_{2j+1}) = 0, \ \ j \ge 1. \end{aligned} \tag{84}$$

[3] If $x(0) = 0$, then the solution $x(t)$ of (83a) is increasing for small $t > 0$ and then decreasing to 0 in a late time. This late time will be consider t_1 instead of $t_1 = 0$.

$$\begin{aligned}
&\tfrac{dx}{dt} = f(t) + \beta(b - x), \\
&t \in [t_{2j+1}, t_{2j+2}] \quad \text{with} \quad x(t_{2j+1}) = 0, \quad x(t_{2j+2}) = x^*, \quad j \geq 0,
\end{aligned} \tag{85}$$

for some sequence $0 < t_1 < t_2 < \ldots < t_n < \ldots$, where the time sequences $\{t_n = t_n(x_0, k, \omega, \beta)\}$ depends on the initial condition x_0, k, $\omega > 0$, and $\beta > 0$. Alternatively we can discuss solutions beginning in S_2 in the same way. Without loss of generality we can consider only solutions starting at S_1. We also have that $t_n(x_0, k, \omega, \beta)$ are continuously differentiable on x_0, k, ω and β.

We are interested in the case in with a solution starting from a point in S_1 returns to S_1 at time $T = \frac{2\pi}{\omega}$.

Let $x_0 \in [0, x^*]$, then the solution $x(t) = x(t, x_0, k, \omega, \beta)$ of the reduced Eqs.(83a)-(83b) has the explicit formulas

$$\begin{aligned}
x(t) &= e^{-\beta t}\left\{x_0 + \int_0^t e^{\beta\tau} f(\tau) d\tau\right\}, \qquad t \in [0, t_1], \\
x(t) &= e^{-\beta t}\int_{t_{2j-1}}^t e^{\beta\tau}\{f(\tau) + \beta b\} d\tau, \qquad t \in [t_{2j-1}, t_{2j}], \\
&= b(1 - e^{-\beta(t - t_{2j-1})}) + e^{-\beta t}\int_{t_{2j-1}}^t e^{\beta\tau} f(\tau) d\tau, \\
x(t) &= x^* e^{-\beta(t - t_{2j})} + e^{-\beta t}\int_{t_{2j}}^t e^{\beta\tau} f(\tau) d\tau\}, \qquad t \in [t_{2j}, t_{2j+1}].
\end{aligned} \tag{86}$$

From the above expressions and the boundary conditions we have

$$x_0 + \int_0^{t_1} e^{\beta\tau} f(\tau) d\tau = 0, \tag{87a}$$

$$x^* e^{\beta t_{2j}} = \int_{t_{2j-1}}^{t_{2j}} e^{\beta\tau}\{f(\tau) + \beta b\} d\tau, \tag{87b}$$

$$x^* e^{\beta t_{2j}} + \int_{t_{2j}}^{t_{2j+1}} e^{\beta\tau} f(\tau) d\tau = 0. \tag{87c}$$

From (87b)-(87c) we have

$$\int_{t_{2j-1}}^{t_{2j+1}} e^{\beta\tau} f(\tau) d\tau = b(e^{\beta t_{2j-1}} - e^{\beta t_{2j}}). \tag{88}$$

Without loss of generality we can assume that $f(t) \leq 0$ on $[0, \frac{T}{2})$, where $T = \frac{2\pi}{\omega}$.

Remark 2.6.1. Since $x_0 + \int_0^{t_1} e^{\beta\tau} f(\tau) d\tau = 0$, we must have $t_1(x_0, k, \omega, \beta) < \frac{\pi}{\omega}$. On the other hand if $t_1(x_0, k, \omega, \beta) > T$ then the solution takes longer than $T = \frac{2\pi}{\omega}$ time to return

to S_1. Hence only those values (x_0, k, ω, β) for which $t_1(x_0, k, \omega, \beta) \in (0, \frac{T}{2})$ will be of our interest.

Since the system (83a)-(83b) is T-periodic, the Poincaré or stroboscopic map (the period one map) $P : [0, x^*] \longrightarrow [0, x^*]$ is defined as:

$$P(x_0, k, \omega, \beta) = x(T, x_0, k, \omega, \beta) = \phi_T(x_0). \tag{89}$$

Let assume that the solution started at S_1 then after T time the solution maybe return to S_1 or maybe is in S_2. Therefore we must distinguish between these two possible cases for a time sequence $\{t_n = t_n(x_0, k, \omega, \beta)\}$.

Case 1: There is an integer $N \geq 1$ such that $T \in [t_{2N}, t_{N+1}]$.

Case 2: There is an integer $N \geq 1$ such that $T \in (t_{2N-1}, t_{2N})$.

Remark 2.6.2. A solution $x(t, x_0, k, \omega, \beta)$ returns to S_1 if and only if $T \in [t_{2N}, t_{2N+1}]$ for some $N \geq 1$. Case 1 implies that a solution complete exactly N cycles around S_1 and S_2 in one time period. In this case we have

$$P(x_0, k, \omega, \beta) = e^{-\beta T} \left(x^* e^{\beta t_{2N}(x_0, k, \omega, \beta)} + \int_{t_{2N}(x_0, k, \omega, \beta)}^{T} e^{\beta \tau} f(\tau) d\tau \right). \tag{90}$$

And case 2 implies that a solution starting at a point in S_1 arrives at S_2 at time T.

Let assume throughout this work that

$$k < \min \left\{ \frac{\delta_2 y^*}{\delta_1}, -2y^* \right\}. \tag{91}$$

From (80) we have that (91) is equivalent to the inequalities

$$x^* > \frac{k}{\beta}, \qquad b > \beta x^* + \frac{k}{2} \qquad \text{or} \quad b > \frac{3k}{2}. \tag{92}$$

Assumption (92) guarantees that a solution of Eqs.(83a)-(83b) is bounded by 0 and x^*.

Notation 2.6.1. We will denote by $P(x_0, k, \omega, \beta) \in [0, x^*]_{S_1}$, if a solution $x(t, x_0, k, \omega, \beta)$ starting at a point in S_1 return to S_1 in one time period ($T \in [t_{2N}, t_{2N+1}]$).

Lemma 2.6.1. *The sequence $\{t_n(x_0, k, \omega, \beta)\}$ has the following properties:*

P1. For each k, $\beta > 0$, and $\omega > 0$ and $0 \le x_1 < x_2 \le x^*$,

$$t_n(x_1, k, \omega, \beta) < t_n(x_2, k, \omega, \beta) < t_{n+2}(x_1, k, \omega, \beta), \qquad n = 1, 2, \ldots. \tag{93}$$

An immediately consequence of the above inequalities is that $P(x_0, k, \omega, \beta)$ is increasing with respect to x_0 whenever $P(x_0, k, \omega, \beta) \in (0, x^*)_{S_1}$.

P2. Let $0 \le x_1 < x_2 \le x^*$ and k, $\beta > 0$, and $\omega > 0$ be fixed. If $P([x_1, x_2], k, \omega, \beta) \subset [0, x^*]_{S_1}$, then there is an $N \ge 1$ such that

$$t_{2N}(x_0, k, \omega, \beta) \le T \le t_{2N+1}(x_0, k, \omega, \beta), \tag{94}$$

for all $x_0 \in [x_1, x_2]$. Hence all solutions $x(t, x_0, k, \omega, \beta)$ have the same number of spikes in T period.

Proof. Let us verify P_2. By the assumption there is an $N \ge 1$ such that

$$t_{2N}(x_1, k, \omega, \beta) \le T \le t_{2N+1}(x_1, k, \omega, \beta). \tag{95}$$

Let define

$$x_M = \sup\{x : x \in [x_1, x_2], \quad t_{2N}(x, k, \omega, \beta) \le T\}. \tag{96}$$

Claim: $x_M = x_2$.

Suppose that $x_M < x_2$. Then by the continuity of t_{2N} we deduce that $t_{2N}(x_M, k, \omega, \beta) = T$. Hence $t_{2N-1}(x_M, k, \omega, \beta) < t_{2N}(x_M, k, \omega, \beta) = T$. So again by the continuity there exists $\hat{x} \in (x_M, x_2]$ such that $t_{2N-1}(\hat{x}, k, \omega, \beta) < T$. However, $\hat{x} > x_M$ implies that (by $P1$)

$$T = t_{2N}(x_M, k, \omega, \beta) < t_{2N}(\hat{x}, k, \omega, \beta). \tag{97}$$

So that $P(\hat{x}, k, \omega, \beta) \notin [0, x^*]_{S_1}$, which leads to a contradiction. □

Notation 2.6.2. Let denote by $\#spikes(x, f, k, \omega)$ the number of spikes generated by a periodic function f with amplitude k and frequency ω on one time period T.

By the previous section we know that $f(t)$ generated spikes for those intervals on $[0, T]$ where $f(t) < 0$. Without loss of generality we can assume throught this section that $f(t) \le 0$ on $[0, \frac{T}{2})$, where $T = \frac{2\pi}{\omega}$.

Definition 2.6.1. *Let $f(t)$ be a piecewise continuous periodic function oscillatory around the t-axis with amplitude $k > 0$, and frequency $\omega > 0$. We define the function $T_j : [0, T] \times [0, \infty) \longrightarrow (0, \infty)$, $j = 1, 2$, such that*

$$T_j(t_a, \omega) > t_a, \qquad j = 1, 2, \tag{98a}$$

and

$$x^* e^{\frac{\beta}{\omega} t_a} + \frac{\beta}{\omega} \int_{t_a}^{T_1(t_a,\omega)} e^{\frac{\beta}{\omega}\tau} f(\tau) d\tau = 0, \tag{98b}$$

$$\frac{\beta}{\omega} \int_{t_a}^{T_2(t_a,\omega)} e^{\frac{\beta}{\omega}\tau} \{f(\tau) + \beta b\} d\tau = x^* e^{\frac{\beta}{\omega} T_2(t_a,\omega)}, \tag{98c}$$

where $T_1(t_a, \omega)$ is the first value satisfying (98b).

Lemma 2.6.2. *Let t_{a_1}, $t_{a_2} \in [0, T]$, and let T_j be define on (2.6.1). For $t_{a_1} < t_{a_2}$ and $\omega_1 < \omega_2$, then*

$$T_j(t_{a_1}, \omega_1) < T_j(t_{a_2}, \omega_2), \qquad j = 1, 2. \tag{99}$$

Proof. Let us proof that $T_1(t_{a_1}, \omega_1) < T_1(t_{a_2}, \omega_2)$.

If $T_1(t_{a_1}, \omega_1) \leq t_{a_2}$ then from the definition of T_1 we get $T_1(t_{a_1}, \omega_1) < T_1(t_{a_2}, \omega_2)$.

Now let us assume that $T_1(t_{a_1}, \omega_1) > t_{a_2}$. By (98b) we have

$$\frac{\omega}{\beta} x^* e^{\frac{\beta}{\omega} t_a} + \int_{t_a}^{T_1(t_a,\omega)} e^{\frac{\beta}{\omega}\tau} f(\tau) d\tau = 0. \tag{100}$$

Let x_j for $j = 1, 2$ be the solution of the equation

$$\dot{x} = f(t) - \frac{\beta}{\omega_j} x, \qquad t > t_{a_j}, \tag{101}$$

with initial conditions $x_j(t_{a_j}) = \frac{\omega_j}{\beta} x^*$.

Now from the definition of T_1 and the assumption $x^* > \frac{k}{\beta}$ we get

$$0 < x_j(t) < \frac{\omega_j}{\beta} x^*, \qquad t \in (t_{a_j}, T_1(t_{a_j}, \omega_j)), \qquad j = 1, 2, \tag{102}$$

and

$$x_2(T_1(t_{a_1}, \omega_1)) = x_1(T_1(t_{a_2}, \omega_2)) = 0. \tag{103}$$

Hence, (102) and $0 < \omega_1 < \omega_2$ imply

$$x_1(t_{a_2}) \leq \frac{\omega_1}{\beta} x^* < \frac{\omega_2}{\beta} x^* = x_2(t_{a_2}). \tag{104}$$

If $T_1(t_{a_1}, \omega_1) \geq T_1(t_{a_2}, \omega_2)$, then (102)-(104) yield that there is a time $t^* \in (t_{a_2}, T_1(t_{a_2}, \omega_2))$ such that

$$x_1(t^*) = x_2(t^*), \quad \text{and} \quad x_1(t) < x_2(t), \quad t \in (t_{a_2}, t^*]. \tag{105}$$

Hence

$$\begin{aligned} \dot{x}_2(t^*) &\leq \dot{x}_1(t^*) = f(t^*) - \tfrac{\beta}{\omega_1} x_1(t^*) \\ &= f(t^*) - \tfrac{\beta}{\omega_1} x_2(t^*) \\ &< f(t^*) - \tfrac{\beta}{\omega_2} x_2(t^*)\} = \dot{x}_2(t^*). \end{aligned} \tag{106}$$

This is a contradiction. Therefore $T_1(t_{a_1}, \omega_1) < T_1(t_{a_2}, \omega_2)$.

The second part of the proof $T_2(t_{a_1}, \omega_1) < T_2(t_{a_2}, \omega_2)$ is similarly to the case above. □

Before we proof our theorem that characterize how the number of spikes change with respect to ω let make the following change of variable

$$t = \frac{t}{\omega}, \quad x(t) = \frac{1}{\beta} x(\frac{t}{\omega}), \quad \text{and} \quad f(t) = f(\frac{t}{\omega}) \tag{107}$$

on (83a)-(83b). Hence we get

$$\frac{dx}{dt} = \frac{\beta}{\omega} \{f(t) - x(t)\}, \qquad 0 \leq x \leq x^*, \tag{108}$$

$$\frac{dx}{dt} = \frac{\beta}{\omega} \{f(t) + \beta b - x(t)\}, \qquad 0 \leq x \leq x^*. \tag{109}$$

Theorem 2.6.3. *Let k and ω be the amplitude and frequency of $f(t)$ respectively and let $x(t)$ be the solution of Eqs.(84)-(85). Then for $0 < \omega_1 < \omega_2$ we have $\#spikes(x, f, k, \omega_2) \leq \#spikes(x, f, k, \omega_1)$. See figure 16*

Proof. For each fixed $x_0 \in [0, x^*]$, $\omega > 0$, $\beta > 0$, let $\{t_j(\omega) = t_j(x_0, k, \omega, \beta)\}$ be the corresponding time sequence. Let us assume that $\#spikes(x, f, k, \omega_1) = n$. Then $t^1_{2n}(x_0, k, \omega_1, \beta) \leq T \leq t^1_{2n+1}(x_0, k, \omega_1, \beta)$ by $P2$ of lemma 2.6.1.

Since $\omega_1 < \omega_2$ it imply that $Period_2 < Period_1$. Then the intervals are different. To easy

the proof let us make the change on variable given on (107) to Eqs.(83a)-(83b). From here Eq.(86) became

$$\begin{aligned} x(t) &= e^{-\frac{\beta}{\omega}t}\left\{x_0 + \frac{\beta}{\omega}\int_0^t e^{\frac{\beta}{\omega}\tau} f(\tau)d\tau\right\}, \qquad t \in [0, \hat{t}_1], \\ x(t)e^{\frac{\beta}{\omega}t} &= \frac{\beta}{\omega}\int_{\hat{t}_{2j-1}}^t e^{\frac{\beta}{\omega}\tau}\left\{f(\tau) + \beta b\right\}d\tau, \qquad t \in [\hat{t}_{2j-1}, \hat{t}_{2j}], \\ x(t) &= x^* e^{-\frac{\beta}{\omega}(t-\hat{t}_{2j})} + \frac{\beta}{\omega}e^{-\frac{\beta}{\omega}t}\int_{\hat{t}_{2j}}^t e^{\beta\tau} f(\tau)d\tau, \qquad t \in [\hat{t}_{2j}, \hat{t}_{2j+1}]. \end{aligned} \tag{110}$$

From the above expressions and the boundary conditions we have

$$x_0 + \frac{\beta}{\omega}\int_0^{\hat{t}} e^{\frac{\beta}{\omega}\tau} f(\tau)d\tau = 0, \tag{111a}$$

$$x(t)e^{\frac{\beta}{\omega}\hat{t}_{2j}} = \frac{\beta}{\omega}\int_{\hat{t}_{2j-1}}^{\hat{t}_{2j}} e^{\frac{\beta}{\omega}\tau}\left\{f(\tau) + \beta b\right\}d\tau, \tag{111b}$$

$$x^* e^{-\frac{\beta}{\omega}\hat{t}_{2j}} + \frac{\beta}{\omega}\int_{\hat{t}_{2j}}^{\hat{t}_{2j+1}} e^{\beta\tau} f(\tau)d\tau = 0. \tag{111c}$$

Now we are going to proof 2.6.3 by induction.

For n=1.

Since $\omega_1 < \omega_2$ and $f(t) \leq 0$ for $t \in [0, \frac{T}{2})$ we have

$$f(k, \omega_1, t) = \frac{\beta}{\omega_1}f(t) < \frac{\beta}{\omega_2}f(t) = f(k, \omega_2, t) = f_1(t) \leq 0, \quad \text{for} \quad t \in [0, \frac{T}{2}). \tag{112}$$

From (134) we have

$$x_0 + \int_0^t e^{\beta\tau} f(k, \omega_1, \tau)d\tau < x_0 + \int_0^t e^{\beta\tau} f(k, \omega_2, \tau)d\tau \quad \text{for} \quad t \in [0, \frac{T}{2}), \tag{113}$$

and

$$\int_0^t e^{\beta\tau} f(k, \omega_1, \tau)d\tau, \qquad \int_0^t e^{\beta\tau} f(k, \omega_2, \tau)d\tau, \tag{114}$$

are decreasinng for $t \in [0, \frac{T}{2})$. Let $\hat{t}_1(\omega_i)$, $i = 1, 2$ the first time such that

$$x_0 + \int_0^{\hat{t}_1(\omega_i)} e^{\beta\tau} f(k, \omega_i, \tau)d\tau = 0, \qquad i = 1, 2. \tag{115}$$

Hence $\hat{t}_1(\omega_1) < \hat{t}_1(\omega_2)$.

By the definition of the functions T_i, $i = 1, 2$, we have

$$T_2(\hat{t}_{2j-1}(\omega_i), \omega_i) = \hat{t}_{2j}(\omega_i), \qquad j = 1, \ldots, \qquad i = 1, 2, \tag{116}$$

and

$$T_1(\hat{t}_{2j}(\omega_i), \omega_i) = \hat{t}_{2j+1}(\omega_i), \qquad j = 1, \ldots, \qquad i = 1, 2, \tag{117}$$

From lemma 2.6.2 and $\hat{t}_1(\omega_1) < \hat{t}_1(\omega_2)$ we have $\hat{t}_2(\omega_1) < \hat{t}_2(\omega_2)$.

Now we assume that $\hat{t}_{2n-1}(\omega_1) < \hat{t}_{2n-1}(\omega_2)$. Using again lemma 2.6.2 yields $\hat{t}_{2n}(\omega_1) < \hat{t}_{2n}(\omega_2)$. This imply that $\#spikes(x, f, k, \omega_1) = n \geq \#spikes(x, f, k, \omega_2)$. □

Proposition 2.6.4. *Let k and $\beta > 0$ be fixed. The time sequence $\{t_n(x_0, k, \omega, \beta)\}$ is strictly monotone decreasing with respect to $\omega > 0$ as long as $t_1(x_0, k, \omega, \beta) \in (0, \frac{T}{2})$.*

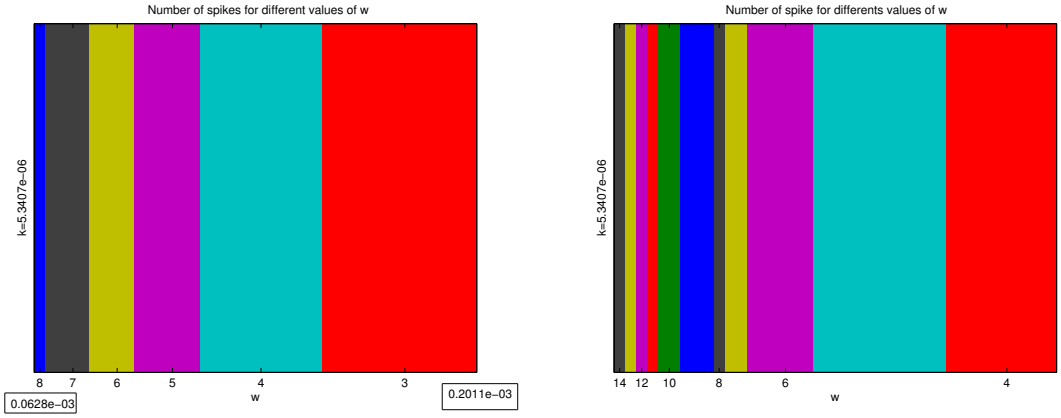

Figure 16: Number of spikes for differents values of ω

Theorem 2.6.5. *Let k and β be fixed. Then there is a sequence of intervals $\{I_N = (\omega_N^*, \omega_N)\}_{N=1}^{\infty}$ with*

$$\omega_1 > \omega_1^* > \omega_2 > \omega_2^* > \ldots > \omega_N > \omega_N^* > \ldots > 0, \tag{118}$$

such that for each $\omega > 0$, $P([0, x^*], k, \omega, \beta) \subset (0, x^*)_{S_1}$ if and only if $\omega \in I_N$ for some $N \geq 1$. In addition, if $\omega \in I_N$, then for each $x_0 \in [0, x^*]$, the solution $x(t, x_0, k, \omega, \beta)$ has exactly N spikes.

Proof. For each fixed $\omega > 0$, by $P2$ of lemma 2.6.1,

$$P([0, x^*], k, \omega, \beta) \subset (0, x^*)_{S_1} \tag{119}$$

if and only if there is an $N \geq 1$ such that

$$t_{2N}(x_0, k, \omega, \beta) < T < t_{2N+1}(x_0, k, \omega, \beta), \quad x_0 \in [0, x^*]. \tag{120}$$

Since $t_n(x_0, k, \omega, \beta)$ is increasing as x_0 increases, (120) is equivalent to

$$t_{2N}(x^*, k, \omega, \beta) < T < t_{2N+1}(0, k, \omega, \beta) \tag{121}$$

(121) is equivalent to $\omega_N^* < \omega < \omega_N$, by proposition 2.6.4.

That is, if and only if $\omega \in (\omega_N^*, \omega_N)$ for some positive integer N. Moreover, $\omega \in I_N$ implies (120). Hence $x(t, x_0, k\omega, \beta)$ has exactly N spikes for all $x_0 \in [0, x^*]$. □

Definition 2.6.2. *Let $f(t)$ be a piecewise continuous periodic function oscillatory around the t-axis with amplitude $k > 0$, and frequency $\omega > 0$. We define the function $T_j : [0, T] \times [0, \infty) \longrightarrow (0, \infty)$, $j = 1, 2$, such that*

$$T_j(t_a, k) > t_a, \qquad j = 1, 2, \tag{122a}$$

and

$$x^* e^{\beta t_a} + \int_{t_a}^{T_1(t_a,k)} e^{\beta\tau} f(\tau) d\tau = 0, \tag{122b}$$

$$\int_{t_a}^{T_2(t_a,k)} e^{\beta\tau} \{f(\tau) + \beta b\} d\tau = x^* e^{\beta T_2(t_a,k)}, \tag{122c}$$

where $T_1(t_a, k)$ is the first value satisfying (122b).

Lemma 2.6.6. *Let t_{a_1}, $t_{a_2} \in [0, T]$, k_1, $k_2 \in (0, \infty)$ and let T_j be define on (2.6.2). Then There exist $k^* > 0$ such that for $t_{a_1} < t_{a_2}$*

(a) and $k_1 < k_2 < k^*$,

$$T_j(t_{a_1}, k_2) < T_j(t_{a_2}, k_1), \qquad j = 1, 2. \tag{123}$$

(b) and for $k_1 < k^* < k_2$

$$T_j(t_{a_1}, k_2) > T_j(t_{a_2}, k_1), \qquad j = 1, 2. \tag{124}$$

Proof. Proof for the case $j = 1$.

From the definition of T_1 we have

$$t_{a_1} < T_1(t_{a_1}, k_2) \qquad \text{and} \qquad t_{a_2} < T_1(t_{a_2}, k_1). \tag{125}$$

Therefore if $T_1(t_{a_1}, k_2) \leq t_{a_2}$ for $k_1 < k_2$ we get $T_1(t_{a_1}, k_2) < T_1(t_{a_2}, k_1)$.

Let us assume that $t_{a_2} < T_1(t_{a_1}, k_2)$. By (122b) we have

$$x^* e^{\beta t_a} + \int_{t_a}^{T_1(t_a,k)} e^{\beta\tau} f(\tau) d\tau = 0, \tag{126}$$

Since f is a periodic function with amplitude k we can write $f(t) = k\hat{f}(t)$ where $\hat{f}(t)$ has amplitude 1.

Now let x_j for $j = 1, 2$ be the solution of the equation

$$\dot{x}_j(t) = e^{\beta t} f_{3-j}(t) \qquad \text{for} \qquad t > t_{a_j} \tag{127}$$

with initial condition $x_j(t_{a_j}) = x^* e^{\beta t_{a_j}}$ and $f_{3-j}(t) = k_{3-j}\hat{f}(t)$.

Since $f_j(t) < 0$ for $t \in (t_{a_j}, T_1(t_{a_j}, k_{3-j}))$ we get

$$0 < x_j(t) < x^* e^{\beta t_{a_j}} \qquad t \in (t_{a_j}, T_1(t_{a_j}, k_{3-j})) \qquad j = 1, 2, \tag{128}$$

and

$$x_1(T_1(t_{a_1}, k_2)) = 0 = x_2(T_1(t_{a_2}, k_1)). \tag{129}$$

But $\beta > 0$ and $t_{a_1} < t_{a_2}$, then

$$x_1(t_{a_2}) < x^* e^{\beta t_{a_1}} < x^* e^{\beta t_{a_2}} = x_2(t_{a_2}). \tag{130}$$

For $t \in (t_{a_2}, \max_{j=1,2} T_1(t_{a_j}, k_{3-j}))$ we have

$$\begin{aligned} \dot{x}_2(t) &= e^{\beta t f_1(t)} = e^{\beta t} k_2 \hat{f}(t) \\ &= \tfrac{k_2}{k_1} e^{\beta t} k_1 \hat{f}(t) = \tfrac{k_2}{k_1} \dot{x}_1(t). \end{aligned} \tag{131}$$

Since x_1 and x_2 are decreasing and $0 < k_1 < k_2$ we obtain

$$\dot{x}_2(t) = \frac{k_2}{k_1} \dot{x}_1(t) < \dot{x}_1(t) \qquad t \in (t_{a_2}, \max_{j=1,2} T_1(t_{a_j}, k_{3-j})). \tag{132}$$

That means that x_2 decrease faster than x_1. Therefore, given $k_1 > 0$ there exist k^* such that

$$T_1(t_{a_1}, k^*) = T_1(t_{a_2}, k_1). \tag{133}$$

Then for all $k_2 \in (k_1, k^*)$ we have $T_1(t_{a_1}, k_2) < T_1(t_{a_2}, k_1)$ anf for all $k_2 \in (k^*, \infty)$ we have $T_1(t_{a_1}, k_2) > T_1(t_{a_2}, k_1)$. The proof for $j = 2$ is similar. □

Now wew are ready to proof the theorem that tell ask how the number of spikes change with respect to the parameter k.

Theorem 2.6.7. *Let k and ω be the amplitude and frequency of $f(t)$, respectively and $x(t)$ be the solution of Eqs.(84)-(85). Then for $\omega > 0$ fixed there is a k^* such that*

(a) For $0 < k_1 < k_2 < k^*$. We have

$\#spikes(x, f, k_1, \omega) \leq \#spikes(x, f, k_2, \omega)$. *See figure 17.*

(b) For $k^* \leq k_1 < k_2$. We have

$\#spikes(x, f, k_1, \omega) \geq \#spikes(x, f, k_2, \omega)$. *See figure 17.*

Proof. We are going to proof part (a) by induction.

For each fixed $x_0 \in [0, x^*]$, $\omega > 0$, $\beta > 0$, let $\{t_j(k) = t_j(x_0, k, \omega, \beta)\}$ be the corresponding time sequence. Let us assume that $\#spikes(x, f, k_1, \omega) = n$. Then $t^1_{2n}(x_0, k_1, \omega, \beta) \leq T \leq t^1_{2n+1}(x_0, k_1, \omega, \beta)$ by $P2$ of lemma 2.6.1.

For n=1.

Since $k_1 < k_2 < k^*$ and $f(t) \leq 0$ for $t \in [0, \frac{T}{2})$ we have

$$f_2(t) = f(k_2, \omega, t) < f(k_1, \omega, t) = f_1(t) \leq 0, \quad \text{for} \quad t \in [0, \frac{T}{2}). \tag{134}$$

From (134) we have

$$x_0 + \int_0^t e^{\beta\tau} f(k_2, \omega, \tau) d\tau < x_0 + \int_0^t e^{\beta\tau} f(k_1, \omega, \tau) d\tau \quad \text{for} \quad t \in [0, \frac{T}{2}). \tag{135}$$

and

$$\int_0^t e^{\beta\tau} f(k_2, \omega, \tau) d\tau, \qquad \int_0^t e^{\beta\tau} f(k_1, \omega, \tau) d\tau, \tag{136}$$

are decreasinng for $t \in [0, \frac{T}{2})$. Let $t_1(k_i)$, $i = 1, 2$ the first time such that

$$x_0 + \int_0^{t_1(k_i)} e^{\beta\tau} f(k_i, \omega, \tau) d\tau = 0, \qquad i = 1, 2. \tag{137}$$

Hence $t_1(k_2) < t_1(k_1)$.

By the definition of the functions T_i, $i = 1, 2$, we have

$$T_2(t_{2j-1}(k_i), k_i) = t_{2j}(k_i), \qquad j = 1, \ldots, \qquad i = 1, 2, \tag{138}$$

and

$$T_1(t_{2j}(k_i), k_i) = t_{2j+1}(k_i), \qquad j = 1, \ldots, \qquad i = 1, 2, \tag{139}$$

From lemma 2.6.6 and $t_1(k_2) < t_1(k_1)$ we have $t_2(k_2) < t_2(k_1)$.

Now we assume that $t_{2n-1}(k_2) < t_{2n-1}(k_1)$. Using again lemma 2.6.6 yields $t_{2n}(k_2) < t_{2n}(k_1)$. This imply that $\#spikes(x, f, k_1, \omega) = n \leq \#spikes(x, f, k_2, \omega)$.

proof of part (b) is similar to part (a). □

Lemma 2.6.8. *Let k and ω be the amplitude and frequency of $f(t)$, respectively. Then for $\omega > 0$ fixed there is a $k^* > 0$ such that $\#spikes(x, f, k^*, \omega) =$ maximun number of spikes for a fixed ω.*

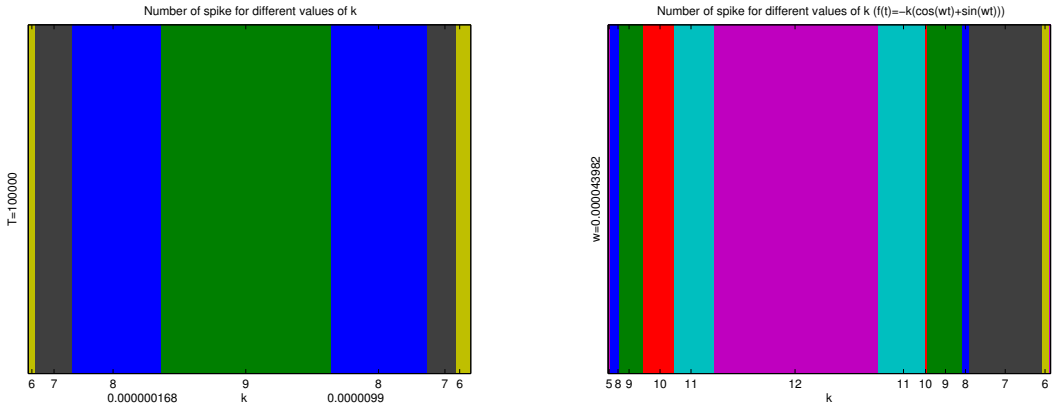

Figure 17: Number of spikes for differents values of k

Lemma 2.6.9. *For each fixed k and β*

$$\lim_{\omega \to 0} \#spikes(f, k, \omega, \beta, 0) = \lim_{\omega \to 0} \#spikes(f, k, \omega, \beta, x^*) = \infty, \tag{140a}$$

$$\lim_{\omega \to \infty} \#spikes(f, k, \omega, \beta, 0) = \lim_{\omega \to \infty} \#spikes(f, k, \omega, \beta, x^*) = 1, \tag{140b}$$

Proof. From Eq.(87a) and $f(t) < 0$ for $t \in (0, \frac{T}{2})$ we get that $t_1(x_0, k, \omega, \beta) < \frac{T}{2}$. Then conclusion of lemma 2.6.9 follows from the fact that decreasing of ω will fasten the oscillation of the solution $x(t, x_0, k, \omega, \beta)$ of Eqs.(83a)-(83b), while an increasing ω will reduce the oscillation of the solution. □

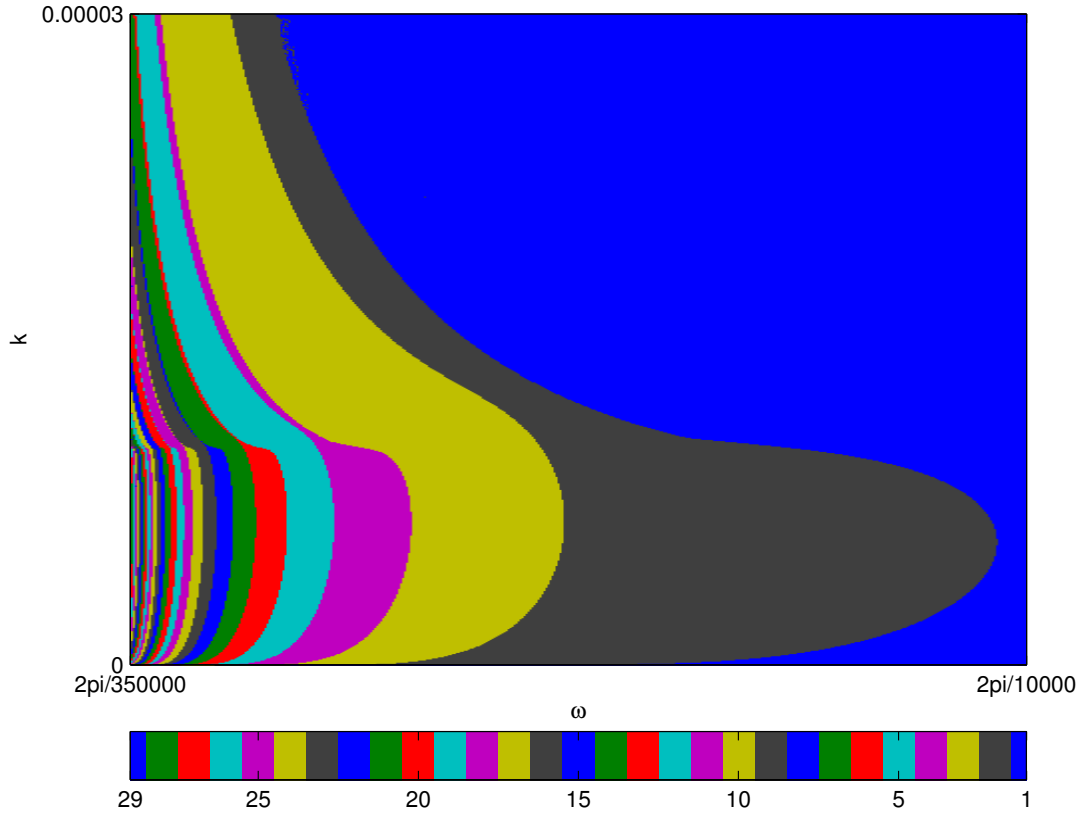

Figure 18: Number of spikes for differents values of k and ω

Figure 18 show the dynamics of how the number of spikes change when the parameters ω and k change. We can see that for k fixed when ω go to zero the number of spikes go to ∞ and for ω fixed there exists $k^* < \infty$ such that the $\#spikes(x, f, k^*, \omega, \beta) =$ maximun number of spikes.

CHAPTER III

COUPLED NONLINEAR CIRCUITS

3.1 Introduction

By interconnecting the circuit unit as shown in figure 19, we obtain a chain structure of generalized "Van Der Pol" type oscillators. The dynamics of this chain structure in the unidirectional case are described by (141) and for the bidirectional case are described by (166). Unidirectional coupling means that only the dynamics of the response subsystem is affected by the drive subsystem through the coupling; the reverse does not hold.

Many investigators have been studied two mutually coupled oscillators (mutual synchronization) because two oscillators' case is a prototype modeling to understand the phenomena in a large number of coupled oscillators. On the other hand forced synchronization is also studied in the filed of physiology [8], chemistry (forced Brusselator [30]) and electric engineering (forced van der Pol [23]). However we cannot find the study of connecting mutual synchronization and forced synchronization.

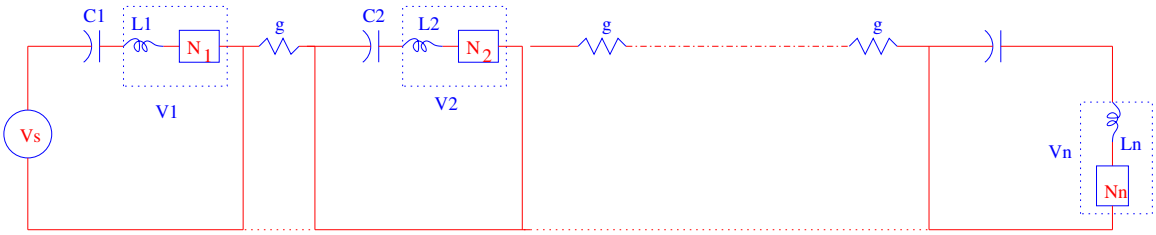

Figure 19: Circuit diagram of the considered chain interconnection of the circuits.

3.2 Unidirectional coupling

In the present section we formulate the problem for a system of two or more oscillators coupled diffusively. We consider a type of unilateral coupling (unidirectional coupling), where the second system is coupled with the first but the first is independent of the second.

- For $k = 1$

$$\begin{cases} \frac{dx_1}{dt} = f(t) - y_1, & (141aa) \\ \epsilon \frac{dy_1}{dt} = x_1 - \varphi(y_1), & (141ab) \end{cases} \tag{141a}$$

- For $k = 2, \ldots, n$

$$\begin{cases} \frac{dx_k}{dt} = -y_k - g(x_k - x_{k-1}), & (141ba) \\ \epsilon \frac{dy_k}{dt} = x_k - \varphi(y_k), & (141bb) \end{cases} \tag{141b}$$

where

$$\varphi(y_n) = \begin{cases} \delta_1 y_k, & if \quad y_k \geq 0, \\ \delta_2 y_k, & if \quad y_0 \leq y_k < 0, \\ \delta_1 y_k + (\delta_2 - \delta_1) y_0, & if \quad y_k < y_0. \end{cases} \tag{142}$$

Let consider the case $n = 2$.

$$\begin{cases} \frac{dx_1}{dt} = f(t) - y_1, \\ \epsilon \frac{dy_1}{dt} = x_1 - \varphi(y_1), \\ \frac{dx_2}{dt} = -y_2 - g(x_2 - x_1), \\ \epsilon \frac{dy_2}{dt} = x_2 - \varphi(y_2), \end{cases} \tag{143}$$

where $0 < \epsilon << 1$ and $g > 0$. Functions x_i and y_i for $i = 1, 2$ in these equations represent voltage and current variables respective, $f(t)$ is a forced period function with amplitude k and frequency ω and $\varphi(y)$ is a piecewise smooth function given on (142).

Let us reduced the number of parameters by introducing the following translation and time scaling

$$\begin{cases} x_1(t) = \frac{1}{\delta_1 k} x_1(\frac{t}{\omega}), \qquad y_1(t) = \frac{1}{k} y_1(\frac{t}{\omega}), \\ x_2(t) = \frac{1}{\delta_1 k} x_2(\frac{t}{\omega}), \qquad y_2(t) = \frac{1}{k} y_2(\frac{t}{\omega}), \\ f_1(t) = \frac{1}{k} f(\frac{t}{\omega}). \end{cases} \tag{144}$$

Then Eq.(143) is therefore transformed to the dimensionless form

$$\begin{cases} \frac{dx_1}{dt} = \alpha(f_1(t) - y_1), \\ \xi\frac{dy_1}{dt} = x_1 - \varphi(y_1), \\ \frac{dx_2}{dt} = -\alpha y_2 - g_1(x_2 - x_1), \\ \xi\frac{dy_2}{dt} = x_2 - \varphi(y_2), \end{cases} \tag{145}$$

where

$$\varphi(y) = \begin{cases} y, & if \quad y \geq 0, \\ \delta y, & if \quad y^* < y < 0, \\ y + b, & if \quad y \leq y^*, \end{cases} \tag{146}$$

and

$$\begin{cases} \alpha = \frac{1}{\omega\delta 1}, \quad \xi = \frac{\epsilon\omega}{\delta_1}, \quad y^* = \frac{y_0}{k}, \quad \delta = \frac{\delta_2}{\delta_1}, \\ x^* = \delta y^* \quad b = \frac{y_0(\delta_2 - \delta_1)}{k\delta_1} = (\delta - 1)y^*, \quad g_1 = \frac{g}{\omega}. \end{cases} \tag{147}$$

Before embarking upon an analysis of phase space trajectories of the coupled system of (145), we briefly recall some facts and terminology from the theory developed for a single relaxation oscillator.

In Eqs.(143) we consider the case $\epsilon \to 0$. In this case y_1 and y_2 moves far faster than x_1

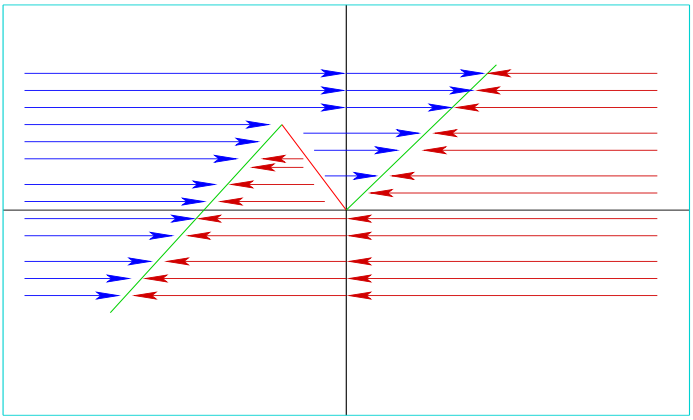

Figure 20: Phase portrait for a relaxation oscillator with piecewise linear function $x = \varphi(y)$. The y nullcline is the graph $\varphi(y)$, and the x nullcline is the x axis. Arrows indicate phase flows.

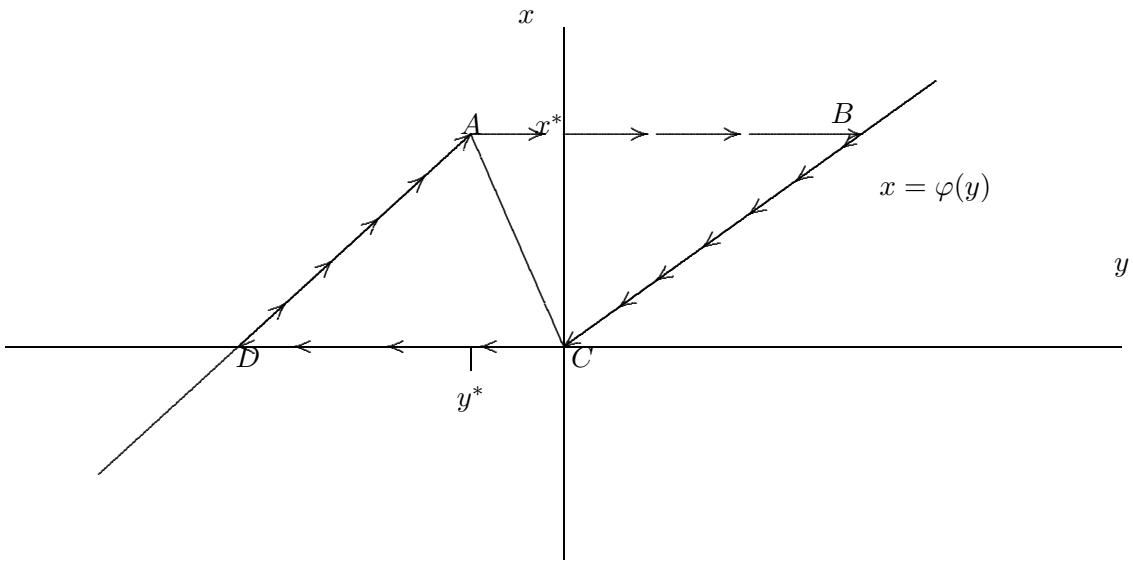

Figure 21: Limit cycle orbit. The limit cycle is labeled as $DABC$, and the arrow heads indicate the direction of motion. Within the limit cycle, AB and CD two fast pieces (indicated by 4 arrowheads) and DA and BC are slow pieces.

and x_2 in the phase space, except for solutions in a neighborhood of the manifold

$$M \equiv \{(x_1, y_1, x_2, y_2) |\ \ x_1 = \varphi(y_1), \quad x_2 = \varphi(y_2)\}\,, \tag{148}$$

and almost all solutions rapidly approach to the stable part of M, where "stable part" is the union of the following half planes:

$$\begin{aligned}
\hat{P}_1 &\equiv \{(x_1, y_1, x_2, y_2) |\ \ x_1 \geq 0, \quad x_2 \geq 0, \quad y_1 = x_1, \quad y_2 = x_2\}\,, \\
\hat{P}_2 &\equiv \{(x_1, y_1, x_2, y_2) |\ \ x_1 \geq 0, \quad x_2 \leq x^*, \quad y_1 = x_1, \quad y_2 = x_2 - b\}\,, \\
\hat{P}_3 &\equiv \{(x_1, y_1, x_2, y_2) |\ \ x_1 \leq x^*, \quad x_2 \geq 0, \quad y_1 = x_1 - b, \quad y_2 = x_2\}\,, \\
\hat{P}_4 &\equiv \{(x_1, y_1, x_2, y_2) |\ \ x_1 \leq x^*, \quad x_2 \leq x^*, \quad y_1 = x_1 - b, \quad y_2 = x_2 - b\}\,.
\end{aligned} \tag{149}$$

That is, almost all stationary solutions are constrained on $\hat{P}_1, \hat{P}_2, \hat{P}_3$, or $\hat{P}_4$. And transitions between each halfplane are done by almost infinitesimal time jumps at each edge, holding x_1 =const and x_2 =const. For example, if a trajectory on $\hat{P}_1$ moves down and if it hits the bottom edge $x_2 = 0$; then it jumps onto $\hat{P}_2$, as show in figure 22. Letting "$\hat{P}_1 \overset{x_2=0}{\longrightarrow} \hat{P}_2$" denotes this transition and so on, all transitions are summarized as above.

We can show that the attracting part of the slow motions are those points (x_1, y_1, x_2, y_2)

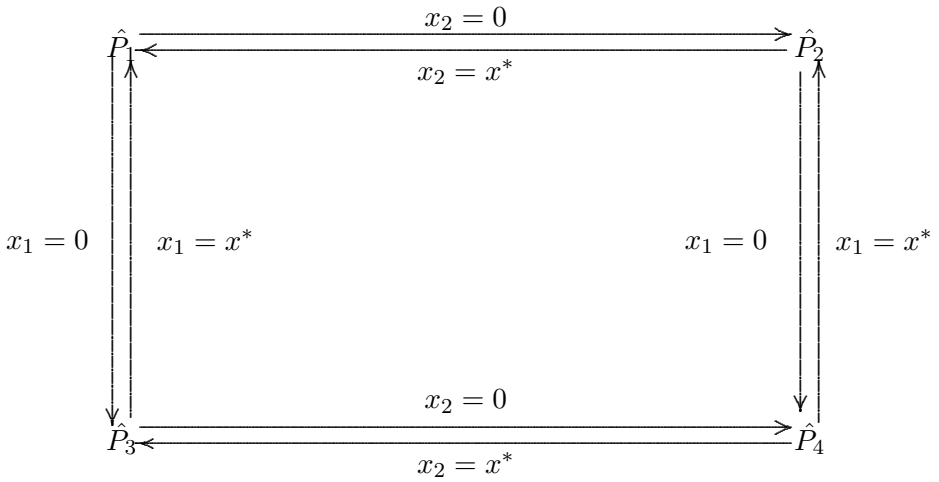

Figure 22: Transition between $\hat{P}_1$, $\hat{P}_2$, $\hat{P}_3$, and $\hat{P}_4$

with $0 \leq x_1 \leq x^*$ and $0 \leq x_2 \leq x^*$, namely,

$$\begin{aligned}
P_1 &= \{(x_1, y_1, x_2, y_2) : \quad y_1 = x_1, \quad y_2 = x_2, \quad 0 \leq x_1 \leq x^* \;\; 0 \leq x_2 \leq x^*\}, \\
P_2 &= \{(x_1, y_1, x_2, y_2) : \quad y_1 = x_1, \quad y_2 = x_2 - b, \quad 0 \leq x_1 \leq x^* \;\; 0 \leq x_1 \leq x^*\}, \\
P_3 &= \{(x_1, y_1, x_2, y_2) : \quad y_1 = x_1 - b, \quad y_2 = x_2, \quad 0 \leq x_1 \leq x^* \;\; 0 \leq x_2 \leq x^*\}, \\
P_4 &= \{(x_1, y_1, x_2, y_2) : \quad y_1 = x_1 - b, \quad y_2 = x_2 - b, \quad 0 \leq x_1 \leq x^* \;\; 0 \leq x_1 \leq x^*\}.
\end{aligned} \tag{150}$$

To be specific, throughout this work we choose the external force to be commonly used sine function $f(t) = ksin(\omega t)$ with k the amplitude and ω the natural frequency. With the above choice of f Eqs.(145)become

$$\begin{cases}
\frac{dx_1}{dt} = \alpha(sin(t) - y_1), \\
\xi \frac{dy_1}{dt} = x_1 - \varphi(y_1), \\
\frac{dx_2}{dt} = -\alpha y_2 - g_1(x_2 - x_1), \\
\xi \frac{dy_2}{dt} = x_2 - \varphi(y_2).
\end{cases} \tag{151}$$

Since the dynamics of the singularly perturbed systems (151) has a close connection with the dynamics of its reduced system as $\xi \to 0$, it is natural way to begin our study on reduced

system on the slow motion. Let write (151) as

$$\begin{cases} \frac{dx_1}{dt} = \alpha(sin(t) - y_1), \\ \frac{dy_1}{dt} = \rho(x_1 - \varphi(y_1)), \\ \frac{dx_2}{dt} = -\alpha y_2 - g_1(x_2 - x_1), \\ \frac{dy_2}{dt} = \rho(x_2 - \varphi(y_2)), \end{cases} \tag{152}$$

where $\rho = \frac{1}{\xi}$ and

$$\varphi(y) = \begin{cases} y, & if \quad y \geq 0, \\ \delta y, & if \quad y^* < y < 0, \\ y + b, & if \quad y \leq y^*. \end{cases} \tag{153}$$

From Eq(152) we see that the reduced system on P_1, P_2, P_3, and P_4 are given respectively by the following differential equations:

$$\begin{cases} \frac{dx_1}{dt} = \alpha(\sin(t) - x_1), & 0 \leq x_1 \leq x^*, \\ \frac{dx_2}{dt} = -\alpha x_2 - g_1(x_2 - x_1), & 0 \leq x_1 \leq x^*, \quad 0 \leq x_2 \leq x^*, \end{cases} \tag{154a}$$

$$\begin{cases} \frac{dx_1}{dt} = \alpha(\sin(t) - x_1), & 0 \leq x_1 \leq x^*, \\ \frac{dx_2}{dt} = \alpha(b - x_2) - g_1(x_2 - x_1), & 0 \leq x_1 \leq x^*, \quad 0 \leq x_2 \leq x^*, \end{cases} \tag{154b}$$

$$\begin{cases} \frac{dx_1}{dt} = \alpha(\sin(t) + b - x_1), & 0 \leq x_1 \leq x^*, \\ \frac{dx_2}{dt} = -\alpha x_2 - g_1(x_2 - x_1), & 0 \leq x_1 \leq x^*, \quad 0 \leq x_2 \leq x^*, \end{cases} \tag{154c}$$

$$\begin{cases} \frac{dx_1}{dt} = \alpha(\sin(t) + b - x_1), & 0 \leq x_1 \leq x^*, \\ \frac{dx_2}{dt} = \alpha(b - x_2) - g_1(x_2 - x_1), & 0 \leq x_1 \leq x^*, \quad 0 \leq x_2 \leq x^*. \end{cases} \tag{154d}$$

Let us describe the dynamics of the original singularly perturbed system (152). A solution of the reduced system (154a)-(154d) is describe as follows:

If a solution starts at P_1 with $x_1(0) = x_{10} \in [0, x^*]$ and $x_2(0) = x_{20} \in [0, x^*]$, then $x_1(t)$ and $x_2(t)$ are subject to Eq.(154a). If there is a first time $t_{11} > 0$ such that $x_1(t_{11}) = x_{11} = 0$ and $x_2(t_{11}) = x_{21} \neq 0$, then the solution is considered jumping to P_3 immediately and

so that $x_1(t)$ and $x_2(t)$ is given by Eq.(154c) with the initial conditions $x_1(t_{11}) = 0$ and $x_2(t_{11}) = x_{21}$. If there is again a fist time $t_{21} > t_{11} > 0$ such that $x_1(t_{21}) = x_{12} < x^*$ and $x_2(t_{21}) = x_{22} = 0$, then the solution is considered jumping to P_4 immediately and so that $x_1(t)$ and $x_2(t)$ is given by Eq.(154d) with the initial conditions $x_1(t_{21}) = x_{12}$ and $x_2(t_{21}) = 0$. If there is again a first time $t_{12} > t_{21} > t_{11} > 0$ such that $x_1(t_{12}) = x_{13} = x^*$ and $x_2(t_{12}) = x_{23} < x^*$, then the solution is considered jumping to P_2 immediately and so that $x_1(t)$ and $x_2(t)$ is given by Eq.(154b) with the initial condition $x_1(t_{12}) = x^*$ and $x_2(t_{12}) = x_{23}$. And so on. In such a way the solution is defined by Eqs.(154a)-(154d).

From (154a) and (154c) we have

$$x_2(t, \alpha, x_1(t_0), x_2(t_0), g_1) = x_2(t_0)e^{-(\alpha+g_1)(t-t_0)} + g_1 \int_{t_0}^{t} e^{-(\alpha+g_1)(t-\tau)} x_1(\tau) d\tau. \tag{155}$$

And from (154b) and (154d) we have

$$\begin{aligned} x_2(t, \alpha, x_1(t_0), x_2(t_0), g_1) = x_2(t_0)e^{-(\alpha+g_1)(t-t_0)} + g_1 \int_{t_0}^{t} e^{-(\alpha+g_1)(t-\tau)} x_1(\tau) d\tau \\ + \frac{b\alpha}{\alpha + g_1}(1 - e^{-(\alpha+g_1)(t-t_0)}). \end{aligned} \tag{156}$$

Notation 3.2.1.

$$\begin{aligned} x_1(t) &= x_1(t, \alpha, x_1(t_0)), \\ x_2(t) &= x_2(t, \alpha, x_1(t_0), x_2(t_0), g_1). \end{aligned} \tag{157}$$

Proposition 3.2.1. *Let $x_1(t)$ and $x_2(t)$ be the solution of (154a)-(154d)*

(a) For all $t > 0$ the solution $0 < x_2(t) \leq x^*$ and $0 \leq x_1(t) \leq x^*$.

(b) There is a $T > 0$ such that for all $t > T$ the solution $x_1(t)$, $x_2(t)$ is on $P_1 \bigcup P_3$.(see figure (23)-(24))

Proof. (a) Since $x^* > 1$ and $b > x^* + \frac{1}{2}$ we have that $0 \leq x_1(t) \leq x^*$. Now from (155)-(156) we get $0 < x_2(t) \leq x^*$.

Now let us show part (b). Assume that $x_1(t_0)$ and $x_2(t_0)$ are in P_1 or P_3. Then $x_2(t)$ is given by (155)

$$\begin{aligned} x_2(t) &\leq x_2(t_0)e^{-(\alpha+g_1)(t-t_0)} + g_1 \quad x^* \int_{t_0}^{t} e^{-(\alpha+g_1)(t-\tau)} d\tau \\ &= x_2(t_0)e^{-(\alpha+g_1)(t-t_0)} + \frac{g_1 x^*}{\alpha + g_1}(1 - e^{-(\alpha+g_1)(t-t_0)}) \\ &= \frac{g_1 x^*}{\alpha + g_1} + (x_2(t_0) - \frac{g_1 x^*}{\alpha + g_1})e^{-(\alpha+g_1)(t-t_0)} \leq x^*. \end{aligned} \tag{158}$$

Hence $0 < x_2(t) \leq x^*$ if $x_1(t_0)$, $x_2(t_0) \in P_1 \bigcup P_3$.

If $x_1(t_0)$ and $x_2(t_0)$ are in P_2 or P_4. Then $x_2(t)$ is given by (156)

$$\begin{aligned} x_2(t) = x_2(t_0)e^{-(\alpha+g_1)(t-t_0)} + g_1 \int_{t_0}^{t} e^{-(\alpha+g_1)(t-\tau)} x_1(\tau) d\tau \\ + \frac{b\alpha}{\alpha+g_1}(1 - e^{-(\alpha+g_1)(t-t_0)}). \end{aligned} \tag{159}$$

Since $b > x^* + \frac{1}{2}$ then $x_2(t)$ is increasing ($x_2(t_1) < x_2(t_2)$ for $t_1 < t_2$). By hypothesis we have $x_2(t) \leq x^*$. We can show that there is a $T > 0$ such that $x_2(T) = x^*$. Therefore for all $t > T$ the solution $x_1(t)$, $x_2(t)$ will be on $P_1 \bigcup P_3$, see figure (23)-(24). □

From (154a)-(154d) we have that the dynamics on each halfplane is describe by

$$\begin{pmatrix} \dot{W}_i(t) \\ \dot{Z}_i(t) \end{pmatrix} = \begin{pmatrix} -\alpha & 0 \\ g_1 & -(\alpha+g_1) \end{pmatrix} \begin{pmatrix} W_i(t) \\ Z_i(t) \end{pmatrix} + \begin{pmatrix} \alpha \sin(t) \\ 0 \end{pmatrix}, \tag{160}$$

for $(x_1, y_1, x_2, y_2) \in P_i, \quad i = 1, 2, 3, 4$, where

$$\begin{pmatrix} W_1 \\ Z_1 \end{pmatrix} = \begin{pmatrix} x_1 \\ x_2 \end{pmatrix}; \qquad \begin{pmatrix} W_2 \\ Z_2 \end{pmatrix} = \begin{pmatrix} x_1 \\ x_2 - q_1 \end{pmatrix}; \tag{161}$$

$$\begin{pmatrix} W_3 \\ Z_3 \end{pmatrix} = \begin{pmatrix} x_1 - p_2 \\ x_2 - q_2 \end{pmatrix}; \qquad \begin{pmatrix} W_4 \\ Z_4 \end{pmatrix} = \begin{pmatrix} x_1 - p_2 \\ x_2 - p_2 \end{pmatrix}; \tag{162}$$

and

$$q_1 = \frac{b\alpha}{\alpha+g_1}, \qquad q_2 = \frac{bg_1}{\alpha+g_1} \quad \text{and} \quad p_2 = b. \tag{163}$$

Using the variation of constants formula we have

$$\begin{aligned} W_i(t) \quad &= Ae^{-\alpha(t-t_0)} + \alpha \int_{t_0}^{t} e^{-\alpha(t-\tau)} \sin(\tau) d\tau, \\ \\ Z_i(t) \quad &= Ae^{-\alpha(t-t_0)} + \alpha \int_{t_0}^{t} e^{-\alpha(t-\tau)} \sin(\tau) d\tau \\ &\quad -Be^{-(\alpha+g_1)(t-t_0)} - \alpha \int_{t_0}^{t} e^{-(\alpha+g_1)(t-\tau)} \sin(\tau) d\tau, \end{aligned} \tag{164}$$

where

$$A = W_i(t_0), \quad B = W_i(t_0) - Z_i(t_0), \quad \text{for} \quad i = 1, 2, 3, 4. \tag{165}$$

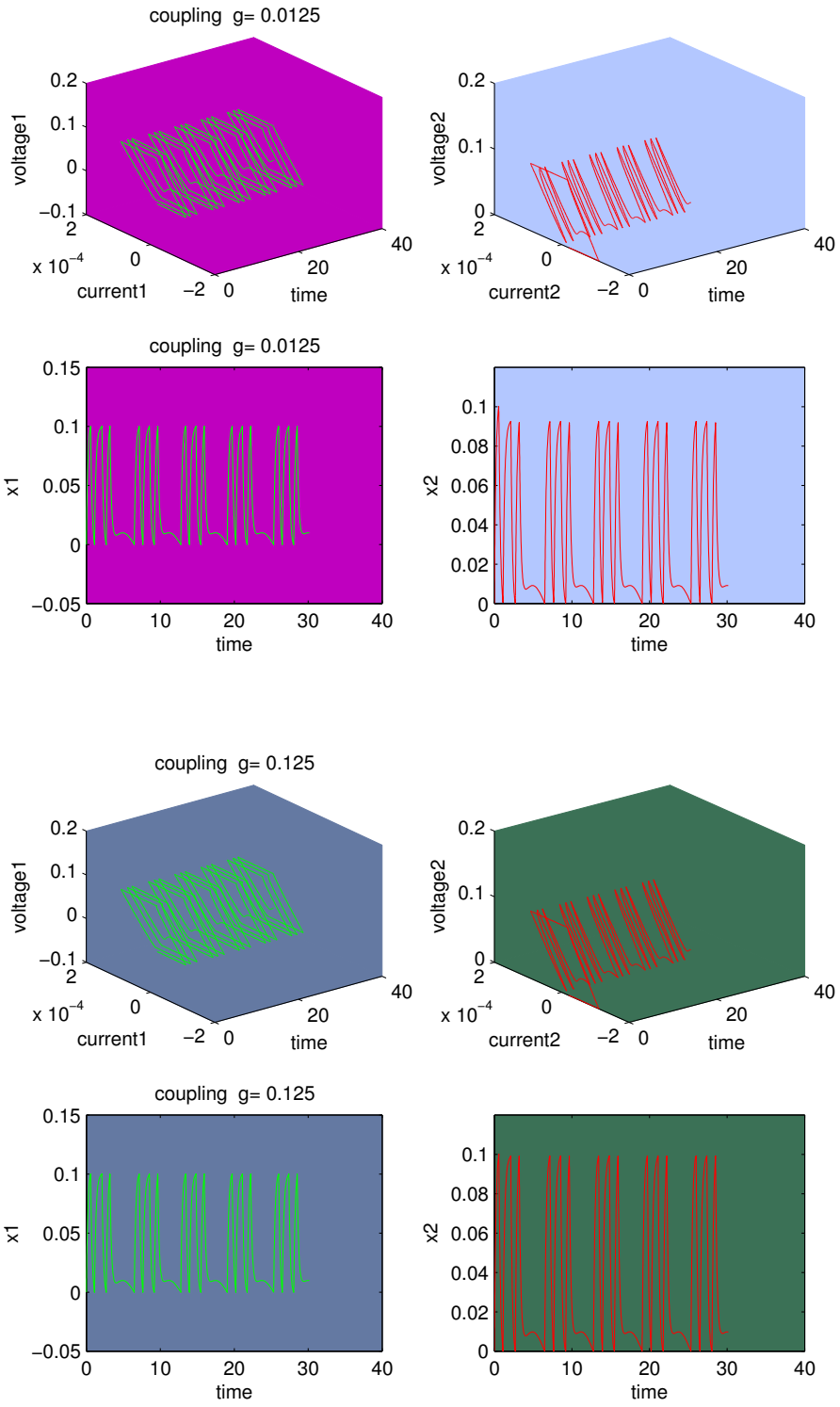

Figure 23: Unidirectional coupling with initial condition on P_2.

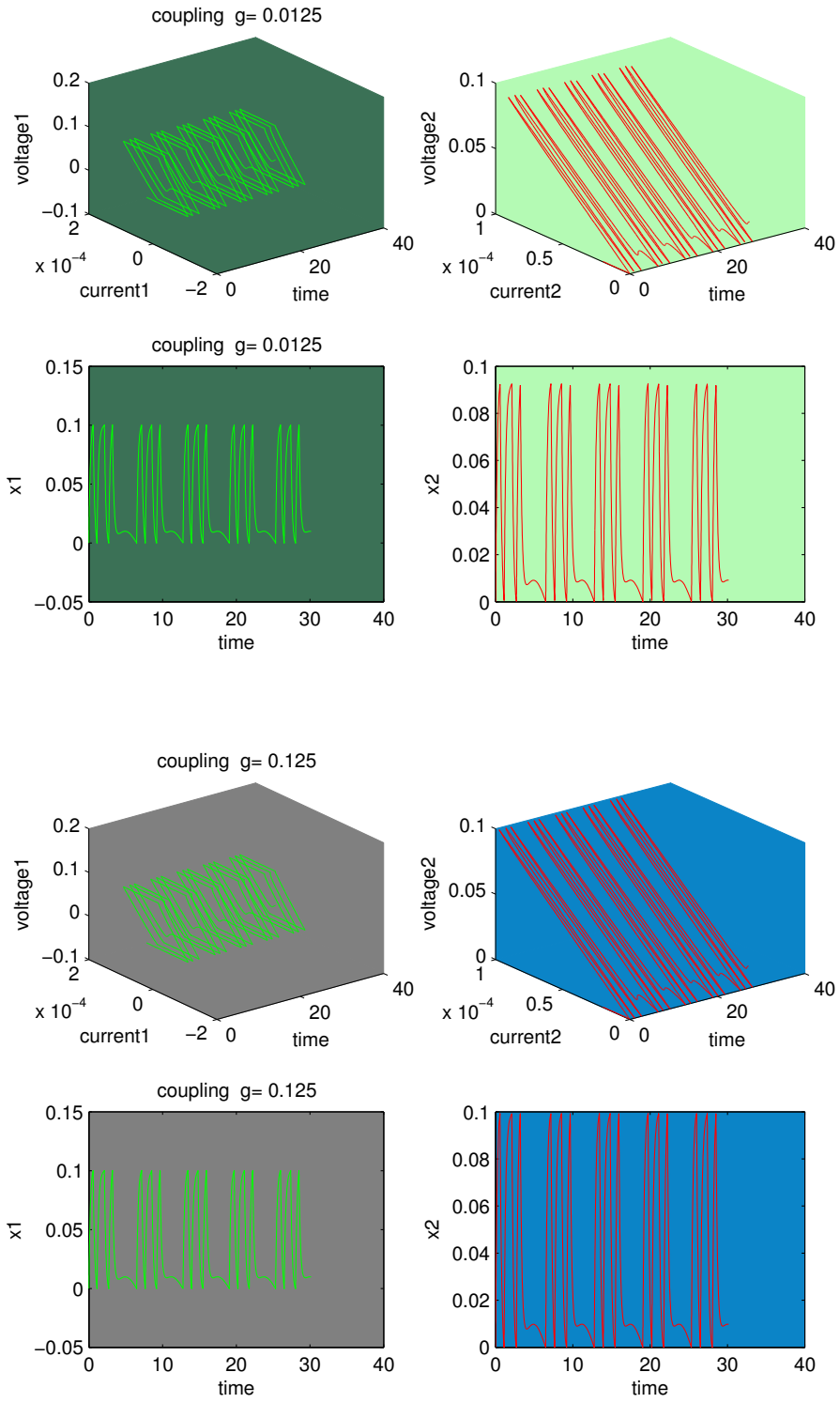

Figure 24: Unidirectional coupling with initial condition on P_1

3.3 Bidirectional coupling

In the present section we formulate the problem for a system of two or more oscillators coupled diffusively. We consider a type of mutually coupling (bidirectional coupling).

- For $k = 1$

$$\begin{cases} \frac{dx_1}{dt} = f(t) - y_1 - g(x_1 - x_2), & (166aa) \\ \epsilon \frac{dy_1}{dt} = x_1 - \varphi(y_1), & (166ab) \end{cases} \tag{166a}$$

- For $k = 2, \ldots, n-1$

$$\begin{cases} \frac{dx_k}{dt} = -y_k + g(x_{k+1} - 2x_k + x_{k-1}), & (166ba) \\ \epsilon \frac{dy_k}{dt} = x_k - \varphi(y_k), & (166bb) \end{cases} \tag{166b}$$

- For $k = n$

$$\begin{cases} \frac{dx_n}{dt} = -y_n - g(x_n - x_{n-1}), & (166ca) \\ \epsilon \frac{dy_n}{dt} = x_n - \varphi(y_n), & (166cb) \end{cases} \tag{166c}$$

where

$$\varphi(y_n) = \begin{cases} \delta_1 y_k, & if \quad y_k \geq 0, \\ \delta_2 y_k, & if \quad y_0 \leq y_k < 0, \\ \delta_1 y_k + (\delta_2 - \delta_1) y_0, & if \quad y_k < y_0. \end{cases} \tag{167}$$

The small parameter $\epsilon > 0$ in front of the time derivative makes (166) a singular perturbed system. The dynamics of such system can be split into two regimes: the slow motion and the fast jumps. The former regime can be formally described by setting $\epsilon = 0$ in (166). Then (166ab), (166bb), and (166cb) yields the equations for the n–dimensional slow manifold, S_d, which can be compactly written using vector notation:

$$S_d = \{x, y \in R^n : \quad x = \varphi(y), \qquad \varphi(y) = (\varphi(y_1), \varphi(y_2), ..., \varphi(y_n))^T\}. \tag{168}$$

Equations (166aa), (166ba), and (166ca) define the vector field on S_d.

On the other hand, the fast dynamics of (166) can be formally obtained by changing to the fast time variable $\tau = \frac{t}{\epsilon}$ and by taking the limit as $\epsilon \to 0$.

Let us consider the case $n = 2$.

$$\begin{cases} \frac{dx_1}{dt} = f(t) - y_1 - g(x_1 - x_2), \\ \epsilon \frac{dy_1}{dt} = x_1 - \varphi(y_1), \end{cases} \tag{169a}$$

$$\begin{cases} \frac{dx_2}{dt} = -y_2 - g(x_2 - x_1), \\ \epsilon \frac{dy_2}{dt} = x_2 - \varphi(y_2), \end{cases} \tag{169b}$$

where $\varphi(y)$ is given by (167).

With $f(t) = k\sin(\omega t)$ and the change of variables given on (144) the Eq.(169) is written as

$$\begin{cases} \frac{dx_1}{dt} = \alpha(\sin(t) - y_1) - g_1(x_1 - x_2), \\ \xi \frac{dy_1}{dt} = x_1 - \varphi(y_1), \\ \frac{dx_2}{dt} = -\alpha y_2 - g_1(x_2 - x_1), \\ \xi \frac{dy_2}{dt} = x_2 - \varphi(y_2), \end{cases} \tag{170}$$

where

$$\varphi(y) = \begin{cases} y, & if \quad y \geq 0, \\ \delta y, & if \quad y^* < y < 0, \\ y + b, & if \quad y \leq y^*, \end{cases} \tag{171}$$

and

$$\begin{cases} \alpha = \frac{1}{\omega\delta 1}, \quad \xi = \frac{\epsilon\omega}{\delta_1}, \quad y^* = \frac{y_0}{k}, \quad \delta = \frac{\delta_2}{\delta_1}, \\ x^* = \delta y^* \quad b = \frac{y_0(\delta_2 - \delta_1)}{k\delta_1} = (\delta - 1)y^*, \quad g_1 = \frac{g}{\omega}. \end{cases} \tag{172}$$

From Eq.(169) we see that the reduced system on P_1, P_2, P_3, and P_4 are given respectively by the following differential equations:

$$\begin{cases} \frac{dx_1}{dt} = \alpha(\sin(t) - x_1) - g_1(x_1 - x_2), & 0 \leq x_1 \leq x^*, \quad 0 \leq x_2 \leq x^*, \\ \frac{dx_2}{dt} = -\alpha x_2 - g_1(x_2 - x_1), & 0 \leq x_1 \leq x^*, \quad 0 \leq x_2 \leq x^*, \end{cases} \tag{173a}$$

$$\begin{cases} \frac{dx_1}{dt} = \alpha(\sin(t) - x_1) - g_1(x_1 - x_2), & 0 \leq x_1 \leq x^*, \quad 0 \leq x_2 \leq x^*, \\ \frac{dx_2}{dt} = \alpha(b - x_2) - g_1(x_2 - x_1), & 0 \leq x_1 \leq x^*, \quad 0 \leq x_2 \leq x^*, \end{cases} \tag{173b}$$

$$\begin{cases} \frac{dx_1}{dt} = \alpha(\sin(t) + b - x_1) - g_1(x_1 - x_2), & 0 \le x_1 \le x^*, \quad 0 \le x_2 \le x^*, \\ \frac{dx_2}{dt} = -\alpha x_2 - g_1(x_2 - x_1), & 0 \le x_1 \le x^*, \quad 0 \le x_2 \le x^*, \end{cases} \tag{173c}$$

$$\begin{cases} \frac{dx_1}{dt} = \alpha(\sin(t) + b - x_1) - g_1(x_1 - x_2), & 0 \le x_1 \le x^*, \quad 0 \le x_2 \le x^*, \\ \frac{dx_2}{dt} = \alpha(b - x_2) - g_1(x_2 - x_1), & 0 \le x_1 \le x^*, \quad 0 \le x_2 \le x^*. \end{cases} \tag{173d}$$

That means the dynamics on each halfplane is describe by

$$\begin{pmatrix} \dot{W}_i(t) \\ \dot{Z}_i(t) \end{pmatrix} = \begin{pmatrix} -(\alpha + g_1) & g_1 \\ g_1 & -(\alpha + g_1) \end{pmatrix} \begin{pmatrix} W_i(t) \\ Z_i(t) \end{pmatrix} + \begin{pmatrix} \alpha \sin(t) \\ 0 \end{pmatrix}, \tag{174}$$

for $(x_1, y_1, x_2, y_2) \in P_i, \quad i = 1, 2, 3, 4,$ where

$$\begin{pmatrix} W_1 \\ Z_1 \end{pmatrix} = \begin{pmatrix} x_1 \\ x_2 \end{pmatrix}; \qquad \begin{pmatrix} W_2 \\ Z_2 \end{pmatrix} = \begin{pmatrix} x_1 + s_1 \\ x_2 + s_2 \end{pmatrix}; \tag{175}$$

$$\begin{pmatrix} W_3 \\ Z_3 \end{pmatrix} = \begin{pmatrix} x_1 - s_2 \\ x_2 - s_1 \end{pmatrix}; \qquad \begin{pmatrix} W_4 \\ Z_4 \end{pmatrix} = \begin{pmatrix} x_1 - s_3 \\ x_2 + s_3 \end{pmatrix}; \tag{176}$$

where

$$s_1 = \frac{bg_1}{\alpha + 2g_1}, \quad s_2 = \frac{b(\alpha + g_1)}{\alpha + 2g_1} \quad \text{and} \quad s_3 = \frac{b\alpha}{\alpha + 2g_1}. \tag{177}$$

Using the variation of constant formula we have

$$W_i(t) = Ae^{-\alpha(t-t_0)} + Be^{-2g_1(t-t_0)} + \tfrac{\alpha}{2} \int_{t_0}^{t} (1 + e^{-2g_1(t-\tau)}) e^{-\alpha(t-\tau)} \sin(\tau) d\tau, \tag{178}$$

$$Z_i(t) = Ae^{-\alpha(t-t_0)} - Be^{-2g_1(t-t_0)} + \tfrac{\alpha}{2} \int_{t_0}^{t} (1 - e^{-2g_1(t-\tau)}) e^{-\alpha(t-\tau)} \sin(\tau) d\tau,$$

$$\text{where} \quad A = \frac{1}{2}(W_i(t_0) + Z_i(t_0)), \quad B = \frac{1}{2}(W_i(t_0) - Z_i(t_0)) \quad \text{for} \quad i = 1, 2, 3, 4. \tag{179}$$

Proposition 3.3.1. *Let $x_1(t)$ and $x_2(t)$ be the solution of (173a)-(173d)*

(a) For all $t > 0$ the solution $0 < x_1(t) \le x^*$ and $0 < x_2(t) \le x^*$.

(b) There is a $\hat{g} > 0$ such that for all $g > \hat{g}$ the solution $x_1(t)$, $x_2(t)$ is on P_3. (see figure (25)-(27))

Proof. The proof is very similar to propostion 3.2.1. □

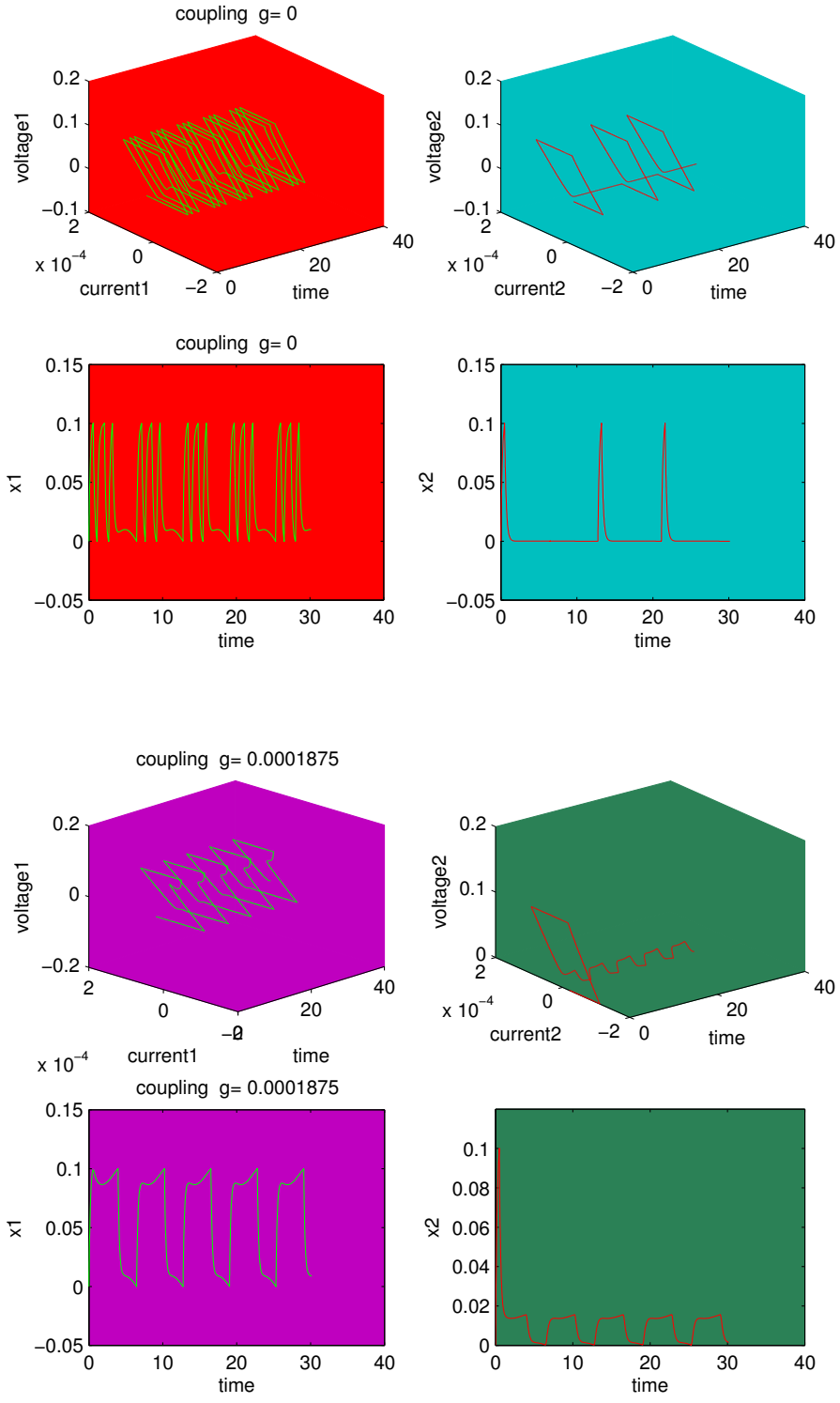

Figure 25: Bidirectional coupling with initial condition on P_2.

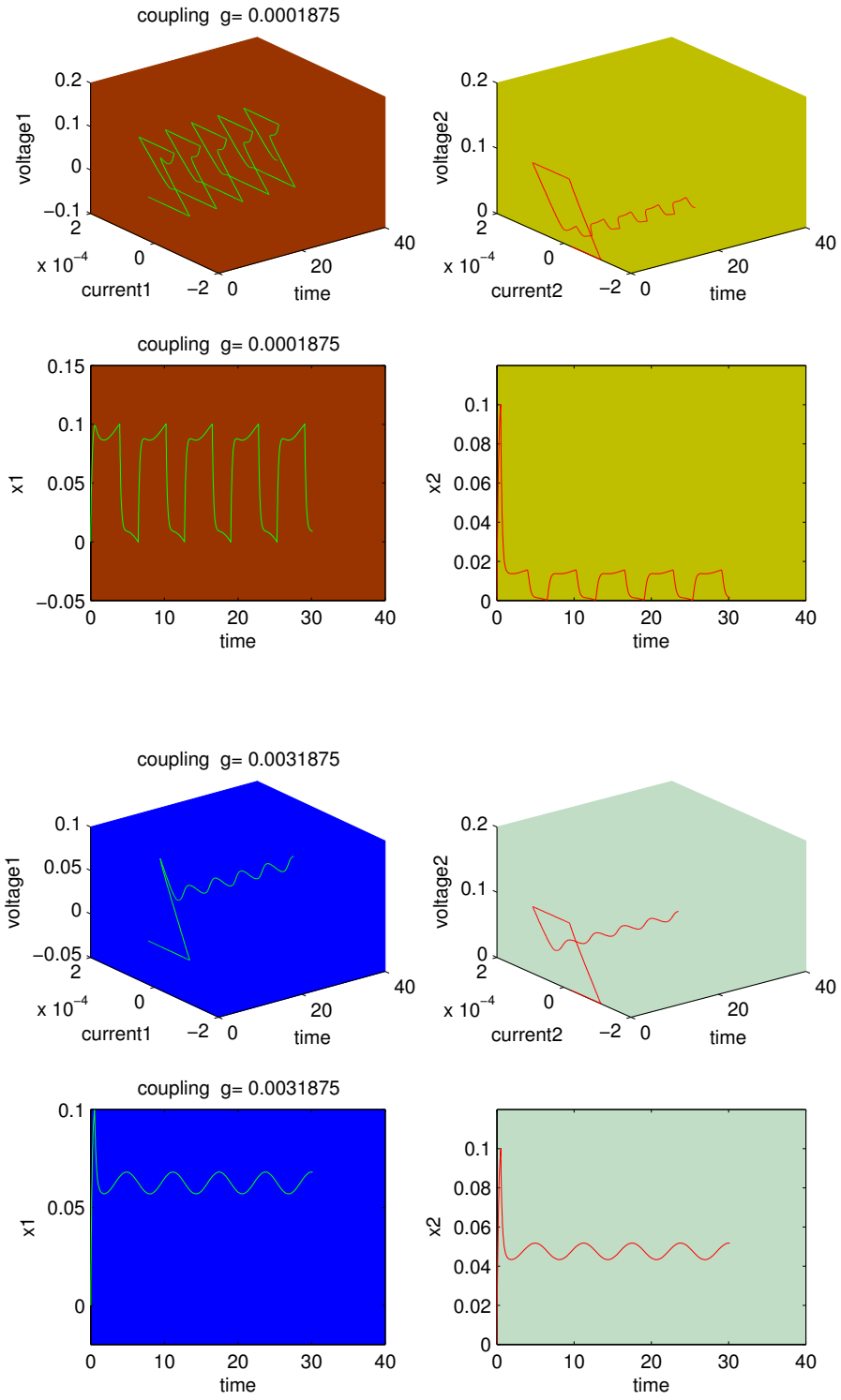

Figure 26: Bidirectional coupling with initial condition on P_1

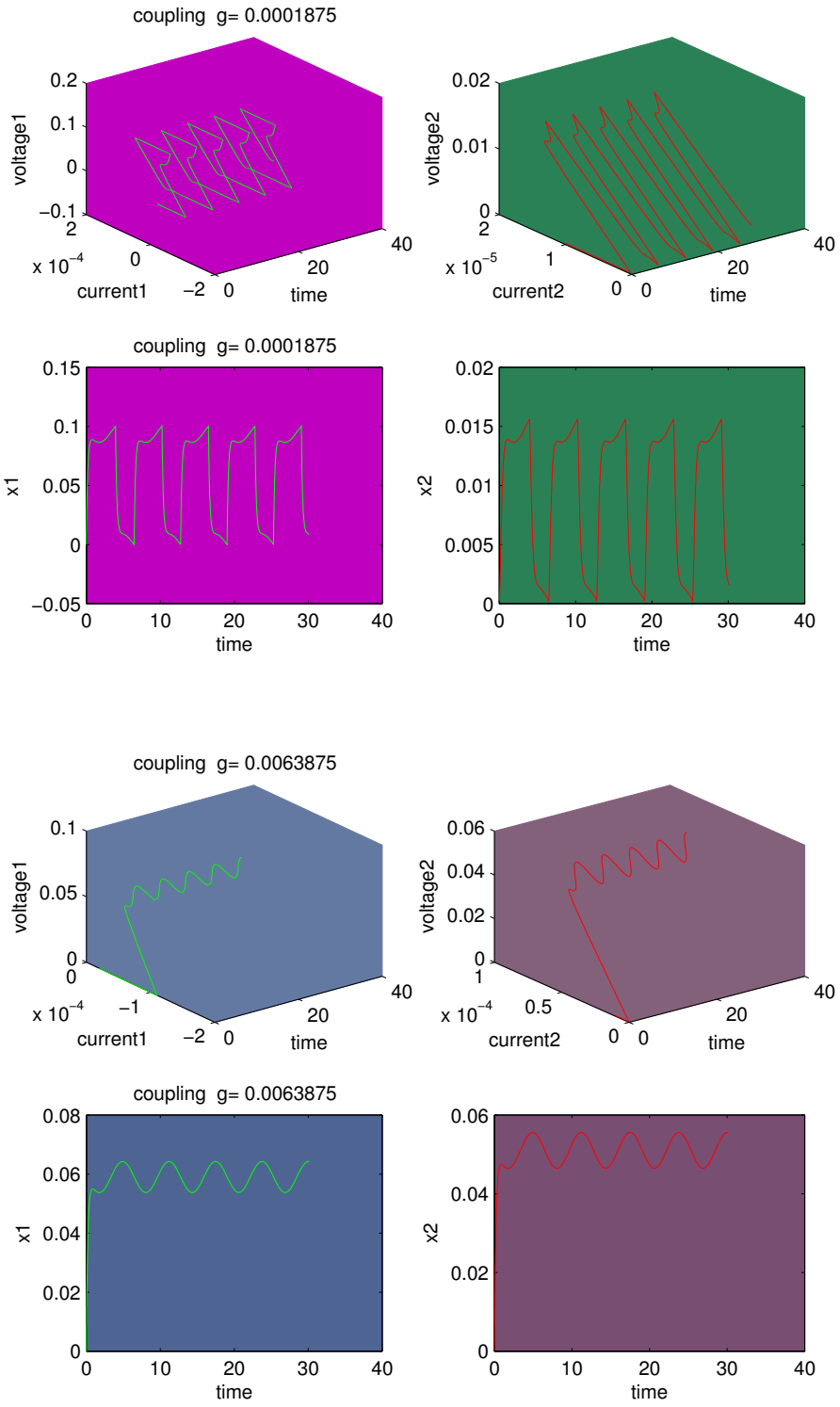

Figure 27: Bidirectional coupling with initial condition on P_3

CHAPTER IV

SYNCHRONIZATION

4.1 Introduction

We understand synchronization as an adjustment of rhythms of oscillating objects due to their weak interaction. Often it is convenient to characterize the rhythm by the number of oscillation cycles per time unit, or by the oscillation cyclic frequency. In the theoretical treatment of synchronization, the angular frequency $\omega = 2\pi f = \frac{2\pi}{T}$ is often more convenient. If two nonidentical oscillators having their own frequencies f_1 and f_2 are coupled together, they may start to oscillate with a common frequency. Whether they synchronize or not depends on the following two factors: coupling strength (this describes how weak or how strong the interaction is) and frequency detuning (frequency detuning or mismatch $\Delta f = f_1 - f_2$ quantifies how different the uncoupled oscillators are.)

Coupled oscillators tend to synchronize–even Hamiltonian systems of them. This suggests that in addition to orbital stability (i.e., stability in amplitudes) there is significant phase–locking, which is asymptotic stability in angular phases.

Synchronization of nonlinear oscillators both in their regular and chaotic states is presently one of the main research topics in the field of nonlinear science since the pioneering work of Pecora and Carrol [34]. But despite the amount of theoretical and experimental results already obtained, a great deal of effort is still required to find optimal parameters to shorten the synchronization time, and avoid loss of synchronization [11] and instability during the synchronization process. This problem is important in all the mentioned fields where synchronization finds or will find practical applications. For instance, in communication systems, the range of time during which the chaotic oscillators are not synchronized corresponds to the range of time during which the encoded message can not be recovered or sent. More than a grave and irreversible loss of information, this is a catastrophe in digital communications since the first bits of standardized bit strings contain the signalization data

or identify card of the message.

4.2 Definitions and Results

The concept of generalized synchronization was introduced to investigate coupling of mismatched or dissimilar systems [4], [25], [38]. Customarily, it is said that coupled systems exhibit generalized synchronization if their states are related by an invertible function. This definition of generalized synchronization must be contained within the information view of synchronization, since an invertible function necessarily preserves the information content of a signal. However, the synchronization of symbolic information is broader and can describe synchronization of more diverse systems. For example, coupling iterated maps to continuous flows is not accommodated by prior definitions of generalized synchronization. Viewing synchronization as an information-matching process, we have the extended synchronization to mismatched or entirely dissimilar oscilltors (see [16]).

The term synchronization may have different meanings in the context of different systems. In general it means that two systems are considered to be synchronized if there is a functional relation between the states of these systems. We want to clarify the meaning of synchronization applicable to the system (166). The following definition of synchronization for a more general system (166) is similar to the definition of the asymptotic synchronization in [22].

Definition 4.2.1. *A solution* $(x_1, y_1, x_2, y_2, ...x_n, y_n) \in R^{2n}$ *of (166) is called synchronous if after some initial lag period* ν*, depending on the initial conditions, it satisfies*

$$|x_i(t) - x_j(t)| \leq \sigma(g), \quad \lim_{g\to\infty} \sigma(g) = 0, \quad t > \nu, \quad 1 \leq i, j \leq n. \tag{180}$$

Remark 4.2.1. We recognize that two arbitrary oscillators are perfectly synchronized in an information sense if they produce the same information –i.e., symbols generated by one systems map injectively to symbols emitted by the other.

Remark 4.2.2. True synchronization requires that the common information be emited at precisely the same time. However, for mismatched oscillators this requirement is too strict, especially when considering flows where the system return time can vary depending on the

precise trajectory. A more practical requirement is that information is emitted at the same average rate or entropy. For unidirectional coupling, a significant delay between the drive and response systems may be allowed for certain applications.

4.3 Coupling

Directional coupling have been studied intensely in combination with different methods for constructing synchronized systems [15], [4], [24]. It may be viewed as a generalization of periodic or quasiperiodic driving that has been used in physics, mathematics, and engineering for a long time. Furthemore, unidirectional coupled systems may lead to interesting applications, for example, in communication systems [12], and [24].

Here we consider the effect of coupling two circuit unidirectionally. Unidirectional coupling means that only the dynamics of the response subsystem (circuit 2) is affected by the drive subsystem (circuit 1) through the coupling (g); the reverse does not hold.

Let us consider a pair of unidirectionally coupled circuit figure (28)

$$\begin{cases} \frac{dx_1}{dt} = k\sin(\omega t) - y_1, \\ \epsilon\frac{dy_1}{dt} = x_1 - \varphi(y_1), \end{cases} \tag{181a}$$

$$\begin{cases} \frac{dx_2}{dt} = -y_2 - g(x_2 - x_1), \\ \epsilon\frac{dy_2}{dt} = x_2 - \varphi(y_2), \end{cases} \tag{181b}$$

where $\varphi(y)$ is given by (142).

The driving signal is given by the voltage x_1 of the first circuit (181a) and the coupling

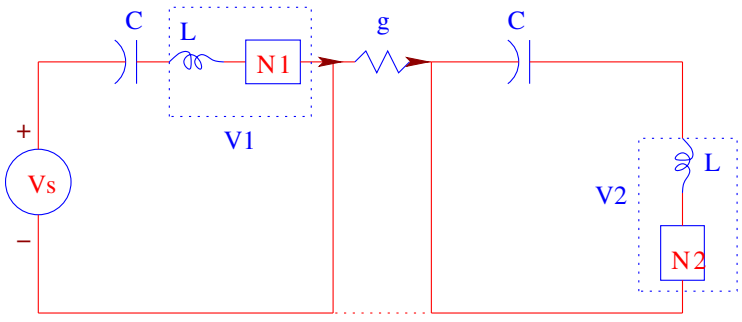

Figure 28: Pair of unidirectional coupled circuits

constant g is varied in order to achieve synchronization. The parameters used for the simulation are $\epsilon = 0.001$, $\delta_1 = 1000$, $\delta_2 = -10000$, $y_0 = -0.00001$, $k = 0.05\omega$, and $\omega = 2\pi 0.000017$, (See figure 32). We did simulation for differents values of k and different values of ω and we got the same figure 32. For $g > 0.85$ this unidirectional coupled system shows the well-known identical synchronization. There exist, however, also parameter intervals for the coupling g where no identical but generalized synchronization occurs.

Now since the dynamics of the singularly perturbed systems (181a)-(181b) has a close connection with the dynamics of its reduced system as $\epsilon \longrightarrow 0$. We are going to prove the following theorem using the reduced system (154a)-(154d). Where f is a piecewise continuous periodic function oscillatory around the t-axis.

Theorem 4.3.1. *Let consider the system (145) where f is a piecewise continuous periodic function oscillatory around the t-axis with amplitude k and frequency ω. Let x_1 and x_2 be the solution of the corresponding reduced systems (154a)–(154d). Then*

$$|x_1(t) - x_2(t)| \leq \sigma(g_1) \longrightarrow 0, \quad \textit{when} \quad g_1 \longrightarrow \infty \quad \textit{for} \quad t - t_0 > \nu. \tag{182}$$

Proof. We have that we can write the reduced system as Eq.(160).

Then from equation 164 we have that the solution of this reduced systems is given by

$$\begin{aligned} W_i(t) &= Ae^{-\alpha(t-t_0)} + \alpha \int_{t_0}^{t} e^{-\alpha(t-\tau)} f(\tau) d\tau, \\ Z_i(t) &= Ae^{-\alpha(t-t_0)} + \alpha \int_{t_0}^{t} e^{-\alpha(t-\tau)} f(\tau) d\tau \\ &\quad -Be^{-(\alpha+g_1)(t-t_0)} - \alpha \int_{t_0}^{t} e^{-(\alpha+g_1)(t-\tau)} f(\tau) d\tau, \end{aligned} \tag{183}$$

where

$$A = W_i(t_0), \quad B = W_i(t_0) - Z_i(t_0), \quad \text{for} \quad i = 1, 2, 3, 4. \tag{184}$$

From here we get

$$\begin{aligned}
|W_i(t) - Z_i(t)| &= |Be^{-(\alpha+g_1)(t-t_0)} + \alpha \int_{t_0}^{t} e^{-(\alpha+g_1)(t-\tau)} f(\tau) d\tau| \\
&\leq |B| e^{-(\alpha+g_1)(t-t_0)} + \alpha \int_{t_0}^{t} e^{-(\alpha+g_1)(t-\tau)} |f(\tau)| d\tau \\
&\leq |B| e^{-(\alpha+g_1)(t-t_0)} + \alpha \int_{t_0}^{t} e^{-(\alpha+g_1)(t-\tau)} d\tau \\
&= \tfrac{\alpha}{\alpha+g_1} + e^{-(\alpha+g_1)(t-t_0)} \left\{ |B| - \tfrac{\alpha}{\alpha+g_1} \right\} \\
&\leq \tfrac{\alpha}{\alpha+g_1} + |B| e^{-(\alpha+g_1)(t-t_0)} \\
&\overset{t-t_0>\nu}{<} \tfrac{\alpha}{\alpha+g_1} + |B| e^{-g_1 \nu} = \sigma(g_1).
\end{aligned} \tag{185}$$

Therefore (185) imply

$$|W_i(t) - Z_i(t)| \leq \sigma(g_1) \longrightarrow 0, \quad \text{when} \quad g_1 \longrightarrow \infty \ \text{ for } \quad t - t_0 > \nu. \tag{186}$$

From proposition 3.2.1 we have x_1, x_2 is on $P_1 \bigcup P_3$. Therefore, we have the two following cases:

Case 1 $x_1, x_2 \in P_1$. then

$$|x_1(t) - x_2(t)| = |W_1(t) - Z_1(t)| \leq \sigma(g_1) \longrightarrow 0, \quad \text{when} \quad g_1 \longrightarrow \infty \ \text{ for } \quad t - t_0 > \nu.$$

Case 2 $x_1, x_2 \in P_3$. then

$$|x_1(t) - p_2 - x_2(t) + q_2| = |x_1(t) - x_2(t) + \tfrac{bg_1}{\alpha+g_1} - b|$$

$$= |W_3(t) - Z_3(t)| \leq \sigma(g_1) \longrightarrow 0, \quad \text{when} \quad g_1 \longrightarrow \infty \ \text{ for } \quad t - t_0 > \nu.$$

Therefore $|x_1(t) - x_2(t)| \longrightarrow 0, \quad \text{when} \quad g_1 \longrightarrow \infty \ \text{ for } \quad t - t_0 > \nu.$

Then according to definition 4.2.1 the system is synchronous. See figure (30)-(32). □

Remark 4.3.1. When generalized synchronization is achieved, the slaves provide some information about the master regime, but other information is lost.

Remark 4.3.2. The importance of this result is that in the conventional communication sytems, thousands of RF carrier cycles are required to reliably extract the information contained in a carrier signal this is because the receiver requieres time to synchronise with the carrier signal. With this circuit we have that information can be decoded in every transmitted cycle since the synchronization depends of the coupling and no the "time". Thus, it

promises very high-speed data transmisssion. For example in order to send information we can use different number of spikes per cycle to represent sets of information symbols and we can do it changing the amplitud for example (see Chapter II) .

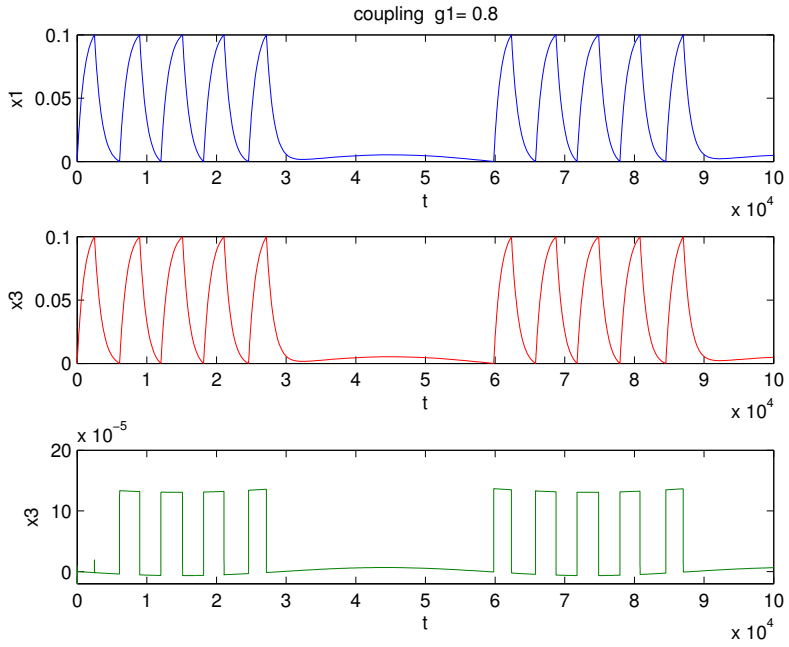

Figure 29: Synchronization of unidirectionally coupled circuit. (a) Drive Blue (x_1), (b) Response Red (x_2), (c) Difference between $x_1 - x_2$, $g = 0.8$.

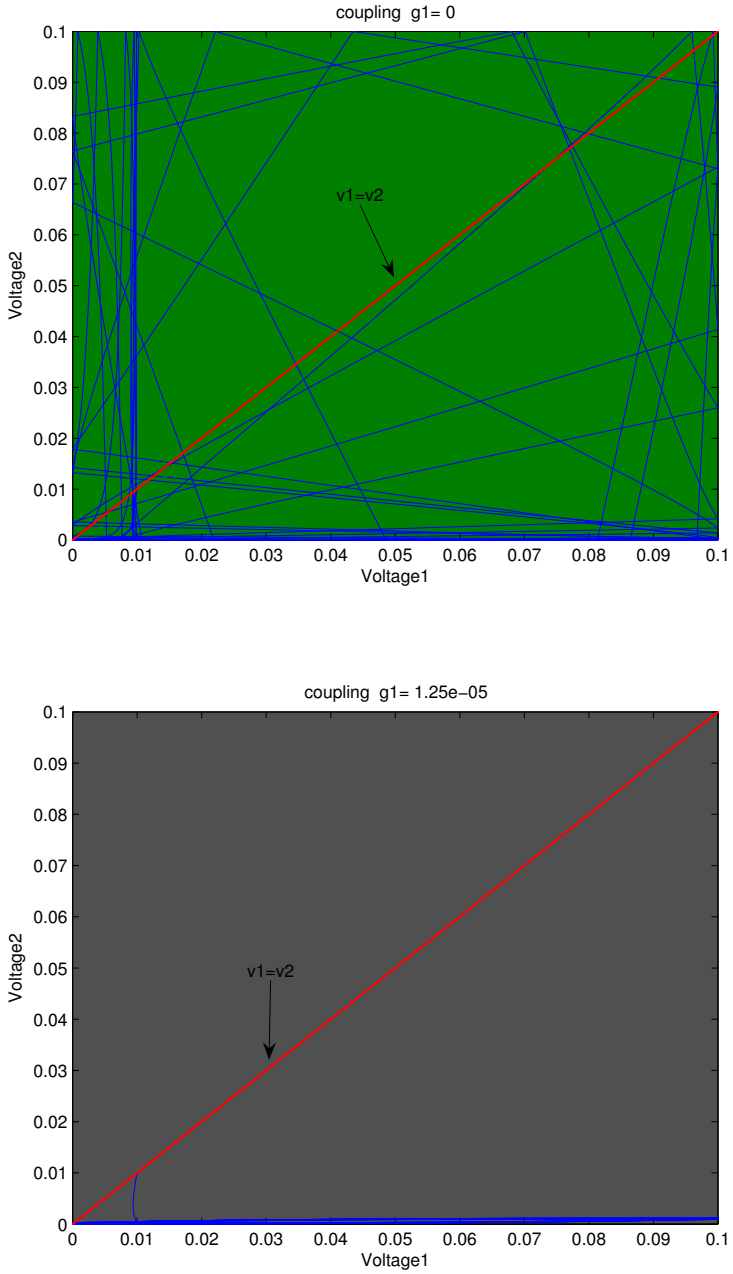

Figure 30: Unidirectional coupling for $g_1 = 0$ and $g_1 = 1.25e - 05$.

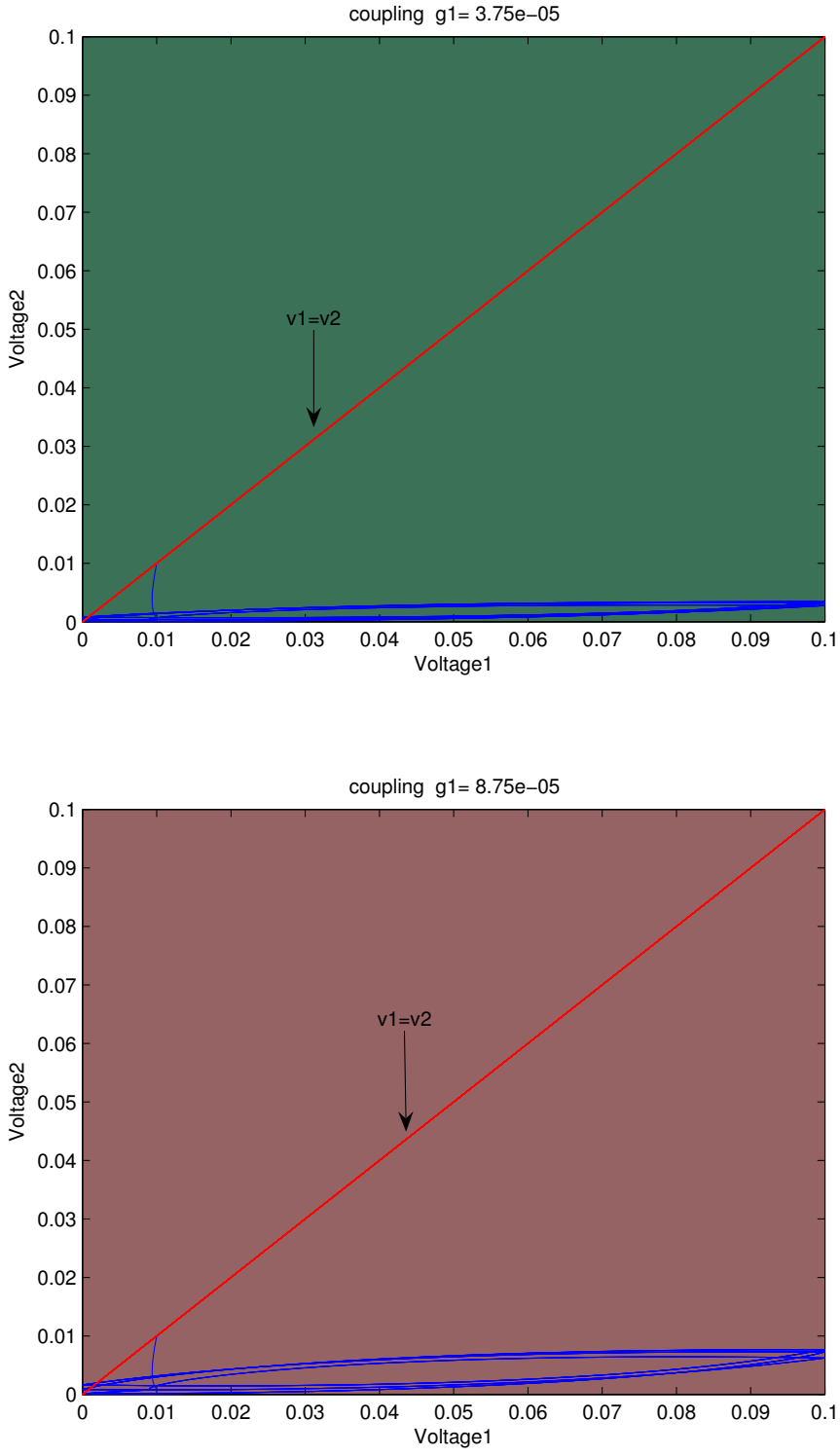

Figure 31: Unidirectional coupling for $g_1 = 3.75e-05$ and $g_1 = 8.75e-05$.

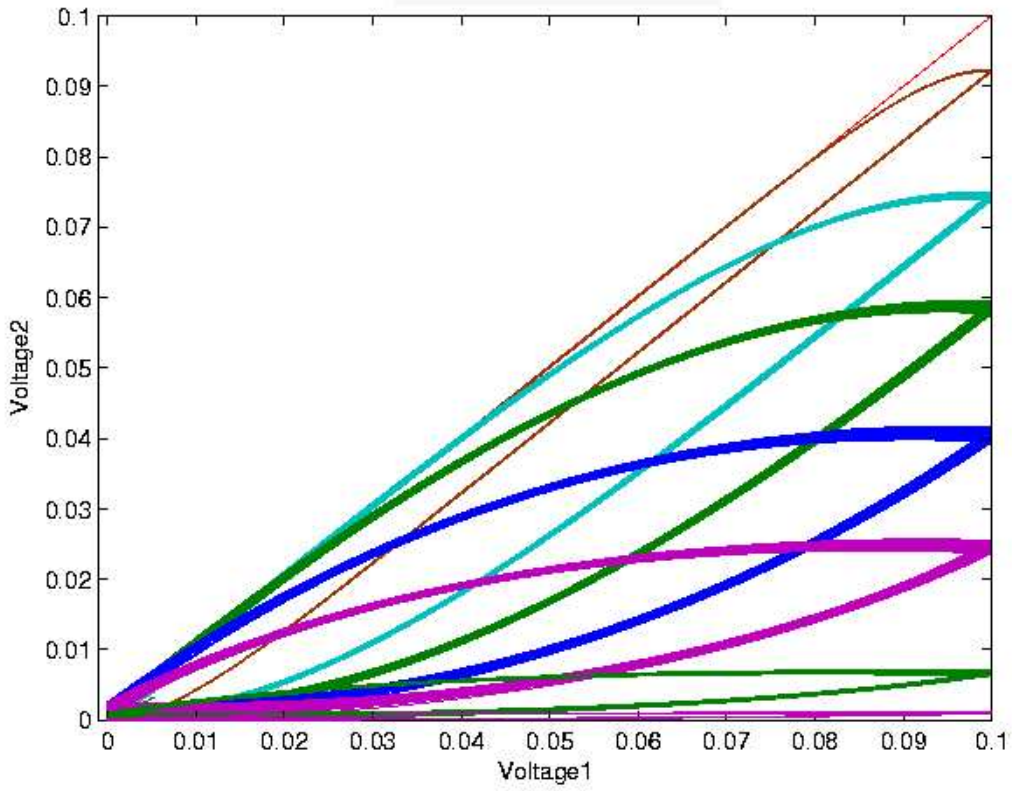

Figure 32: Unidirectional coupling for different values of g.

Table 3: Values of g for the figure 32. The figure are counting from bottom (f_1) to top (f_8).

$g \times e-03$	0.0375	0.0875	0.3875	0.7875	1.5875	3.188	12.79	13110
fig	f_1	f_2	f_3	f_4	f_5	f_6	f_7	f_8

Now we are going to consider the effect of coupling two circuit bidirectionally. Let us consider a pair of bidirectionally coupled circuit figure 33.

$$\begin{cases} \frac{dx_1}{dt} = k\sin(\omega t) - y_1 - g(x_1 - x_2), \\ \epsilon\frac{dy_1}{dt} = x_1 - h(y_1), \end{cases} \tag{187a}$$

$$\begin{cases} \frac{dx_2}{dt} = -y_2 - g(x_2 - x_1), \\ \epsilon\frac{dy_2}{dt} = x_2 - h(y_2), \end{cases} \tag{187b}$$

where $h(y)$ is given by (142).

The coupling constant g is varied in order to achieve synchronization. The parameters

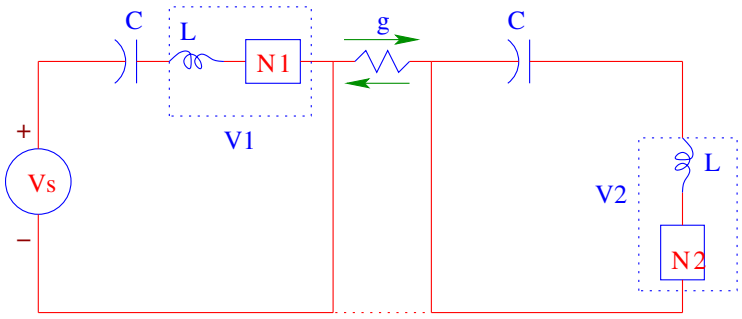

Figure 33: Pair of bidirectional coupled circuit.

used for the simulation are $\epsilon = 0.001$, $\delta_1 = 1000$, $\delta_2 = -10000$, $y_0 = -0.00001$, $k = 0.05\omega$, and $\omega = 2\pi 0.000017$, (See figure 35). Now since the dynamics of the singularly perturbed systems (181a)-(181b) has a close connection with the dynamics of its reduced system as $\epsilon \longrightarrow 0$. We are going to prove the following theorem using the reduced system (154a)-(154d). Where f is a piecewise continuous periodic function oscillatory around the t-axis.

Theorem 4.3.2. *Let consider the system (169) where f is a piecewise continuous periodic function oscillatory around the t-axis with amplitude k and frequency ω. Let x_1 and x_2 be the solution of the corresponding reduced systems (173a)–(173d). Then*

$$|x_1(t) - x_2(t)| \leq \sigma(g_1) \longrightarrow 0, \quad \textit{when} \quad g_1 \longrightarrow \infty \quad \textit{for} \quad t - t_0 > \nu. \tag{188}$$

Proof. We have that we can write the reduced system as Eq.(174).

Then from equation 178 we have that the solution of this reduced systems is given by

$$\begin{aligned} W_i(t) &= Ae^{-\alpha(t-t_0)} + Be^{-2g_1(t-t_0)} + \tfrac{\alpha}{2}\int_{t_0}^{t}(1 + e^{-2g_1(t-\tau)})e^{-\alpha(t-\tau)}\sin(\tau)d\tau, \\ Z_i(t) &= Ae^{-\alpha(t-t_0)} - Be^{-2g_1(t-t_0)} + \tfrac{\alpha}{2}\int_{t_0}^{t}(1 - e^{-2g_1(t-\tau)})e^{-\alpha(t-\tau)}\sin(\tau)d\tau, \end{aligned} \tag{189}$$

where

$$A = \frac{1}{2}(W_i(t_0) + Z_i(t_0)), \quad B = \frac{1}{2}(W_i(t_0) - Z_i(t_0)) \quad \text{for} \quad i = 1, 2, 3, 4. \tag{190}$$

From here we get

$$\begin{aligned}
|W_i(t) - Z_i(t)| &= |2Be^{-2g_1(t-t_0)} + \alpha \int_{t_0}^{t} e^{-(\alpha+2g_1)(t-\tau)} \sin(\tau) d\tau| \\
&\leq |2B|e^{-2g_1(t-t_0)} + \alpha \int_{t_0}^{t} e^{-(\alpha+2g_1)(t-\tau)} |\sin(\tau)| d\tau \\
&\leq |2B|e^{-2g_1(t-t_0)} + \alpha \int_{t_0}^{t} e^{-(\alpha+2g_1)(t-\tau)} d\tau \\
&= |2B|e^{-2g_1(t-t_0)} + \tfrac{\alpha}{\alpha+2g_1} \left\{1 - e^{-(\alpha+2g_1)(t-t_0)}\right\} \\
&= \tfrac{\alpha}{\alpha+2g_1} + |2B|e^{-2g_1(t-t_0)} - \tfrac{\alpha}{\alpha+2g_1} e^{-(\alpha+2g_1)(t-t_0)} \\
&\overset{t-t_0>\nu}{<} \tfrac{\alpha}{\alpha+2g_1} + 2|B|e^{-2g_1\nu} = \sigma(g_1).
\end{aligned} \tag{191}$$

Therefore (191) imply

$$|W_i(t) - Z_i(t)| \longrightarrow 0, \quad \text{when} \quad g_1 \longrightarrow \infty \quad \text{for} \quad t - t_0 > \nu. \tag{192}$$

From proposition 3.3.1 we have $x_1, x_2 \in P_3$ for $t > T$. Therefore,

$$\begin{aligned}
&|(x_1(t) - s_2) - (x_2(t) - s_1)| = |(x_1(t) - x_2(t)) - (\tfrac{bg_1}{\alpha+2g_1} - \tfrac{b(\alpha+g_1)}{\alpha+2g_1})| \\
&= |(x_1(t) - x_2(t)) - \tfrac{b\alpha}{\alpha+2g_1}| = |W_3(t) - Z_3(t)| \longrightarrow 0, \\
&\quad \text{when} \quad g_1 \longrightarrow \infty \quad \text{for} \quad t - t_0 > \nu.
\end{aligned} \tag{193}$$

Then according to definition 4.2.1 the system is synchronous. See figure 34–35. □

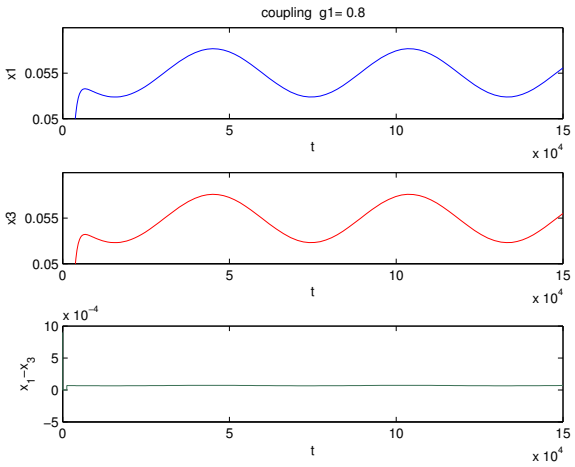

Figure 34: Synchronization of bidirectionally coupled circuit. (a) x_1 Blue , (b) x_2 Red , (c) $x_1 - x_2$, $g = 0.8$.

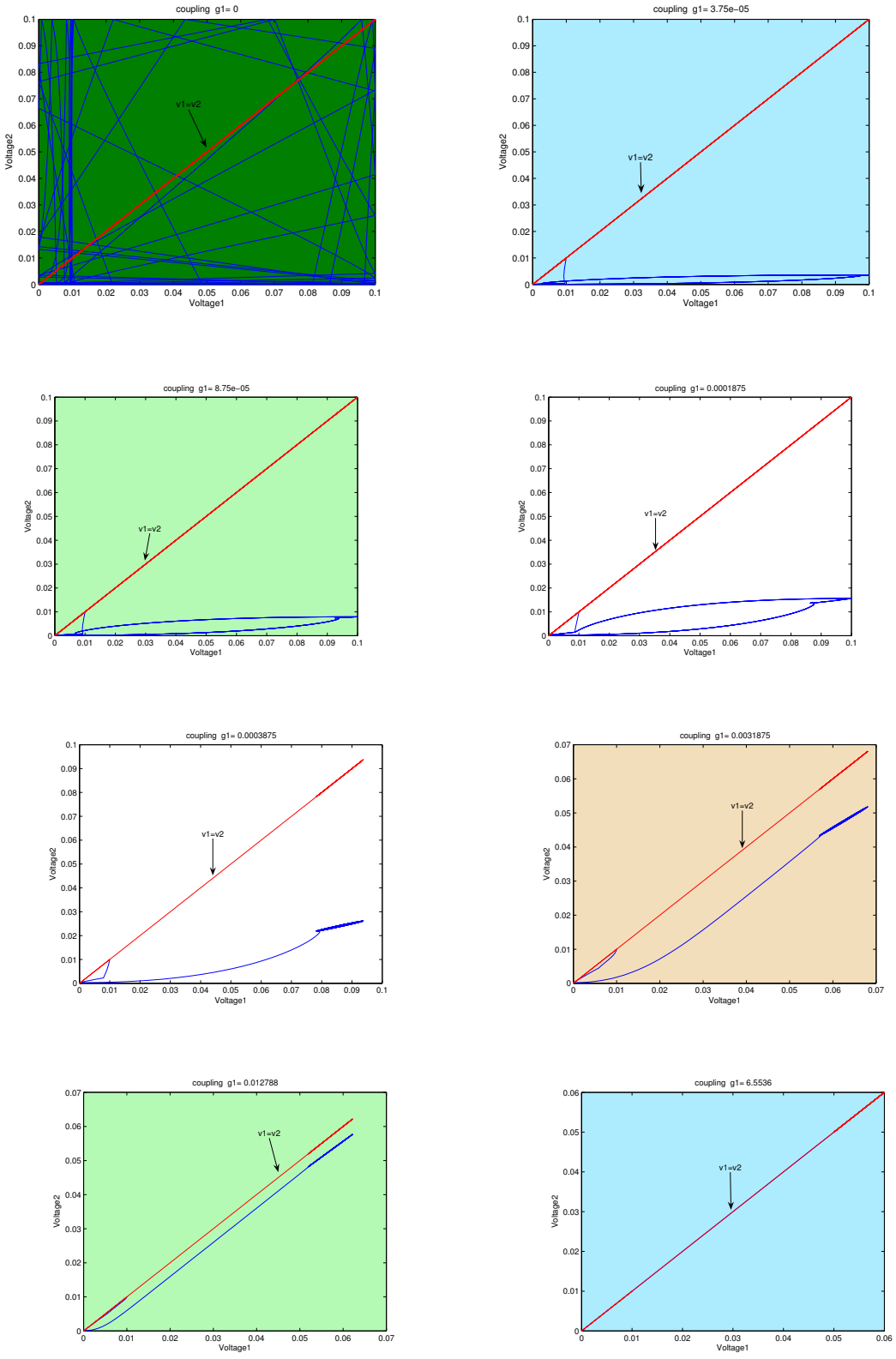

Figure 35: synchronization of bidirectional coupling

Before finish the chapter let me explain with the following example the diferences between the unidirectional and bidirectional coupling. For the unidirectional coupling does not matter what information has the circuit two (x_2) before it coupled with circuit one ($x_1(t)$). The information coming from circuit one (x_1) will be copy for circuit two (x_2). Let assume that before coupling the information given by the driver (x_1) and the response (x_2) is given by figure 36. Then from the simulation figure 36 we get that for $g = 0.8$ x_2 copy the information from x_1.

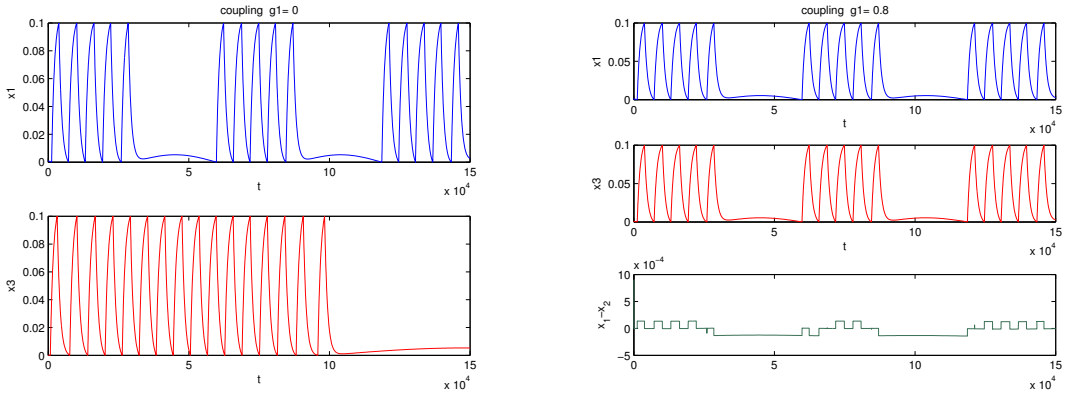

Figure 36: when circuit 1 and circuit 2 have different information before coupling (unidirectional case).

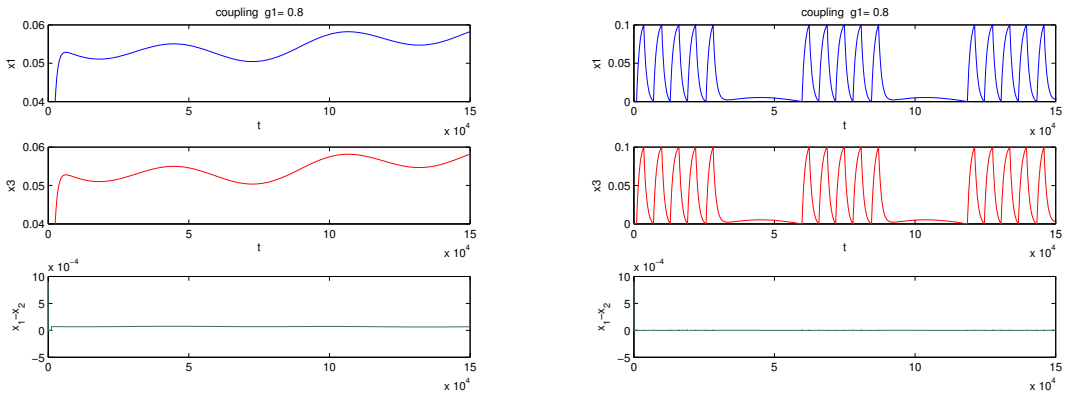

Figure 37: when circuit 1 and circuit 2 have the same information before coupling (dibirectional case).

CHAPTER V

NUMERICAL SIMULATION

5.1 Introduction

Using interactive software, such as Matlab, it is now possible to place more emphasis on learning new and difficult concepts than on programming algorithms. Interesting practical examples can be discussed, and useful problems can be explored. Matlab is an interactive, matrix-based system for scientific and engineering numeric computation and visualization. Its strength lies in the fact that complex numerical problems can be programed easily and in a fraction of the time required with a programming language such as Fortran or C.

Concerning the phenomena of synchronization, two basic questions are particularly interested and important. The first one is: giving a coupled chaotic system or a chaotic system, when the system possesses synchronization or self–synchronization. For coupled identical systems the diagonal of the system is invariant. Synchronization is equivalent to the attracting property of the diagonal, which in turn is determined by the Lyapunov exponents normal to the diagonal. More precisely, if all the Lyapunov exponents normal to the diagonal are negative, then the coupled oscillators synchronize.

If we consider two close trajectories in the phase space, i.e., the unperturbed and the perturbed ones, then we see that in the radial direction they converge with time, while in the direction along the cycle neither converge nor diverge. In terms of nonlinear dynamics, the convergence/divergence properties of nearby trajectories are characterized by the Lyapunov exponents. Convergence of trajectories along some direction in the phase space corresponds to a negative Lyapunov exponent. The absolute value of this exponent quantifies the rate of convergence. Convergence and divergence of trajectories is characterized by Lyapunov exponents. Suppose we consider a cloud of initial conditions around some point on the limit cycle (figure 38). This phase volume decreses during the evolution, resulting in an elliptical form. This corresponds to a negative Lyapunov exponent in the direction transversal to the

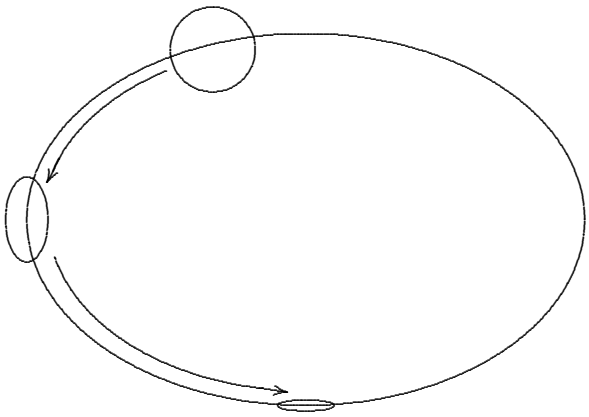

Figure 38: Meaning of Lyapunov exponents.

cycle, and to a zero Lyapunov exponent in the tangential direction (see figure 38).

There are as many Lyapunov exponents as dimensions of the phase space. Considering a region (circle, sphere, hypersphere, etc) in phase space then at a later time all trajectories in this region form an n-dimensional elliptical region. The Lyapunov exponent can be calculated for each dimension. When talking about a single exponent one is normally referring to the largest, this convention will be assumed from now onwards. If the Lyapunov exponent is positive then the system is chaotic and unstable. Nearby points will diverge independently of how close they are. The magnitude of the Lyapunov exponent is a measure of the sensitivity to initial conditions, the primary characteristic of a chaotic system. If the Lyapunov exponent is less than zero then the system attracts to a fixed point or stable periodic orbit. These systems are non conservative (dissipative). The absolute value of the exponent indicates the degree of stability.

If the Lyapunov exponent is zero then the system is neutrally stable, such systems are conservative and in a steady state mode.

Any continuous time-dependent dynamical system without a fixed point will have at least one zero exponent [19], corresponding to the slowly changing magnitude of a principal axis tangent to the flow. Axes that are on the average contracting (expanding) correspond to negative (positive) exponents. The sum of the Lyapunov exponents is the time-averaged divergence of the phase space velocity; hence any dissipative dynamical system will have

Table 4: General character of Lyapunov exponents in $3-D$ flows:

I_1	I_2	I_3	Attractor
neg	neg	neg	equilibrium point
0	neg	neg	limit cycle
0	0	neg	2-torus
pos	0	neg	strange(chaotic)

Table 5: For flows in dimension higher than 3

$(0,0,0,-,\ldots)$	$3-$torus, etc.
$(+,+,0,-,\ldots)$	hyperchaos, etc

at least one negative exponent, the sum of all of the exponents is negative, and the post-transient motion of trajectories will occur on a zero volume limit set, an attractor.

The exponential expansion indicated by a positive Lyapunov exponent is incompatible with motion on a bounded attractor unless some sort of folding process merges widely separated trajectories. Each positive exponent reflects a "direction" in which the system experiences the repeated streching and folding that decorrelates nearby states on the attractor. Therefore, the long-term behavior of an initial condition that is specified with any uncertainty cannot be predicted; this is chaos. An attractor for a dissipative system with one or more positive Lyapunov exponents is said to be "strange" or "chaotic".

5.1.1 Unilateral coupling (unidirectional coupling)

It is shown numerically, using MATLAB, that the unidirectional coupling are perfectly synchronized in an generalized sense according to definition 4.2.1 and information sense. That is, they produce the same information –i.e., symbols generated by one systems map injectively to symbols emitted by the other.

We carried out computer calculations where the parameters values of $\delta_1 = 1000$, $\delta_2 = -10000$, $k = 1.0681e-04$, $y^* = -0.00001$, $\epsilon = 1000$ and the error tolerance $10e-05$. The parameters $\omega > 0$ was choosen randomly each time that we start the simulation after that we start to increases the coupling g in order to get synchronization with respect to

the variables x_1 and x_2. On figure 39 and figure 40, the first three pictures from left to right is the figure of x_1 and x_2 before coupling. We can see clearly how x_2 change when g increase. There are five differents color, this is because we choose five random frequency and construct the period as $T = \frac{2\pi}{\omega_1} + \ldots + \frac{2\pi}{\omega_5}$. Then each color represents the number of spikes that correspond to each frequency. The table 6 correspond to the position of the spike for figure 39.

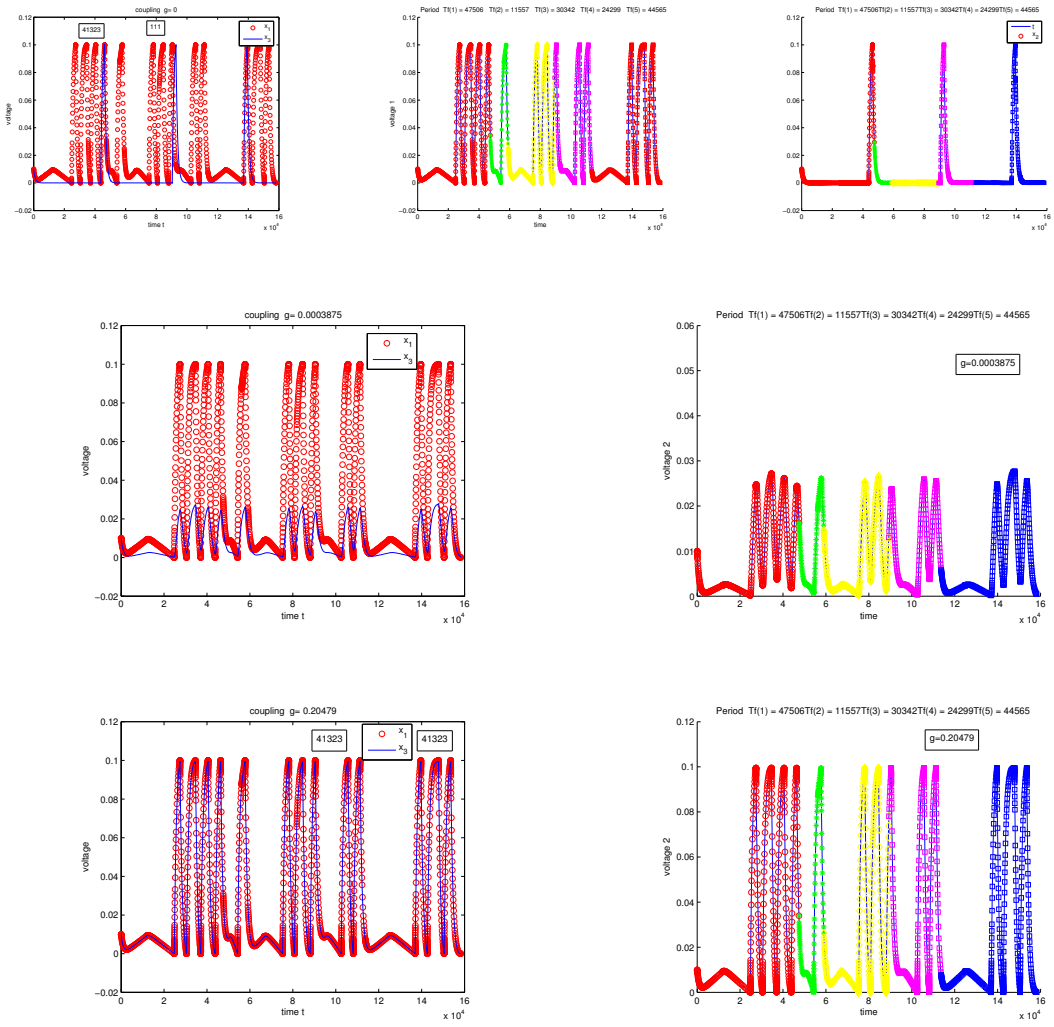

Figure 39: Synchronization of information between driver and receiver

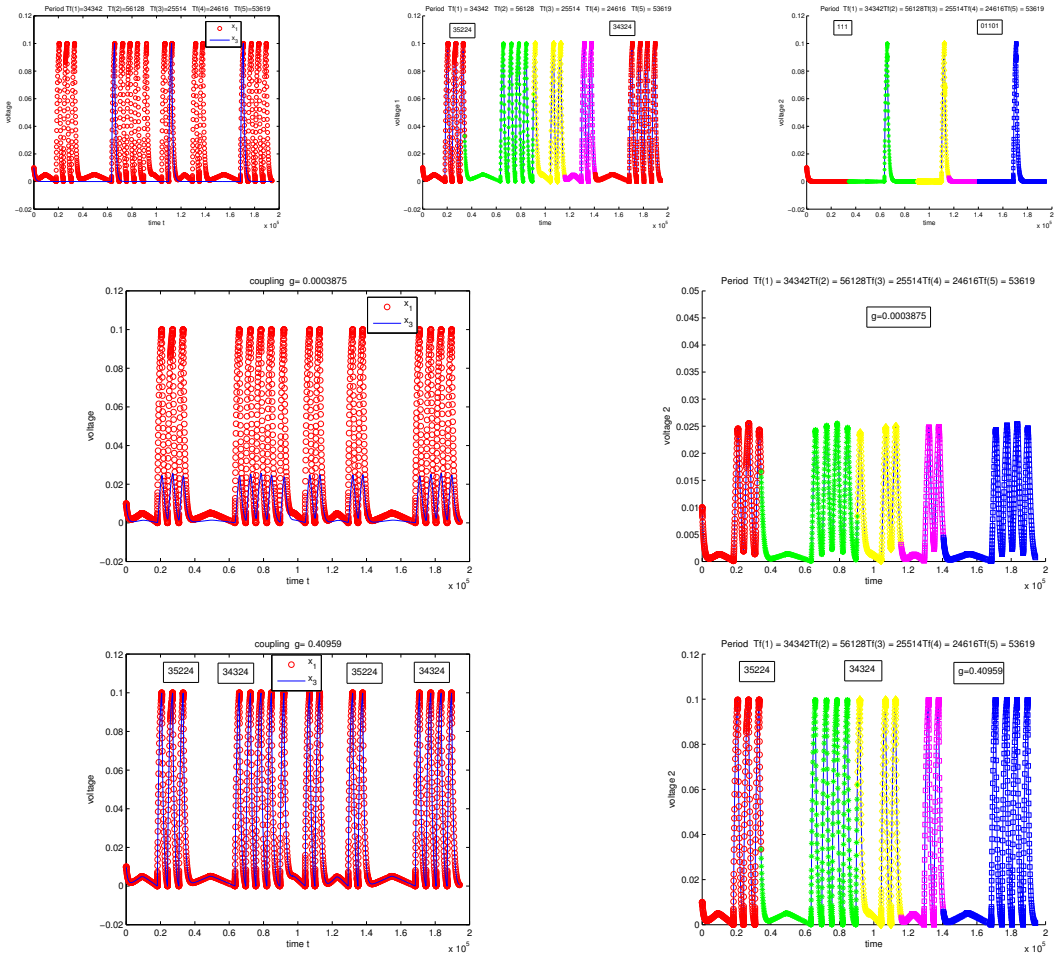

Figure 40: Continue

The following table show the position of each spike with respect to each period.

Table 6: Location of the spikes on circuit 1 and circuit 2

s_{dist11}	6137	6634	23531	6481	5887	7321	14573	5872	16272	5885	9116
s_{dist13}	6163	6638	23525	6478	5890	7324	14569	5872	16272	5887	9115

Now for example let us assume that we are sending an information from circuit one (driver) to circuit two (response) but these information is represented by color. For example, if the number of spike is less of equal than 3 then we have red otherwise we have green. In this simulation we took the following values $\delta_1 = 1000$, $\delta_2 = -10000$, $y^* = -0.00001$, $k = 0.0000053407$, and the values of $w = \frac{2\pi}{T}$ was taking randomly. We show using MATLAB that this two circuit perfectly synchronized according to definition 4.2.1.

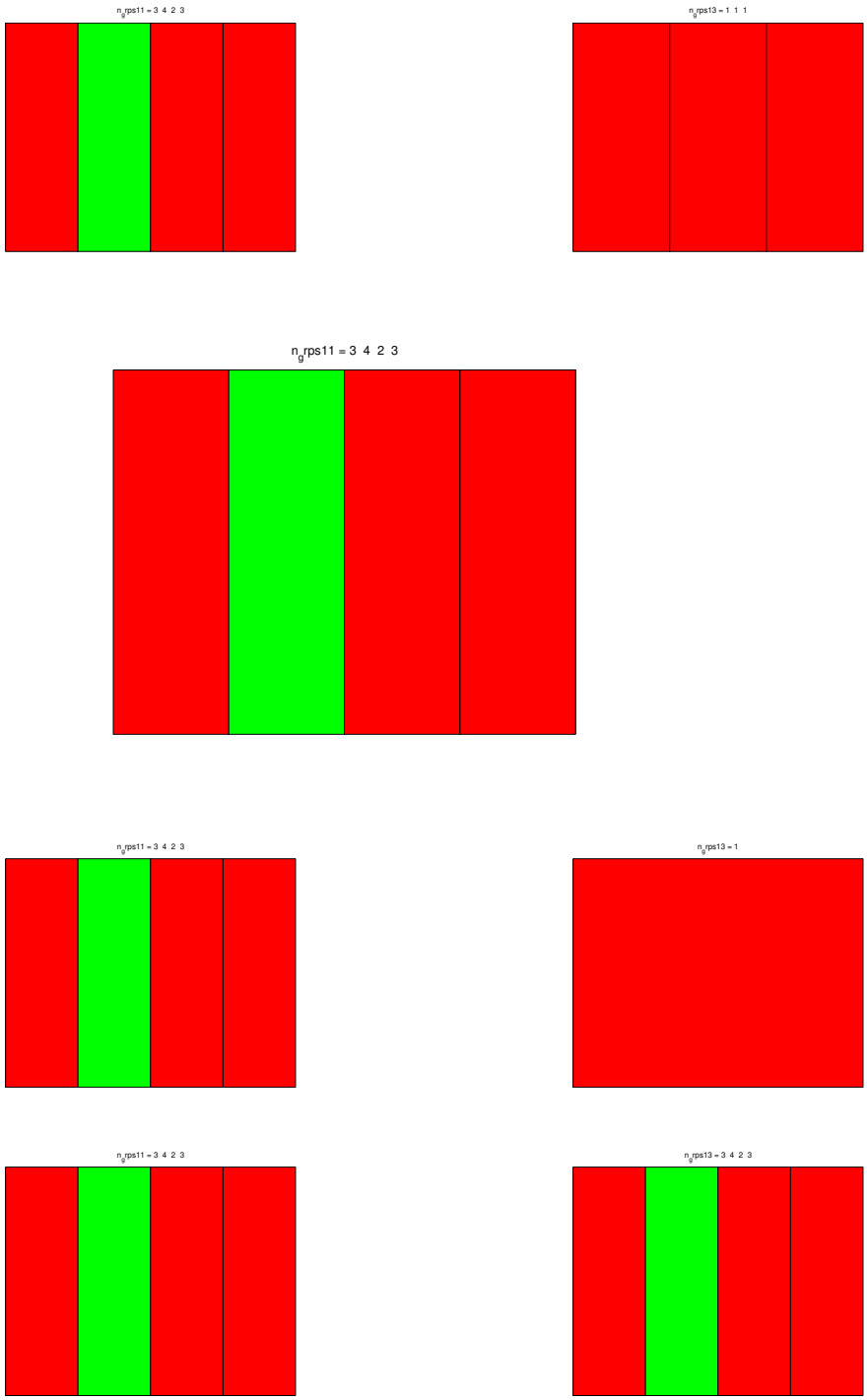

Figure 41: Generalize synchronization.

5.1.2 Bidirectional coupling

It is shown numerically, using MATLAB, that the bidirectional coupling exhibit generalized synchronization but this synchronization is not on an information sense according to remark

4.2.1. That is, they do not produce the same information –i.e., symbols generated by one systems no map injectively to symbols emitted by the other. What they are doing here is they destroy the initial information at less that they have the same information before they are coupled.

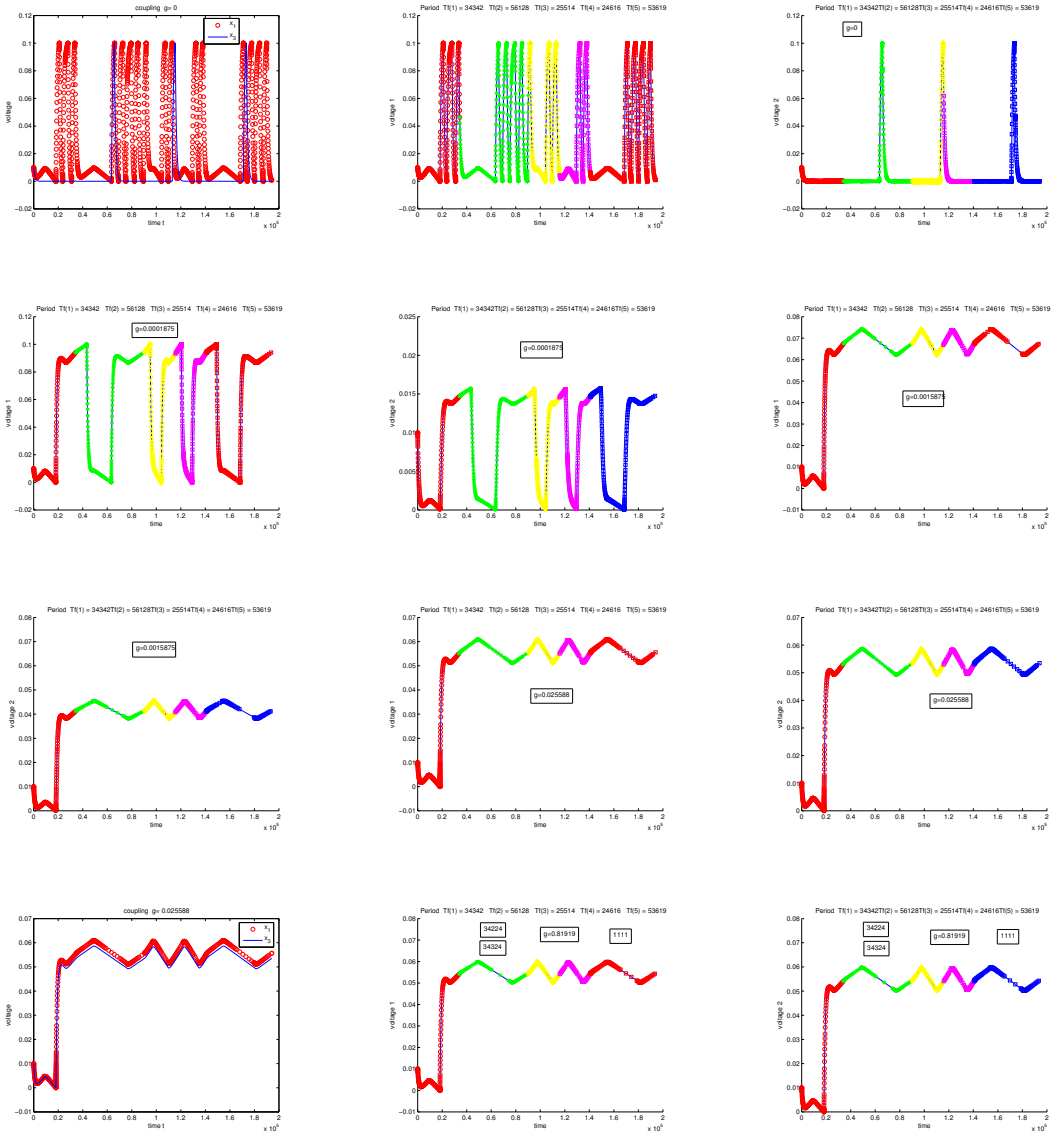

Figure 42: Synchronization of information (Bidirectional coupling).

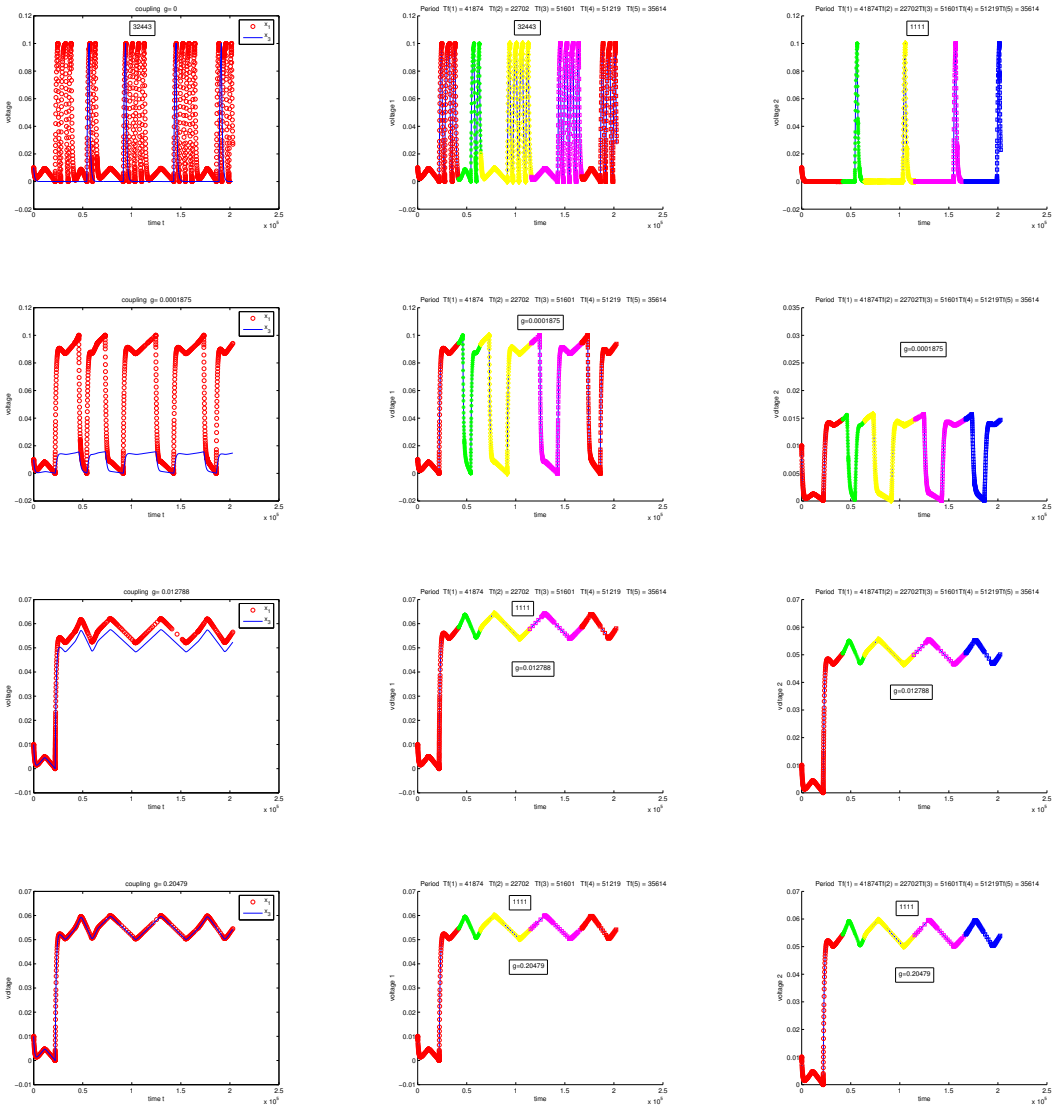

Figure 43: Continue.

5.2 Lyapunov Exponents

The Lyapunov exponents of a system are a set of invariant geometric measures which describe, in an intuitive way, the dynamical content of the system. In particular, they serve as a measure of how easy it is to perform prediction on the system. When talking about a system here, it is easiest to think of it as a set of trajectories in phase space, i.e., an attractor.

Lyapunov exponents quantify the average rate of convergence or divergence of nearby trajectories, in a global sense. A positive exponent implies divergence, a negative one

convergence, and a zero exponent indicates the temporally continuous nature of a flow. Consequently a system with positive exponents has positive entropy, in that trajectories that are initially close together move apart over time. The more positive the exponent, the faster they move apart. Similarly, for negative exponents, the trajectories move together. A system with both a positive and negative Lyapunov exponents is said to be chaotic.

Any continuous time-dependent dynamical system without a fixed point will have at least one zero exponent [19], corresponding to the slowly changing magnitude of a principal axis tangent to the flow. Axes that are on the average contracting (expanding) correspond to negative (positive) exponents. The sum of the Lyapunov exponents is the time-averaged divergence of the phase space velocity; hence any dissipative dynamical system will have at least one negative exponent, the sum of all of the exponents is negative, and the post-transient motion of trajectories will occur on a zero volume limit set, an attractor.
The exponential expansion indicated by a positive Lyapunov exponent is incompatible with motion on a bounded attractor unless some sort of folding process merges widely separated trajectories. Each positive exponent reflects a "direction" in which the system experiences the repeated streching and folding that decorrelates nearby states on the attractor. Therefore, the long-term behavior of an initial condition that is specified with any uncertainty cannot be predicted; this is chaos.

We carried out computer calculations. Table 7 show the values of δ_1, δ_2, k, and y^* that we used in this simulation. The values of ω were choosen randomly.

Table 7: Values of δ_1, δ_2, k, and y_0

δ_1	δ_2	k	y_0
1000	-10000	$1.0681e-04$	-0.00001

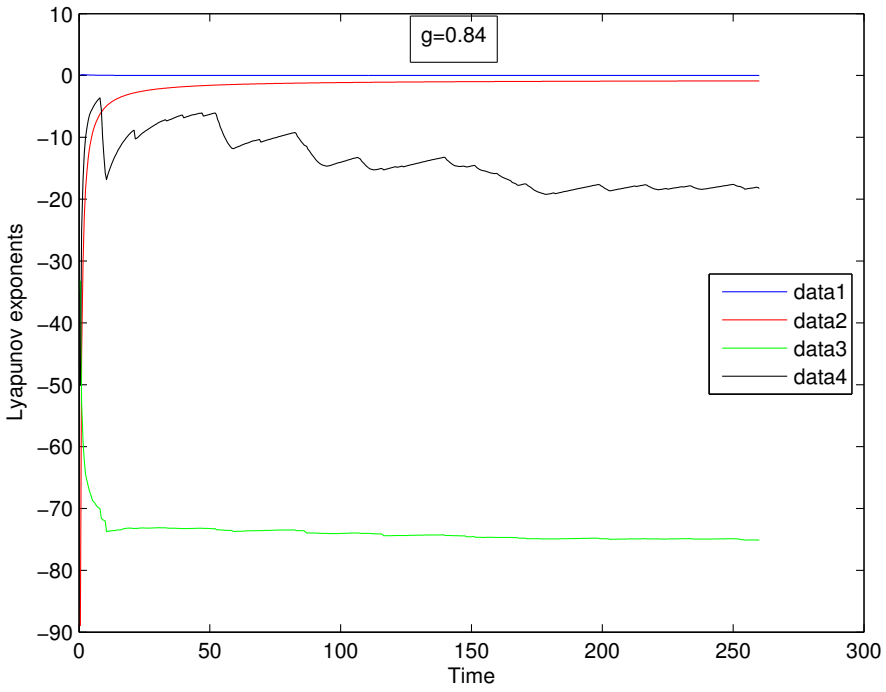

Figure 44: Dynamics of Lyapunov exponents

REFERENCES

[1] Abarbanel, H. D. I. Rulkov, N. F. and Sushchik, M. M., "Generalized synchronization of chaos: The auxiliary system approach," *Phys. Rev. E*, vol. 53, pp. 4528–4535, May 1996.

[2] Afraimovich, V. S., Chow, S.-N., and Hale, J. K., "Synchronization in lattices of coupled oscillators," *Phys. D*, vol. 103, pp. 442–451, 1997.

[3] Afraimovich, V. S. and Rodrigues, H. M., "Uniform ultimate boundedness and synchronization for nonautonomous equations," *CDSNS94-202*, vol. 29, no. 9, pp. 1050–1060, 1994.

[4] Afraimovich, V. S., Verichev, N. N., and Robinovich, M. I., "Stochastic synchronization of oscillators in dissipitative systems," *Sov. Radiophys*, vol. 29, pp. 795–800, 1986.

[5] Andronov, A. A. and Vitt, A. A., "On mathematical theory of entrainment," *J. Appl. Phys.*, vol. 7, no. 4, 1930 (in Russian).

[6] Appleton, E. V., "The automatic synchronization of triode oscillator," *Proc. Cambridge Phil. Soc. (Math. and Phys. Sci.)*, vol. 21, no. 9, pp. 231–248, 1922.

[7] Arnold, V. I., "Small denominators. i. mappings of the circumference onto itself," *AMS Transl. Ser.*, vol. 46, no. 2, pp. 213–284, 1961.

[8] Barnes, B. and Grimshaw, R., "Numerical studies of the periodically forced bonhoeffer van der pol system," *Int. J. Bifurcation and Chaos*, vol. 7, pp. 2653–2689, December 1997.

[9] Cartwright, M. L., "Forced oscillations in nearly sinusoidal systems," *J. Inst. Elec. Eng.*, vol. 95, p. 88, 1948.

[10] Cartwright, M. L. and Littlewood, J. E., "On nonlinear differential equations of the second order," *J. London Math. Soc.*, vol. 20, pp. 180–189, 1945.

[11] Corron, N. J., "Loss of synchronization in coupled oscillators with ubiquitous local stability," *Phys. Rev. E*, vol. 63, no. 055203, 2001.

[12] Cuomo, K. M. and Oppenheim, A. V., "Circuit implementation of synchronized chaos with applications to communications," *Phys. Rev. Lett*, vol. 71, pp. 65–68, July 1993.

[13] Denjoy, A., "Sur les courbes défines par les équations différentielles á la syrface du tore," *J. de Matheématiques Pures at Appliquées*, vol. 78, pp. 333–375, May 1971.

[14] Fenichel, N., "Geometrical singular perturbation theory for ordinary differential equations," *J. Diff. Eq.*, vol. 31, pp. 53–98, 1979.

[15] Fujisaka, H. and Yamada, T., "Stability theory of synchronized motion in coupled-oscillator systems," *Progress of Theoretical Physics*, vol. 69, no. 1, pp. 32–47, 1983.

[16] Georgi, S. M. and Kopell, N., "Synchronization and transient dynamics in the chains of electrically coupled fitzhugh–nagumo oscillators," *Siam J.Appl. Math*, vol. 61, no. 5, pp. 1762–1801, 2001.

[17] Grasman, J., *Asymptotic Methods for Relaxation Oscillations and Applications*. New York: Probus Publishing Company, 1987.

[18] Gray, C. M., "Synchronous oscillations in neural systems: Mechanism and functions.," *J. Computat. Neuroscience*, vol. 1, pp. 11–38, 1994.

[19] Haken, H., "At least one lyapunov exponent vanishes if the trajectory of an attractor does not contain a fixed point," *Physics Letters A*, vol. 94, pp. 71–72, February 1983.

[20] Hale, J., "Coupled oscillators on a circle," *Resenhas IME-USP*, vol. 1, pp. 441–457, 1994.

[21] Hale, J., "Attracting manifolds for evolutionary equations," *CDSNS96-257*, 1996.

[22] Hale, J., "Diffusive coupling, dissipation and synchronization," *J.Dynam. Differential Equations*, vol. 9, pp. 1–52, 1997.

[23] Itoh, M. and Murakami, H., "Chaos and canards in the van der pol equation with periodic forcing," *Int. J. Bifurcation and Chaos*, vol. 4, pp. 1023–1029, August 1994.

[24] Kocarev, L. and Parlitz, U., "General approach for chaotic synchronization with applications to communication," *Phys. Rev. Lett*, vol. 74, pp. 5028–5031, June 1995.

[25] Kocarev, L. and Partlitz, U., "Generalized synchronization, predictability, and equivalence of unidirectionally coupled dynamical systems," *Phys. Rev. Lett*, vol. 76, no. 11, pp. 1816–1819, 1996.

[26] Kopell, N., "Chains of coupled oscillators, in brain theory and neural networks," *M. A. Arbib, ed., MIT Press, Cambridge, MA*, 1995.

[27] Kuramoto, Y., *Chemical Oscillations, Waves, and Turbulence*. Tokyo: Springer–Verlag, 1984.

[28] Meyer, A., "On the theory of coupled vibrations of two self-excited generators," *Proc. Gorky State University.*, vol. 2, p. 3, 1935.

[29] Nayfeh, A. H., *Perturbation Method*. New York: Wiley–interscience, 1973.

[30] Olesen, M. W. and Knudsen, C., "Destruction of dominant arnol'd tonges in forced oscillators," *Int. J. Bifurcation and Chaos*, vol. 4, pp. 737–739, June 1994.

[31] O'Malley, R. E., *Singular Perturbation Methods for Ordinary Differential Equations*. Springer-Verlag, 1991.

[32] Parlitz, U. and Junge, L., "Subharmonic entrainment of unstable period orbits and generalized synchronization," *Phys. Rev. Lett.*, vol. 79, pp. 3158–3161, October 1997.

[33] Pecora, L. and Carroll, T. L., "Synchronization in chaotic systems," *Phys. Rev. Lett.*, vol. 64, pp. 821–824, February 1990.

[34] Pecora, L. and Carroll, T. L., "Driving systems with chaotic signals," *Phys. Rev. A*, vol. 44, pp. 2374–2383, August 1991.

[35] Peskin, C. S., *Mathematical Aspects of Heart Physiology*. Courant Institute of Mathematical Sciences, New York, 1975.

[36] Pyragas, K., "Synchronization of coupled time-delay systems: Analytical estimations," *Phys. Rev. E*, vol. 58, pp. 3067–3071, September 1998.

[37] Rand, R. H. Cohen, A. H. and Holmes, P. J., "Systems of coupled oscillators as models of central pattern generators, in neural control of rhythmic movements in vertebrates," *Cohen, A. H, Grillner, S, and Rossignol, S, eds., Wiley, New York*, pp. 369–413, 1987.

[38] Rulkov, N. F. Sushchik, M. M. and Tsimring, L., "Generalized synchronization of chaos in directionally coupled chaotic systems," *Phys. Rev. E.*, vol. 51, no. 2, pp. 980–994, 1995.

[39] Shaw, R., "Strange attractors, chaotic behavior, and information flow," *Z. Naturforsch*, vol. 36A, pp. 80–112, 1980.

[40] Shui-Nee, C. and Weishi Liu, E. S., "Synchronization, stability and normal hyperbolicity," *Resenhas IME-USP*, vol. 3, no. 1, pp. 139–158, 1997.

[41] Stoker, J., *Nonlinear Vibrations in Mechanical and Electrical Systems*. New York: Wiley–Interscience, 1950.

[42] Terman, D. and Wang, D., "Global competition and local cooperation in a network of neural oscillators," *Phys. D*, vol. 81, pp. 148–176, 1995.

[43] Van Der Pol, B., "On relaxation oscillations," *Phill. Mag.*, vol. 2, pp. 978–992, 1926.

VITA

José Luis Sánchez was born in Carúpano, a small town located in the northeast of Venezuela. He earned the title of Licenciado en Matematicas at the Universidad Central de Venezuela. Then he started a master's program in mathematics at Universidad Central de Venezuela while he was teaching. He did some research in Set-Value Functions and Composition Operators that resulted in his master thesis. He worked as assistant professor at the Universidad Central de Venezuela, before been admitted for the Ph.D. program at the Georgia Institute of Technology, in Fall 1999.